THERMAL IMAGING FOR POTENTIAL USE IN CEREALS AND OILSEEDS HANDLING

BY

MANICKAVASAGAN ANNAMALAI

A Thesis
Submitted to the Faculty of Graduate Studies
The University of Manitoba
in Partial Fulfillment of the Requirements
for the Degree of

DOCTOR OF PHILOSOPHY

Department of Biosystems Engineering
University of Manitoba
Winnipeg, Manitoba, CANADA

THE UNIVERSITY OF MANITOBA

FACULTY OF GRADUATE STUDIES

*****

COPYRIGHT PERMISSION

THERMAL IMAGING FOR POTENTIAL USE IN CEREALS AND OILSEEDS HANDLING

BY

MANICKAVASAGAN ANNAMALAI

A Thesis/Practicum submitted to the Faculty of Graduate Studies of The University of Manitoba in partial fulfillment of the requirement of the degree

DOCTOR OF PHILOSOPHY

ABSTRACT

Canada produces around 57 Mt of grains every year and about 46% of that is exported. Wheat is the major grain in Canada, and the annual production is about 43% (24.5 Mt) of the total grain production. To minimize the losses by stored-product insects, early detection of infestations is required to carry out control measures. Knowledge on heating behavior and quality changes during drying using different methods such as microwave heating are essential to develop alternative grain drying systems. Similarly, in grain handling facilities, quick, reliable machine vision methods are needed to assist the grain inspectors in the determination of grain grading factors such as class identification. Therefore, the potential uses of an infrared thermal imaging method were studied for five similar applications in grain handling operations.

An un-cooled focal planar array type infrared thermal camera (Model: ThermaCAM ^{TM} SC500 of FLIR systems, Burlington, ON, Canada; spectral range: 7.5 to 13.0 μm), with 320×240 pixels, was used to take thermal images of the grain bulk samples. For single kernel analysis, a 50 μm close-up lens was attached to the original lens of the camera to get magnified thermal images.

Non-uniform heating patterns were observed on the surface of barley, canola and wheat after microwave treatment in a pilot-scale drier. The difference between maximum and minimum temperatures (ΔT) on the surface of the grain bulk were 62.9 to 69.5°C, 64.3 to 75.6°C and 39.5 to 59.2°C for wheat, barley and canola, respectively, when the applied microwave power and exposure time were 500 W and 56 s. Germination percentages and fat acidity value (FAV) were determined for the wheat samples collected from the high temperature and normal temperature regions of bulk grain after microwave treatment. The germination percentages were significantly (α=0.05) lower for samples

collected from high temperature region than those from the normal temperature zones. Similarly, the FAV was significantly different for the samples collected from the high temperature and normal temperature regions.

The capability of a thermal imaging method to detect a hot spot in a stored grain silo was determined. The hot spot was detected from the thermal images of the silo wall and grain bulk (as a high temperature region) when it was located at 0.3 m from the silo wall and below the grain surface, respectively. Hot spots were not detected in thermal images during wind and cold weather conditions. Thermal imaging can not be used as an independent method to detect the hot spot in a silo by monitoring the surface temperature of the silo wall.

A thermal imaging system was developed to identify eight western Canadian wheat classes using bulk sample (20 g) analyses. The overall classification accuracies of a quadratic discriminant method with 8 classes mixed, red classes mixed (4 classes), white classes mixed (4 classes) and pairwise comparison (2 classes) were; 76, 87, 79 and 95%, and 64, 87, 77 and 91% using bootstrap and leave-one-out validation techniques, respectively.

The efficiency of a thermal imaging system was determined to detect the presence of *Cryptolestes ferrugineus* (Stephens) inside wheat kernels at six developmental stages (four larval, pupal and adult). The overall classification accuracy for a quadratic discriminant method was 83.5 and 77.7% for infested and sound kernels, respectively, and for a linear discriminant method it was 77.6 and 83.0% for infested and sound kernels, respectively.

ACKNOWLEDGEMENTS

I express my deep sense of gratitude and hearty thanks to Dr. D.S. Jayas for giving me the opportunity to work on this project, excellent guidance, keen interest, timely suggestions, constant encouragements and help rendered during the entire course of study. I am very grateful to my other committee members Dr. N.D.G. White, Dr. J. Paliwal and Dr. Rob Roughley for their valuable suggestions, encouragements, and endless help during this study.

I am very thankful to the Natural Sciences and Engineering Research Council of Canada (NSERC) for offering the Canada Graduate Scholarship (CGS) for my Ph.D. program. I thank C.J. Demianyk, Matt McDonald, Dale Bourns and Gerry Woods for their technical support, and Debby Watson and Evelyn Fehr for their administrative support.

On a personal note, I express my gratitude to the fellow researchers Dr. Abdul Rehman Tahir, Aishwarya Balasubramanian, Anandakumar Palanichamy, Aravind Mohan Lokhamoorthi, Chandra Bhan Singh, Dr. Chitra Karunakaran, Chelladurai Vellaichamy, Dipali Narvankar, Feng Wang, Dr. Fuji Jian, Gayathri Pitchai, Govindarajan Sureshbabu, Haiyan Li, Dr. Hao Zhang, Jun Wu, Mahesh Sivakumar, Nithya Udayakumar, Prabal Ghosh, Rajarammanna Ramachandran, Dr. Ruplal Choudhary, Sun Ke, Sathya Gunasekaran, Dr. Shashikant Sadistap, Sujala Balaji, Sureshraja Neethirajan, and Vadivambal Rajagopal, and summer students Kelly Griffiths and Caroline Shields.

Finally, I express my hearty appreciations to my beloved wife Meenu Manickavasagan and daughter Shivaani Manickavasagan for their love, cooperation and

moral support during this work and throughout my life.

Dedicated to my parents
... who are living in my memory

TABLE OF CONTENTS

LIST OF TABLES

LIST OF FIGURES

1. INTRODUCTION

1.1 Canadian Grain Industry

The Canadian grain industry has a significant role in the nation's agricultural sector and the world's grain trade. On an average, Canada produces about 57 Mt of grains annually and around 46% of that is exported (Canadian Wheat Board 2005). Wheat is the major grain in Canada, and the annual production is about 42.9% (24.5 Mt) of the total grain production (Canadian Wheat Board 2005). Canada is the sixth largest producer and third largest exporter of wheat in the world. Canada also ranks second in the production and first in the export of Durum wheat in the world. Canada has a global reputation for being a consistent supplier of quality grains to more than 70 countries.

The harvested grain must be dried to safe storage moisture levels before storing. Conventional drying methods such as hot-air drying and near-ambient drying are still followed in the grain industry. Knowledge on heating patterns and quality changes during drying using different methods such as microwave heating are essential to develop alternative grain drying systems.

Insects, molds and rodents can cause severe damage (qualitative and quantitative) to the grain during storage. In Canadian grain industry, around 162 to 475 million dollars is lost every year due to the stored-product pests and microorganisms (White 1993). Hot spots (localized high temperature zones) can develop anywhere inside the grain bulk and grow in all directions due to the accelerated chain reaction of insects, moulds and the respiration of grains. Therefore, early detection of hot spots is required to carry out control measures. Furthermore, quick, reliable machine vision methods are needed to assist the grain inspectors in quality assessment tasks such as identification of classes and

detection of insect infestation. Therefore, the potential uses of infrared thermal imaging for five similar applications in grain handing operations were studied in this research.

1.2 Infrared Thermal Imaging

In thermal imaging, the invisible radiation pattern (temperature) of an object is converted into a visible image. The region in the infrared band with wavelengths from 3 to 14 μm is called the thermal infrared region. This band is useful in imaging applications that use heat signatures (Gonzalez and Woods 2002). An infrared thermal imaging system provides the surface temperature of any object in two dimensions, and these data could be used (directly or indirectly) for many applications. It is essential to create a suitable thermal environment on the object of interest before imaging to obtain useful information. In some cases, "steady state" imaging (at ambient conditions) may reveal the status of the object and the abnormalities. Whereas in other cases, heating or cooling may be required before imaging to classify the objects or to identify the abnormality within the object. This technique is becoming popular in many fields including the agricultural and food industries. However, the published works for the applications of thermal imaging in the grain industry are limited.

1.3 Objectives

1. To determine the non-uniformity of heating on the surface of grain after microwave treatment using a pilot-scale drier.
2. To determine the germination percentage and fat acidity value (FAV) of the wheat samples collected from the high temperature and the normal temperature regions of bulk grain after microwave treatment.

3. To determine the capability of thermal imaging to detect a hot spot in a stored grain silo.
4. To determine the efficiency of a thermal imaging technique to identify western Canadian wheat classes by bulk sample analysis.
5. To determine the efficiency of a thermal imaging technique to detect the presence of *Cryptolestes ferrugineus* (Stephens) inside wheat kernels at six developmental stages (four larval, pupal and adult).

1.4 Thesis Outline

Chapter 1 describes the general introduction about the Canadian grain industry, infrared thermal imaging and objectives of this research. Chapter 2 deals with the review of literature pertaining to each objective, and theory and agricultural applications of infrared thermal imaging. Chapters 3 to 7 are presented in paper format, and the details are explained in Table 1.1. The overall conclusions and recommendations are discussed in Chapter 8.

Table 1.1 Status of the manuscripts.

Objective	Chapter	Status of the manuscript	Journal
1	3	Published, Vol. 24:1559-1567, 2006	Drying Technology
2	4	Submitted in June 2006	Canadian Biosystems Engineering
3	5	Published, Vol. 22(6):891-897, 2006	Applied Engineering in Agriculture
4	6	Submitted in September 2006	Transactions of the ASABE
5	7	Submitted in November 2006	Journal of Stored Products Research

2. LITERATURE REVIEW

2.1 Thermal Imaging

Temperature measurement is an important phenomenon in almost all industrial and agricultural sectors. Several instruments and methods have been developed to measure the temperature of objects. Temperature measurements in the agricultural and food industries have mostly relied on conventional contact methods such as thermocouples, thermometers, and thermistors, which provide limited information (Nott and Hall 1999). Non-contact methods and temperature mapping techniques are becoming popular due to higher temporal and spatial resolutions. Several techniques such as x-ray tomography, infrared thermography, electrical impedance tomography, ultrasound imaging, microwave radiometry, and magnetic resonance imaging (MRI) are available to map the temperatures of biological materials (Nott and Hall 1999; Sun et al. 1993, 1994; Kantt et al. 1997, 1998; Hulbert et al. 1995). However, infrared thermal imaging has great potential for both pre-harvest and post-harvest operations in agriculture due to the portability of the equipment and simple operational procedure. This chapter describes the fundamentals of the infrared thermal imaging method and a review of its applications in agriculture.

The region in the infrared band with wavelengths from 3 to 14 μm is called the thermal infrared region. This band is useful in imaging applications that use heat signatures (Gonzalez and Woods 2002). Thermal imaging is a non-contact technique to convert the radiation pattern of an object into a visible image called a thermogram or thermal image (Agerskans 1975). By this method, the surface temperature of any object can be mapped at a high resolution. Thermal imaging is a passive technique which does

not require any external source of illumination. Another advantage of this technique is the penetration capacity of thermal radiation through smoke and mist. However, many factors such as sun, wind, fog, and rain affect the performance of the thermal imaging method while measuring the temperature of outdoor objects (Davis and Lettington 1988).

2.1.1 Fundamentals of thermal imaging

Infrared radiation was discovered by an astronomer, Sir William Herschel, in 1800 (Anonymous 2002). He measured the temperature of different colors in sunlight to determine the color which was responsible for heating. Herschel discovered that the hottest temperature existed beyond the red region and it was not visible. He named this radiation as "calorific rays" and it is now known as infrared radiation. Many characteristics of infrared radiation are similar to visible light. For instance, infrared radiation can be focused, refracted, reflected, and transmitted. All objects with a temperature greater than absolute zero (–273°C) emit infrared radiation (Anonymous 2002). The emissivity, absorptivity, transmissivity, and reflectivity to infrared radiation vary for different materials. In general, the objects which are good absorbers of infrared radiation are also good emitters. Examples of materials that have good and poor infrared radiation properties are given in Table 2.1.

Table 2.1 Materials with good and poor infrared radiation properties Anonymous (2002).

Property	Good	Poor
Transmissivity	Sodium chloride, germanium, zinc selenide, diamond	Biological materials
Reflectivity	Clean metals, aluminum foil	Paper, rubber
Emissivity/ Absorptivity	Black electric tape, water, paper, rubber, non-metalic flat paints	Clean metals, aluminum foil

The relationship between absorptivity (α), reflectivity (ρ), and transmissivity (τ) of an object is expressed by Kirchhoff's law as:

$$\alpha + \rho + \tau = 1 \quad (2.1)$$

At thermal equilibrium of an object, the absorption is equal to emission. In many thermographic applications, the law can further be simplified for opaque objects ($\tau = 0$) as:

$$\alpha + \rho = 1 \quad (2.2)$$

or

$$\epsilon + \rho = 1 \quad (2.3)$$

where ϵ is emissivity.

The infrared sensors in a thermal camera receive the total infrared radiation emitted from the surface of objects. According to Stefan-Boltzmann law (Eqn 2.4), the total amount of radiation emitted by an object per unit area is directly related to the emissivity of the object and its temperature:

$$E = \sigma \epsilon T^4 \quad (2.4)$$

where:

E = total amount of radiation emitted by an object per unit area ($W\ m^{-2}$)

σ = Stefan-Boltzman constant = 5.67×10^{-8} ($W\ m^{-2}\ K^{-4}$)

ϵ = emissivity of the object, decimal

T = temperature of the object (K)

Therefore, if the total radiation emitted and the emissivity of a material are known, its temperature can be calculated. For quantitative temperature measurement, the emissivity of the objects must be known but for qualitative differentiation, the emissivity may be neglected (Hellebrand et al. 2002).

Infrared detectors in a thermal camera sense the radiation emitted from the surface of the object in the spectral range of 3-5 μm (short wave) or 8-12 μm (long wave). These two wavelength regions are selected for infrared radiation measurement as these wave bands have good transmission in the atmosphere (Anonymous 2002).

2.1.2 Applications in agriculture

An infrared thermal imaging system provides the surface temperature of any object and these data may be used directly or indirectly for many applications. This method is suitable for making qualitative determination of surface temperature than quantitative measurement (Davis and Lettington 1988). This technique has been used in various fields such as medicine, electrical, mechanical, and civil engineering for a long time (Agerskans 1975). The reductions in cost of the equipment and simple operational procedure have created opportunities for the application in several fields of the agricultural and food industries. This technology can be used for temperature measurement of all agricultural materials and processes, where heat is generated or lost in space and time (Hellebrand et al. 2002). Small variations (below 1°C) can also be successfully measured with proper equipment and methodology. If the temperature difference is too small, a suitable

environment should be created such as increasing or decreasing the temperature of the sample and measuring the rate of cooling or heating (Danno et al. 1980).

2.1.2.1 ***Pre-harvest operations*** Plant leaves possess a complex heterogeneous internal structure and because of this different parts of the leaf contain different amounts of water per unit area, affecting thermal properties. The important parameters in plant physiology such as transpiration rate, heat capacity per unit area of the leaf, and the water flow velocity can be measured to high temporal and spatial resolution by thermal imaging techniques (Christoph et al. 2002). Identification of diseases in the field nursery before visible symptoms occur, irrigation scheduling based on soil moisture content and plant parameters, detection of fruits and vegetables on the plants to guide mechanical harvesting, and yield forecasting are the potential areas in which thermal imaging methods may be utilized effectively in the agricultural fields.

2.1.2.1.1 *Detection of diseases in field nursery* Local microclimatic changes in the field seedling nursery will cause severe damage to the tender seedlings. Early detection of dampness and disease in a nursery is very important to take early control measures. The microclimatic changes inside the nursery site can be mapped with great spatial accuracy using infrared thermography. In a field nursery, significant positive correlation was found between seedling temperature and degree of damage (Hellebrand et al. 2002). The warmest seedlings had a lower survival rate than the cooler seedlings (Egnell and Orlander 1993). Kim and Lee (2004) developed algorithms to detect the quality of potato transplants using visual and thermal imaging. Potato transplants were grown at three photosynthetic photon flux (PPF) levels of 50, 150, 250 $\mu mol.m^2s^{-1}$ and four electrical conductivity levels of 700, 1400, 2100, 2800 $\mu s.cm^{-1}$. The leaf temperature was higher

(by about 0.5 to 2.0°C) for the transplants grown at PPF of 50 $\mu mol.m^2s^{-1}$ than the other two treatments. The authors stated that thermal and visual characteristics of potato transplants can be used to monitor the transplants grown at low PPF.

2.1.2.1.2 *Scheduling of irrigation* Infrared thermometry may be used to schedule irrigation based on soil moisture content and plant parameters such as evapo-transpiration, stomatal conductance, and closing of stomata (Jones 1999). Inoue et al. (1990) determined the transpiration and stomatal conductance using infrared thermometry. Temperature of the canopy was taken with the help of a handheld infrared thermal camera in a cotton field. Transpiration rate and stomatal conductance were calculated using canopy temperature and other meteorological data in a model. A porometer was used to measure transpiration and stomatal conductance in the field simultaneously. Crop stress indices calculated by remote infrared thermometry were linearly related with porometer values and R^2 were 0.79 and 0.93 for transpiration and stomatal resistance, respectively. Berliner et al. (1984) determined the crop stress for wheat using infrared thermometry. A thermal camera was installed on a platform located on the top of a pole (3.3 m height) in the field. In addition to canopy temperature, wet and dry bulb temperatures, wind speed, and solar radiation were recorded simultaneously. Stomatal resistance and water potential had a linear relationship with canopy temperature and the R^2 were 0.64 and 0.65, respectively. For the implementation of canopy temperature as a water stress index, no meteorological data other than infrared measurement is required. Landsat thermal bands could be used to study the irrigation status of the field and different stages of growth of crops (Perdikou et al. 2002). Kalma and Jupp (1990) used infrared thermometry data to develop a model for estimating the

evaporation from a pasture. All metabolic activities of a plant cause variation in temperature and hence, research on the quantification of changes in temperature on the canopy with respect to various plant parameters would yield valuable information required for precision farming.

2.1.2.1.3 *Prediction of yield* Time series data models are commonly used methods to estimate yield for many crops in almost all parts of the world. But most of the time, high deviation is observed in the actual yield from the forecasted yield. Smith et al. (1985) analyzed the relationship between wheat yield and one-time measurement (daytime) of temperature difference between foliage and ambient air temperature (T_f-T_a). For foliage temperature measurement, they used a thermal camera (3° field of view lens) which received the infrared radiation in the spectral wavelength of 8-14 μm. The camera was held at 1.5 m height in the field and focused on the foliage at 30°. In addition to ambient and foliage temperatures, associated micrometeorological data were collected during the wheat growing stages from jointing to maturity. The experiment was conducted for two crop seasons (1982 and 1983) on a red-brown soil in Australia. Transpiration and the associated aerodynamic characteristics and canopy stomatal resistances to water vapor transport were predicted from the collected temperature data. They determined that the predicted transpiration and CO_2 assimilation rates were closely related to yield within each year but not between years. The regression coefficients for T_f-T_a and various yield parameters are shown in Table 2.2. It was stated that infrared thermometry would be a useful technique for studying yield variations in agronomic experiments.

Table 2.2 Relationship between yield parameters of wheat and mean T_f-T_a for years 1982 and 1983 (Smith et al. 1985).

Period	Yield Parameter	R^2	
		1982	1983
Jointing to maturity	Grain yield	0.94	0.87
Jointing to anthesis + 7 days	Kernel numbers	0.88	0.75
Grain filling	Kernel weight	0.57	0.40

In Europe, around 20% deviations were observed in the harvested yield of apple from the forecasted yield using a time series data model during the 2000 crop season (Stajnko et al. 2004). An algorithm to analyze thermal images was developed by Stajnko et al. (2004) to count the number and measure the diameter of fruits in an apple orchard. Thermal images of the apple trees were taken five times during the vegetation period. Each time around 120 images of 20 apple trees were taken from both the sunny and shadowy side of the tree from a distance of 2 m. The acquired images were processed to obtain the number and diameter of fruits. At the same time, on each imaged tree, all fruits were manually counted and diameters of the fruits were measured with sliding calipers. The R^2 values between thermal imaging and manual methods were in the range of 0.83 to 0.88 for fruit number and 0.68 to 0.70 for fruit diameter measurement. The R^2 value increased during the ripening period for both number and diameter of the fruits. It was suggested that thermal imaging techniques may be employed to provide an objective and easy counting of apples and measurement of their diameters required in calculating the apple yield. Since the accuracy of yield forecasting by thermometry is very promising, this technique may be used as a complementary method to other methods.

2.1.2.1.4 *Detection of fruits distribution for harvesting* Mechanical harvesting requires precise determination of the location of fruits on trees. Xu and Ying (2003)

suggested infrared thermal imaging to identify citrus fruits in a tree canopy. Around 1°C difference was observed between the mean temperatures of citrus, leaves, and branches. It was stated that infrared thermal imaging would be the easiest and most accurate method in locating the citrus for mechanical harvesting as opposed to other machine-vision methods.

2.1.2.1.5 *Detection of heat distribution within commercial greenhouses* The environmental conditions inside a greenhouse chamber should be maintained carefully because the small plants and seedlings are sensitive to small changes in the microclimate. Thermography is a useful tool to detect temperature anomalies at various locations inside the greenhouse. Ljungberg and Jonsson (2002) conducted an infrared survey to investigate the temperature profile at various locations inside a greenhouse such as surface of the tables used for plant production, radiation tubes, and plants at different stages of growth. The survey was conducted in greenhouses under two different conditions, production benches without plants and with plants. A thermal camera (wavelength 8-12 μm), mounted on a two wheeled cart was used for the survey. In the greenhouse with plants, the difference between maximum and minimum temperatures on the production benches was 4.3°C, whereas it was 11°C in the greenhouse without plants. The difference was more than 100°C on the radiation pipes in the greenhouse with plants and only 6.5°C in the greenhouse without plants. The authors suggested that thermography can be used as a tool to calibrate heating systems, evaluate its function, and to indicate anomalies in the growth process of plants inside a greenhouse. Infrared thermography may be used as an effective tool in research and evaluation of the growth process of plants at different energy related greenhouse conditions.

2.1.2.1.6 *Detection of damage by termite* In tropical countries termites are a major problem for coconut and other trees. Failure to detect termites in a timely manner, and not taking a preventive measure often leads to the death of the perennial trees. Termites are also a serious problem in farm buildings and in all wooden structures in domestic buildings. In Australia, the estimated economic loss in buildings by termites is around $70 million (James and Rice 2002). Thermal imaging has been used as a non-destructive and fast method to detect termites in trees and buildings, compared to the traditional methods such as knocking and drilling in wood (James and Rice 2002).

2.1.2.1.7 *Inspection of farm machinery* Unexpected failure of farm equipment during peak operational season can result in severe economic losses. All mechanical and electrical equipment can be inspected by a thermal camera for wear and tear. By this method, it is possible to identify the excessive heat produced by components due to friction or any other reason. For instance, hay making equipment, planters, combines, tractors, and other mechanical equipment may be inspected by infrared thermography and proactive steps can be taken to change parts before they fail or cause an interruption in production (Hellebrand et al. 2002). Utter (2003) demonstrated the use of infrared thermography to identify the backfiring and oil leakage in agricultural aircraft.

In many developing countries, millions of people are involved in agricultural field operations. To maximize work efficiency and field safety, ergonomic factors are being considered in the design of farm machinery and the work environment. Thermography would be an excellent choice to map the body temperature of workers during field work.

2.1.2.2 *Post-harvest Operations*

2.1.2.2.1 *Evaluation of fruit maturity* Maturity evaluation of fruits and vegetables is a crucial operation in both pre-harvest and post-harvest stages. Even though several automatic methods are available for this purpose, visual inspection is used in many parts of the world. This manual method of maturity evaluation is a time consuming process and human fatigue frequently influences the results (Danno et al. 1980). The maturity of tomato, Japanese pear, and Japanese persimmon were evaluated using infrared thermometry by Danno et al. (1980). Fruits and vegetables were divided into three grades of maturity such as, immature, mature, and over-ripe based on color, firmness, and sugar content. Since the difference in surface temperatures of fruits and vegetables at different stages of maturity was small at a steady state (before treatment), the produce was kept at high (30°C) and low (5°C) temperatures in constant temperature rooms for more than 24 h before temperature measurement. The surface temperature of fruits and vegetables was different in three grades of maturity and the difference was in the range of 0.5 to 1.0°C. The surface temperature of immature fruits stored at lower temperature was slightly higher than that of mature and over-ripe fruits. Whereas, the surface temperature of immature fruits stored at higher temperature was slightly lower than that of mature and over-ripe fruits.

2.1.2.2.2 *Detection of bruises in fruits and vegetables* Bruises and scratches are the most common damage on the surface of fruits and vegetables during transportation and handling. Danno et al. (1978) determined the effect of surface defects on temperature distribution for apple, Satsuma mandarin, and natsudaidai (similar to grape) fruits. Artificial bruises were made on the fruits by pressing and scratching. The

bruised fruits were kept at high (30°C) and low (10°C) temperatures in temperature-regulated rooms for more than 24 h. Then the fruits were imaged with a thermal camera (wavelength 8-14 μm). In all fruits, the temperature at the bruises was slightly lower than that of unbruised skin. A temperature difference of 0.2 to 1.0°C was measured between sound and bruised skin.

While detecting the bruises in apple manually, the dark-colored skin easily confuses and misleads human vision. The capability of the thermal imaging method to detect bruises in apple was determined by Varith et al. (2003). Red delicious, Fuji, and Macintosh varieties were bruised by dropping them from 0.46 m onto a smooth concrete floor. After creating bruises, the apples were kept at 26°C and 50% relative humidity for 48 h for the development of bruises. Then the apples were refrigerated at 3°C for at least 3 h. Apples were subjected to two heating and one cooling treatments (Treatment A- heating with forced convection using ambient air at 50% relative humidity, 26°C; Treatment B- heating with forced convection using the same air heated to 37°C; Treatment C- cooling with forced convection using ambient air at 50% relative humidity, 26°C after heating in 40°C water for 2 to 3 min). After treatments the apples were thermally imaged for 3 min using a thermal camera with 3.4 to 5 μm spectral bands. It was determined that at steady state (before treatment) thermal imaging could not detect the bruises in apple. But after all treatments the bruised tissue showed at least 1 to 2°C difference from sound tissue within 30 to 180 s after treatments. The authors stated that the temperature difference between sound and bruised tissue was possibly due to the differences in thermal diffusivity and not due to the emissivity. The correctly identified bruises by thermal imaging method in different treatments are shown in Table 2.3 (Varith

et al. 2003). Vanlinden et al. (2003) used thermal imaging method to detect bruises in tomato. Artificially bruised tomatoes were heated in microwave oven for 14 s and then thermally imaged. The temperature difference between the intact and bruised parts was in the range of 0.5 to1.0°C.

Table 2.3 Correctly identified bruises in apple by thermal imaging after heating and cooling treatments (n=15) (Varith et al. 2003).

Variety	Treatment*	Successful bruise detection (%)
Fuji	A	100.0
	B	86.7
	C	86.7
Macintosh	A	100.0
	B	100.0
	C	86.7
Red Delicious	A	66.6
	B	40.0
	C	60.0

* A- heating with forced convection using ambient air (26°C and 50% relative humidity)
B- heating with forced convection using heated air (37°C)
C- cooling with forced convection using ambient air (26°C and 50% relative humidity), after heating in 40°C water for 2– 3 min

2.1.2.2.3 *Detection of foreign substances in food* The thermographic technique may be used as a supplementary method to detect foreign materials, which could not be separated by mechanical and optical methods. Meinlschmidt and Margner (2003) developed a thermal imaging system to detect foreign materials (rotten nuts, hard shells, and stones) in hazelnuts (Fig. 2.1). Algorithms were developed for pulse and online thermography using three image processing techniques namely histogram analysis, texture analysis, and an object-oriented method. The quality of detection was affected by the physical behavior of the food and the foreign body, their form, and the noise in the images.

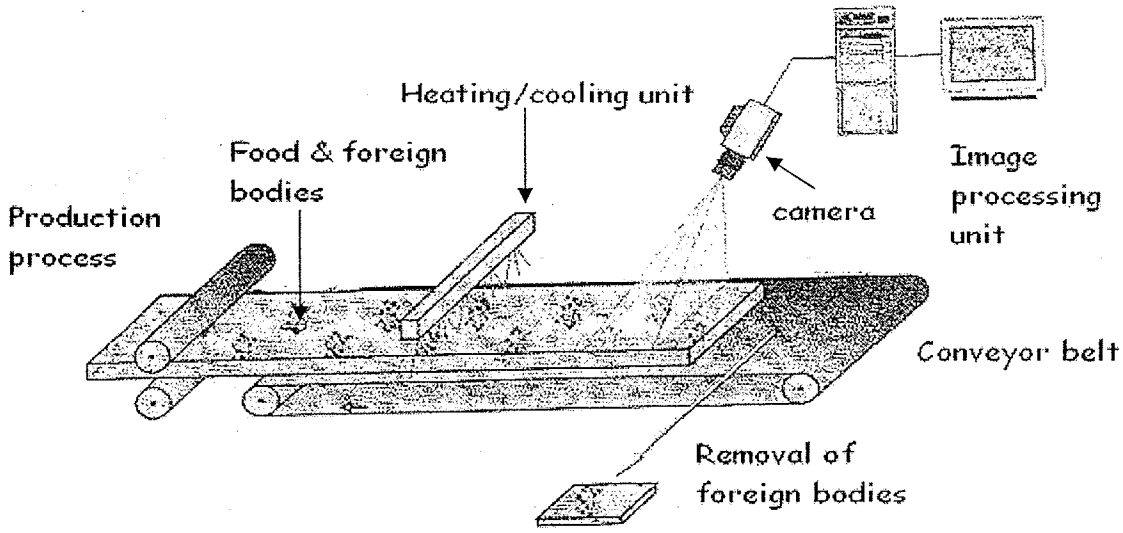

Figure 2.1 **Online thermography apparatus for detecting foreign bodies in a moving food stream** (Meinlschmidt and Margner 2003).

2.1.2.2.4 *Detection of heat distribution in wood during drying* Thermal imaging has the potential to evaluate the heating pattern during and after various heating methods. For instance, it is possible to make continuous measurement of the uniformity of heating by microwaves. Antti and Perre (1999) evaluated a microwave applicator used for online wood drying. Thermal camera and CT-scan were used to map the surface temperatures and moisture distribution, respectively, in wood during the drying operation. Dry and wet specimens of birch, pine-heartwood, and pine-sapwood were used in this experiment. Before drying, the moisture content was 6 and 50% for dry and wet birch, 6 and 29% for dry and wet pine-heartwood, and 6 and 19% for dry and wet pine-sapwood. The initial temperature was 22°C for the dry specimen and between 5 and 12°C for the wet specimens in all types of wood. The temperature gradient at the surface of wood in dry specimens was 6°C after 1 min heating and reached 25°C after 7 min

whereas the temperature gradient at the surface of wet specimens was 13 and 30°C after 1 and 7 min of heating, respectively. The authors stated that accurate determination of microwave power consumed for drying may be possible with the help of measured temperature using an infrared camera.

2.1.2.3 Other applications The damage to fruits and vegetables due to microbial activities may be evaluated by thermography (Hellebrand et al. 2002). The quality and palatability of beef are directly related to the stress level of animals and hence, it is necessary to separate highly stressed animals in the slaughter house. Infrared imaging can be used to segregate stressed animals before being slaughtered (Wurzbach 2003).

The thermal imaging method has potential to be used in many pre-harvest and post-harvest operations of agriculture. However, the opportunities are still in the experimental stage. Intensive research should be conducted for the real-time applications to increase the productivity and ultimately the net profit to farmers. Plant, soil, and water relationships has been studied in detail using thermal imaging by several researchers (Berliner et al. 1984; Inoue et al. 1990; Kalma and Jupp 1990; Jones 1999; Perdikou et al. 2002) and the outcome of this kind of research would yield valuable data required for the site-specific management and precision farming. Similarly in post harvest operations, thermal imaging methods can be used for classification of agricultural produce based on certain criteria which would otherwise not be detected by visual methods. Unlike other methods, with thermal imaging it may not be possible to develop universal methodologies for agricultural operations because the thermal behavior of plants and

agricultural produces vary with climatic conditions. It may be required to develop different protocols for similar operations under different growing conditions.

2.2 Microwave Treatment of Grains and Oil Seeds

When a food product is subjected to microwave treatment, heat is generated due to molecular friction resulting from the dipolar rotation of polar molecules (mainly water molecules), and from the conducive migration of dissolved ions (Oliveira and Franca 2002). This heat may be utilized for drying or to obtain any other desired changes within the product. Several researchers have investigated the suitability of microwaves for drying and other applications in grains and oil seeds (Anthony 1983; Borchers et al. 1972; Campana et al. 1993; Nelson 1976). The potential applications of microwaves in grain are drying and disinfestations.

2.2.1 Microwave drying

In conventional hot air drying, the drying process begins at the surface of the grain and then proceeds inside. As a result of this process, hardening, splits, and cracks may develop on the surface of the kernel. In addition to this damage, diffusion of moisture near the surface may be restricted because of the reduced permeability of the outer layer (John and Otten 1989). But in microwave drying, heat generation takes place within and throughout the kernel. Therefore, a positive temperature gradient and outward moisture driving potential is created leading to a faster heating rate and shorter processing time (John and Otten 1989; Gunasekaran 1990; Oliveira and Franca 2002).

John and Otten (1989) evaluated thin layer drying of peanuts using microwaves (2450 MHz magnetron and 250-1000 W) which resulted in a drying rate from 10 to 94 times the rate obtained using conventional drying for pods and 8 to 32 times for kernels.

The external damage after microwave drying was minimal but uneven drying was observed. The physical quality was improved with a decreased power level, and there was no visual damage observed in kernels dried at 250 W. It was also stated that more microwave power was absorbed by pods than kernels.

Parboiled rice has been dried using a microwave-vacuum technique with the same finished product quality as with a conventional drying method (Velupillai et al. 1989). Gunasekaran (1990) investigated the drying behavior of corn using continuous and pulsed microwave energy. In that experiment, about 25 g sample was taken in a glass dish (single layer of kernels) and dried by microwaves in continuous and pulsed modes using an experimental microwave oven (250 W). The power-on time in the pulsed mode was 10 and 15 s, and power-off time ranged from 20 to 75 s. The drying was more rapid in continuous mode. Within pulsed mode, faster drying was achieved in the longer power-on time. It was concluded that the moisture removal rate in microwave drying was several times faster than the conventional hot-air drying. Adu and Otten (1996) developed drying characteristics curves for microwave drying of white beans.

Although grain drying by microwaves is faster than by conventional drying, process optimization with respect to energy efficiency and final product quality have yet to be achieved (Shivhare et al. 1992a).

2.2.2 Microwave disinfestations

Microwaves can also be used as a non-chemical insect control method (Baker et al. 1956, Hurlock et al. 1979, Hamid and Boulanger 1969). As microwaves have high penetration capacity through grain, more uniform drying and efficient insect control could simultaneously be achieved (Boulanger et al. 1969). The capability of microwaves for

inactivating the *Fusarium graminearum* Schwabe in wheat was studied by Reddy et al. (1998). The eradication of the pathogen increased with the total microwave energy however, seed viability and seedling vigour decreased accordingly. Watters (1976) used microwaves to kill *Tribolium confusum* J. duVal in wheat and flour. It was determined that the mortality was related to microwave exposure time and the moisture content of the wheat and higher in wheat than in flour. The mortality of *T. confusum* was 70% at 55°C and 100% at 65°C while using microwaves for disinfestations (Hamid and Boulanger 1969). Vadivambal et al. (2005) used a pilot scale microwave system (2.45 GHz) and obtained 45, 58, 85 and 100%, mortality for *Tribolium castaneum* (Herbst) at 250, 300, 400 and 500 W, respectively.

2.2.3 Grain quality after microwave treatment

Although microwaves have potential for many applications in the grain industry, its complete utilization will be determined by the quality changes during treatment. Campana et al. (1993) investigated the effect of microwave drying on the physical, chemical and baking properties of wheat. In their experiment, 1500 g of wheat was taken in a plastic tray (grain thickness 20 mm) and heated using microwaves (2450 MHz). The temperature of the grain was measured at 12 places using a thermometer. Hot spots were observed due to non-uniform heating, however entire grain was mixed before further quality analysis. It was determined that the total protein was not affected by microwave treatment but the functionality was affected. The wet-gluten content decreased with increasing microwave power. The microwave exposure time and the initial moisture content of the grain determined the level of damage.

Microwave drying of rice and soybeans under partial vacuum improved the product quality (Gardner and Butler 1981 cited by Nelson 1987). Anthony (1983) determined that microwave and vacuum drying of cotton improved the marketing qualities of cotton seed oil. Kadlec et al. (2001) reported that the combined effect of germination, microwave treatment and drying by hot air and at 80°C decreased the high content of α-galactooligosaccharides (desired quality change) in yellow pea.

Walde et al. (2002) reported that microwave drying could reduce the power consumption in wheat milling, but it was not suitable where the final products made out of that flour needed to be soft in textural characteristics. Velu et al. (2006) determined that protein and starch content of maize were not affected by microwave drying. However, viscosity of the flour decreased with increasing microwave drying time. It was also reported that the color of the microwave dried samples was brighter than the convective dried samples. Doty and Baker (1977) investigated the effect of microwave conditioning (625 W) of wheat on the effect of flour and wheat quality. It was reported that the increased ash content, increased dough strength, decreased β-amylase activity, increased flour viscosity and decreased loaf volume were the important degradation qualities due to microwave conditioning. The effect of microwave radiation and storage on the quality of wheat flour was studied by MacArthur and Appolonia (1981). The experiment was conducted using a domestic microwave oven (2450 MHz, 625 W) and 2000 g flour was used. The sample was taken in a bowl (150 mm diameter) and the depth of the flour was 90 mm at the center of the bowl. During treatment, the bowl was rotated by hand at every 60 s to avoid hot spots. The samples were cooled, and then stored in an

air tight container. The total sugar content and starch intrinsic viscosity decreased in the microwave treated samples after storing for six months.

Seed treatment is one of the important applications of microwaves in agricultural operations (Nelson 1987). Nelson and Stetson (1985) reviewed the germination responses of seeds to radio frequency (RF) electric treatment. Seed dormancy due to hard seed coat or biochemical nature may be changed by microwave or RF electric treatment for a short time (Nelson and Stetson 1985). Treatment time should be in the range of a few seconds to a minute based on the dielectric properties and moisture content of seeds, and frequency and electric field intensity. Dielectric heat treatment increased or accelerated the germination of small-seeded legumes (alfalfa, red clover, arrowleaf clover). However several vegetable and ornamental seeds, grasses, and seeds of woody plants did not respond to RF electric treatment on germination (Nelson and Stetson 1985).

2.3 Hot Spot in Stored Grain

A hot spot in a grain silo is a localized high temperature zone in the grain bulk. Generally, the spoilage of stored grain begins in these spots. Based on origin, the hot spot may be classified as fungi-induced hot spot in damp grain and insect induced hot spot in dry grain (Sinha 1967). The temperature and moisture in a hot spot provide favorable conditions for the growth of insects and moulds. A hot spot can develop anywhere inside the grain bin. The temperature of the hot spots may go up to 380 to 400°C in crops such as soybeans and fababeans where chemical oxidation of the oil in the seed continues even after the cessation of biological respiration (Christensen and Meronuck 1986 as cited by Muir and White 2001).

Loading wet grain on top of the dry old crop, entry of rain through roof leaks, blowing of snow through ventilators, rising of moisture through a cracked floor or moisture migration within a grain bulk may cause damp grain pockets in granaries. In high moisture zones, moulds begin to grow and produce heat and moisture. The growth of moulds is arrested at 65°C but bacteria can grow up to 80°C (Muir and White 2001). *Penicillium* spp., *Aspergillus* spp., and *Absidia* spp. are the commonly associated species in fungi-induced hot spot (Wallace and Sinha 1962).

Sinha (1961) studied the physical conditions of insect-induced hot spots in 13 farm granaries of Manitoba and Saskatchewan. Grain temperature and moisture content were measured at several sampling points in and around the hot spot. Moisture content and temperatures were measured with a dielectric moisture meter and thermocouple, respectively. High density of insects and mites at all life stages were found within a hot spot, particularly in damp grain. *Cryptolestes ferrugineus* (Stephens) was the most common insect species encountered in heating grain. The most significant feature of the grain bulk with hot spot was uneven distribution of moisture content. The grain within a hot spot and its surrounding area could be divided into three regions based on its moisture content: "damp" (about 17%); "tough" (14.6 to 17%); and "dry" (below 14.6%). The fully matured hot spot made up of tough and damp layers had the shape of a mushroom. In general, the grain temperature increased with the increase in depth of the hot spot. The maximum temperature in the hot spot was found immediately below the surface of sprouting grain. In hot spot locations, the temperature gradient was as high as 20°C per 0.31 m. The difference between the maximum temperature in the hot spot and the

temperature of surrounding cool grain was in the range of 12 to 48°C in different granaries.

Sinha and Wallace (1965) described the ecology of fungus-induced hot spot. Two identical bins were filled with 13.5 t of hard red spring wheat at 14% moisture content to a depth of 1.8 m. In one of the experimental bins, 25 kg of high moisture wheat (23%) was introduced at 0.6 m below the top surface of the grain and the other bin was kept as a control. The temperature profile and moisture content at various locations were measured in both bins during five winter months in Manitoba. Microorganisms started appearing after introducing the damp grain in the treated bin, and the temperature increased rapidly. The temperature of hot spot reached a maximum of 64°C in three months, and then cooled down immediately in two weeks. The probable reasons for heating between 55 and 64°C were due to the action of bacteria and biochemical activity, as fungi could not grow above 55°C.

Periodic inspection is essential to monitor temperature and moisture content of the grain bulk. Slight rise in temperature on the surface of the bulk indicates that some spoilage is occurring inside the bulk, because grain is a good insulator (Malvik 2002). Immediate care should be taken to find out the location and size of the hot spot, and damaged grain should be removed from the storage bin.

2.4 Identification of Wheat Classes

Wheat class is determined by hardness (hardness versus softness), color (red versus white), and growth habit (spring versus winter) whereas, varieties represent different breeding lines within a class. As each class of wheat is used for a specific purpose, mixing of classes at any stage in handling operations is not allowed.

In North America, identification of wheat classes and varieties is routinely performed as part of the grading system. Varieties which are unregistered in Canada are not eligible for top quality Canadian wheat grades and little contamination is allowed in other grades (Lookhart et al. 1995). In some situations, primary elevator managers and grain inspectors have difficulties in identifying unregistered varieties and this can lead to serious quality deficiencies. Biochemical identification procedures are used to supplement the visual inspection by grain inspectors. In Canada, polyacrylamide gel electrophoresis (PAGE) and high performance liquid chromatography (HPLC) are two common methods used for the measurement of variety specific-proteins in the laboratory (Canadian Grain Commission 2005a). In the PAGE method, the identification of wheat varieties is carried out based on their gliadin protein fingerprint. The protein finger print of the testing material is compared with the reference catalog. Similar to PAGE in the HPLC method, varieties are identitified by grain protein composition with the additional advantage of automatic data acquisition (Wrigley and Batey 1995). Because of the similarity in genetic background, some registered varieties cannot be distinguished from each other by the above methods (Lookhart et al. 1995).

In routine grain handling operations most of the grading factors such as soundness, vitreousness, varietal purity, and foreign materials are measured by human inspection. This subjective method of inspection leads to error in several circumstances (Majumdar and Jayas 2000a). A reliable and rapid method is required for online testing of wheat classes and varieties.

Neuman et al. (1987) developed algorithms to discriminate Canadian wheat classes and varieties by digital image analysis using shape features and Fourier

descriptors of kernel perimeter for whole grain. They obtained perfect classification for sound and mature kernels of Canada western red spring (CWRS) and Canada western amber durum (CWAD) in admixture with wheat of other classes. However, significant confusion existed among Canada western red winter (CWRW), Canada western soft white spring (CWSWS), Canada prairie spring (CPS) and Canada utility (CU) classes. While classifying different varieties into corresponding classes, the accuracy was between 2.1 and 100%. The accuracy was in the range of 15 to 96% for the identification of different varieties of wheat within a class.

Zayas et al. (1986) investigated the capability of digital image analysis methods to identify three classes of wheat from the USA (hard red winter (HRW), soft red winter (SRW) and hard red spring (HRS)) and their varieties. They used kernel length, width, length ratio, tangent, sine and length of arc of parabolic segment for classification. The average of correctly classified kernels were 85% for the training set and 83% for the experimental set while mixing three varieties of either HRW or SRW wheat. Whereas for the mixture of two varieties from either HRW or HRS wheat, the average classification accuracy was 78% for calibration samples and 77% for test samples.

Neuman et al. (1989) identified three Canadian wheat classes (HRS, CWAD and CWSWS) using color, and achieved 62 to 76% accuracy. Myers and Edsall (1989) classified five wheat varieties from Australia using size and shape features and achieved 44 to 96% classification accuracy. Almost all published papers used kernel morphological features for class and variety identification. Varieties in different classes of Canadian wheat tend to be relatively uniform in kernel type because of the limited genetic resources used by the breeders (Sapirstein 1995). Hence the classification

efficiencies of imaging methods are poor and inconsistent. It would be highly desirable to have an alternative method for online classification of wheat classes and varieties, which may use some characteristics of the kernels other than morphological features (Lookhart et al. 1995).

2.5 Infestation Detection Methods

Around 10 to 30% of the produced grain in the world is lost every year, and most of its results from the invasion of the grain mass by moulds, insects and rodents (White 1995). Many countries have started setting limits for live and dead insects in grain and flour before buying or selling. In the United Stated of America, the presence of 2 live insects in 1000 g of representative sample indicates that the wheat is infested (United States Department of Agriculture 2004). But Canada has set zero tolerance for live insects in wheat for both export and domestic markets. For wheat flour, the United States Food and Drug Administration (FDA) has established a defect action level of 75 insect fragments per 50 g of flour (Perez et al. 2003). Whereas the acceptable concentration of insect fragments is 10 per 50 g of wheat flour in Canada (Health Canada 1999). It is becoming important to detect the insects at all life stages in grain handling facilities and take control measures before they start multiplying. Several techniques have been developed to detect live and dead insects in grain.

Probe traps are cylindrical tubes with perforations in the upper section through which insects drop into the trap. These traps have a pointed tip for easy insertion into the grain. Traps must be removed from the grain bin and inspected periodically to determine the number and kind of insects that have been captured (White et al. 1990). A brass probe trap developed by Loschiavo and Atkinson (1967) for detecting insects in stored grain

has been redesigned several times using newer and less expensive plastic materials (White et al. 1990). White and Loschiavo (1986) developed a stacked version of the probe trap for investigating insect activity at different grain depths. Epsky and Shuman (2001) developed an electronic grain probe insect counter (EGPIC) to provide automated real time monitoring of insects. EGPIC used infrared beam sensors to count insects quickly and record the time of day as they dropped through the probe trap. Whenever an insect falls into the trap, an electronic count is generated. They used *Cryptolestes ferrugineus*, *Oryzaephilus surinamensis* (L.) and *Tribolium castaneum* insects to test the counting accuracy of the developed system. The counting accuracy was directly proportional to the size of the insects and it was 93.6% for the smallest insect (*C. ferrugineus*) and 99.5% for the largest insect (*T. castaneum*). Interpretation of trap catch is difficult because many factors (insect species, grain moisture content, temperature and relative humidity) influence trap catch. Trap catch also increased proportionally with an increase in trapping duration (Fargo et al. 1989).

Insect infestation in a grain silo can be detected acoustically by amplification and filtering the sounds produced by their movement and feeding. Hagstrum et al. (1988) determined that sounds of the lesser grain borer (*R. dominica*) larvae can be used to estimate larval population densities without removing grain samples. Shuman (2003) developed an automated system with acoustic sensors to detect insect infestation in 135 kg wheat in the laboratory. Acoustical sensors detected infestation by *T. castaneum*, *R. dominica* (F.) and *S. oryzae* (L.), but could not detect smaller insects such as *C. ferrugineus* and *O. surinamensis.*

Ridgway et al. (2002) developed a rapid machine vision method to detect insects (adult beetles), rodent droppings and ergot in bulk grains. Freshly killed insects (*O. surinamensis, S. granarius, T. castaneum, R. dominica, C. ferrugineus* and *Ahasverus advena* (Waltl)) and other contaminants were dropped at random locations within the area of wheat sample (25 kernels, monolayer). A charge coupled device (CCD) camera (256×256 pixels) was used to capture the artificially prepared wheat samples. The images were analyzed using various image processing algorithms to identify insects and other contaminants. Identification accuracy was 93, 87 and 98 to 99% for insects, ergots and rodent droppings, respectively. Zayas and Flinn (1998) investigated the application of machine vision to detect adult insects (*R. dominica*) in bulk wheat samples. A CCD camera (1488×1180 pixels) was used to take the images of the bulk wheat samples, and the images were analyzed using multi-spectral analysis and pattern recognition techniques. The position of the insect (ventral, dorsal, and side) and the adhering particles affected the classification accuracy. The identification accuracy was more than 90% to detect *R. dominica* in bulk wheat.

Soft X-rays can be used as a non-destructive method to detect insect infestations in grain kernels. Karunakaran (2002) investigated the capability of soft X-ray (15 kV potential and 65 μA current) in detecting the infestation by several insects and achieved an identification accuracy of 84 to 98%. While detecting the infestation by *S. oryzae* in wheat kernels, Karunakaran et al. (2003) achieved an accuracy of more than 95% for the samples infested by larval stages and more than 99% for the samples infested by pupae and adults. The classification accuracy of a soft X-ray method to detect the infestation in wheat by larval stages of *T. castaneum* was more than 86% (Karunakaran et al. 2004a).

At present, the "Berlese funnel" method is commonly used by the Canadian Grain Commission to detect infestations, which takes 6 h to extract live insects. In this method, a grain sample is exposed to light and heat to stimulate the live insects. One kilogram of grain sample is taken in a funnel and heated with a 60 W bulb. A 2 mm mesh screen is placed at the bottom of the funnel to hold the grain but allow the insects to go through. A container, partially filled with water is placed at the bottom of the funnel to receive the insects when they come out of the grain (Canadian Grain Commission 2005b). The extraction efficiencies of this method were 34 to 44% for implanted larvae, 66 to 86% for free living larvae and 96% for adults of the rusty grain beetle (Minkevich et al. 2002). An alternative method is required to detect the early stages of hidden infestation inside grains.

As identified through this literature search there is a need to develop alternative methods for various applications in grain handling activities. Therefore, five related studies were conducted and results are reported in chapters 3 to 7. The studies were:

1. Non-uniformity of heating of barley, canola and wheat after microwave heating using a pilot-scale drier was studied. The temperature rise (mean surface temperature), the difference between maximum and minimum temperatures (ΔT), and the maximum temperature on the surface of the grain bulk were measured for barley and wheat at four moisture levels and for canola at five moisture levels.
2. Germination and free-fatty-acid values of wheat grains were analyzed for the samples collected from the high temperature (caused due to the non-uniformity of microwave heating) and normal temperature regions after microwave treatment using a pilot-scale dryer.

3. The capability of a thermal imaging technique to detect a hot spot placed at various locations inside an experimental silo filled with barley was studied. The effect of wind and cold weather on the detection accuracies was also determined.
4. An infrared thermal imaging system was developed to identify eight western Canadian wheat classes (at 14% m.c. wet basis) by bulk sample analysis.
5. An infrared thermal imaging system was developed to identify the infestation inside wheat kernels by *Cryptolestes ferrugineus* at six developmental stages (four larval, pupal and adult).

3. NON-UNIFORMITY OF SURFACE TEMPERATURES OF GRAIN AFTER MICROWAVE TREATMENT IN A PILOT-SCALE MICROWAVE DRIER

3.1 Summary

In this study, temperature rise and non-uniformity of heating of grain with different moisture contents after microwave treatment were investigated. The temperature anomalies after microwave treatment were measured for barley and wheat at four moisture levels (12, 15, 18, and 21% wet basis) and for canola at five moisture levels (8, 12, 15, 18, and 21% wet basis). Fifty grams of grain samples were heated in a continuous-type pilot-scale microwave drier (2450 MHz) at five power levels (100, 200, 300, 400, and 500W) and two exposure times (28 and 56 s). Grain samples were thermally imaged using an infrared thermal camera as soon as they came out from the microwave chamber. Average, maximum, and minimum temperatures were extracted from each thermal image and the difference between maximum and minimum temperatures (ΔT) was calculated. The grain type had a significant effect on the surface temperatures after microwave treatment. The surface temperatures increased with microwave power and exposure time but decreased with moisture content. The average surface temperatures after microwave treatment were between 72.5 and 117.5°C, 65.9 and 97.5°C, and 73.4 and 108.8°C for barley, canola and wheat, respectively, when the applied microwave power was 500 W. At the same power level, the maximum surface temperature was between 100.3 and 140.0°C, 77.8 and 117.7°C, and 98.3 and 130.9°C for barley, canola, and wheat, respectively. Non-uniform heating patterns were observed for all three grain types at all moisture contents, power levels, and exposure times. The ΔT was in the range of 7.2 to 78.9°C, 3.4 to 59.2°C, and 9.7 to 72.8°C for barley, canola, and

wheat, respectively. The location of hot and cold spots may vary in different driers based on the position of magnetron and other components, but an almost similar non-uniform heating pattern is expected in all microwave driers. Therefore, this non-uniformity must be taken into consideration while developing microwave processing systems for grains.

3.2 Introduction

In conventional hot air drying, the drying process begins at the surface of the grain and then proceeds inside. As a result of this process, hardening, splits, and cracks may develop on the surface of the kernel. In addition to this damage, diffusion of moisture near the surface may be restricted because of the reduced permeability of the outer layer (John and Otten 1989). Hence, the drying process will be less effective during the final stage in conventional drying (Gunasekaran 1990). But in microwave drying, heat generation takes place within and throughout the kernel. Therefore, a positive temperature gradient and outward moisture driving potential will be created, leading to a faster heating rate and shorter processing time (John and Otten 1989; Gunasekaran 1990; Oliveira and Franca 2002). The capabilities of microwaves for drying of grains and oilseeds have been investigated by several researchers (Nelson 1987; Velupillai et al. 1989; Shivhare et al. 1992a, 1992b, 1992c; Adu and Otten 1996). Thin-layer drying of peanuts using microwaves (2450 MHz and 250 to 1000 W) revealed that the drying rate was higher in microwave drying and it was 10 to 94 times the rate of conventional drying for pods and 8 to 32 times for kernels. After microwave drying, the external damage to the kernels was less but significant uneven drying and shrinkage were observed in 10% of the samples during the internal inspection of kernels (John and Otten 1989). Parboiled rice can be dried using a microwave-vacuum method with the same finished product

quality as from conventional drying (Velupillai et al. 1989). During a study on the drying behavior of corn study by Gunasekaran (1990), about 25 g samples were placed in a glass dish (single layer of kernels) and dried in an experimental microwave oven (250 W) with continuous and pulsed mode microwave applications. The power-on time in the pulsed mode was 10 and 15 s and power-off time ranged from 20 to 75 s. The drying was more rapid in the continuous mode and with longer power-on time in the pulsed mode.

Microwaves can also be used as a non-chemical insect control method (Baker et al. 1956; Hurlock et al. 1979). As microwaves have high penetration capacity through grain, more uniform drying and efficient insect control could simultaneously be achieved (Boulanger et al. 1969). The capability of microwaves for inactivating the fungus *Fusarium graminearum* Schwabe in wheat was studied by Reddy et al. (1998). The eradication of the pathogen increased with the total microwave energy; however, seed viability and seedling vigour decreased accordingly. Watters (1976) used microwaves to kill *Tribolium confusum* J. duVal in wheat and flour. It was determined that the mortality was high with an increase in microwave exposure time and increase in moisture content of the wheat, and higher in wheat than in flour. The mortality of *T. confusum* was 70% at 55°C and 100% at 65°C when microwaves were used for disinfestations (Hamid and Boulanger 1969). While using an industrial microwave system (2.45 GHz), Vadivambal et al. (2005) obtained 45, 58, 85, and 100% mortality for *T. castaneum* (Herbst) at 250, 300, 400, and 500 W, respectively.

Although grain drying by microwaves is faster than conventional drying, process optimization with respect to energy efficiency and final product quality yet has to be achieved (Shivhare et al. 1992a). Un-even heating is the major problem in microwave

cooking or heating of any agricultural and food product. Even though uniform heating is expected within a kernel during grain drying by microwaves, the sinusoidal wave pattern of microwaves develops hot and cold spots on the bulk grain sample (Vadivambal et al. 2005). Grain temperature is the most crucial factor than air temperature during grain drying and the former should not go beyond 60°C at any point of time (Okazaki and Ishihara 1980). In microwave drying, the quality of the grain that is present in the hot spot regions may be severely affected due to the elevated temperature. Similarly, during grain disinfestation by microwaves, the insects have the ability to identify the cold spot and escape from the high temperature. To achieve 100% mortality, the power level should be selected in such a way that the minimum temperature generated at that power should be able to kill the insects.

Knowledge of temperature rise and non-uniformity of temperature when microwaves are used for heating grains at different moisture contents would be helpful to select power level and treatment time while developing microwave systems for various applications in the grain industry. Furthermore, the heating behavior of each grain type should be clearly understood before using this technology because the microwave heating pattern depends on various factors of food such as size, shape and ingredients. (Fakhouri and Ramaswamy 1993). In most of the published reports on heating patterns of microwave ovens, thermocouples and fiber-optic probes were placed at some locations in the food materials to measure the temperature. In these methods, measurements were taken at single points; therefore, it may not be possible to determine the actual non-uniformity pattern. Furthermore, we could not find any published result on non-uniformity of heating pattern for grains. In this study, an infrared thermal camera was

used to take thermal images and measure the surface temperatures of grains. The objectives of this research were (a) to determine the average surface temperatures of barley, canola and wheat samples after microwave treatment, (b) to determine the maximum temperature on the surface of barley, canola and wheat samples after microwave treatment, and (c) to determine the non-uniformity of heating (difference between maximum and minimum temperatures) on the surface of barley, canola, and wheat samples after microwave treatment.

3.3 Materials and Methods

A continuous type pilot-scale microwave drier operated at 230 VAC, 60 Hz, 23 A, (Model No: P24YKA03, Industrial Microwave Systems, Morrisville, NC) was used in this study. The microwave drier consisted of a conveyer belt assembly, microwave applicator, fan, and a control panel (Fig. 3.1). The speed of the conveyor and the power output of the microwave generator could be adjusted to the desired level. The fan was set on at all time during the experiments and the air inlet temperature was set at 30°C.

The non-uniformity of heating was investigated for wheat and barley at four moisture contents (12, 15, 18, and 21% wet basis) and for canola at five moisture contents (8, 12, 15, 18, and 21% wet basis). Microwave treatment was given to the grain at five power levels (100, 200, 300, 400, and 500 W) and two exposure times (28 and 56 s). Canadian hard red spring (HRS) class wheat and commercial grade canola and barley were obtained from the Cereal Research Centre, Agriculture and Agri-Food Canada, Winnipeg, and used in this research. The length of major and minor axes of kernels was 8.79±0.16 and 3.52±0.07 mm, and 6.68±0.16 and 3.36±0.13 mm for barley and wheat, respectively,

and the diameter of the canola seed was 1.78±0.13 mm (measured by a vernier caliper, n = 20).

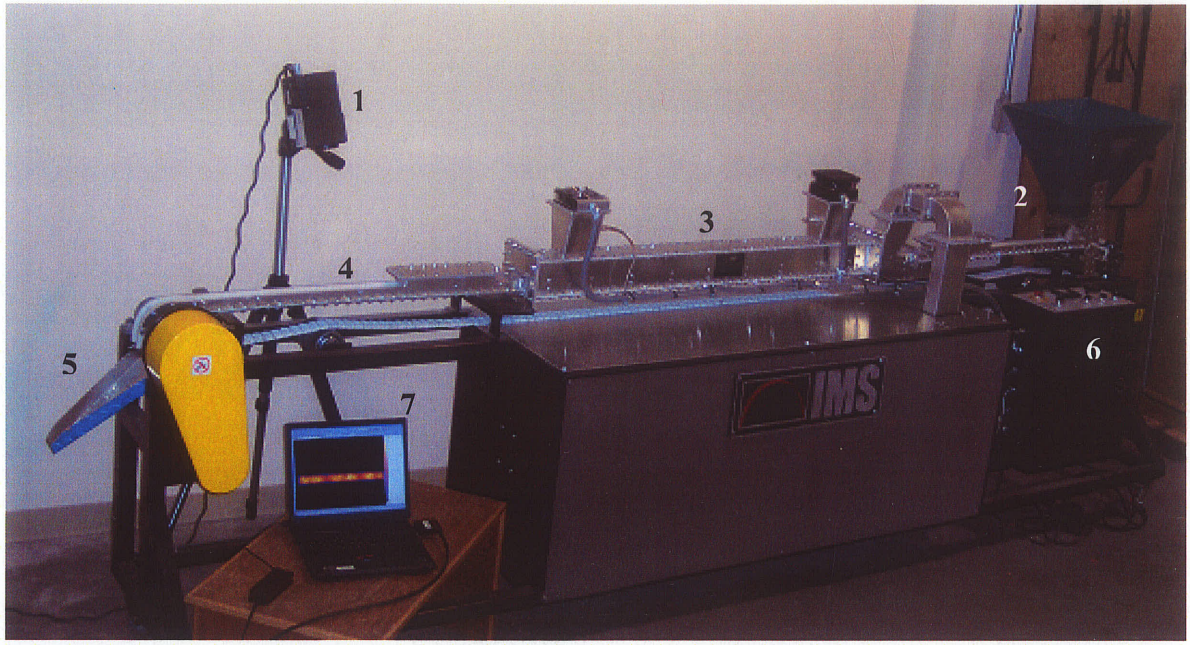

1. thermal camera 2. grain inlet 3. microwave chamber 4. conveyor 5. grain outlet chute 6. control panel 7. data acquisition system

Figure 3.1 Experimental setup of microwave drier and thermal camera to study non-uniformity of heating in grain.

In each experiment, a 50 g sample was spread on the conveyor (top surface was made flat) and allowed to enter the chamber where the grain was subjected to microwave treatment. The approximate volume of the grain sample on the conveyor during treatment was 300×30×10 mm (length of the belt×width of the belt × depth of grain on the belt). Two microwave exposure times were achieved by changing the speed of the conveyor.

An un-cooled focal planar array type infrared thermal camera with 320×240 pixels was used to take thermal images of the microwave heated grain (Model: ThermaCAM ™ SC500 of FLIR systems, Burlington, ON, Canada; spectral range: 7.5 to

13.0 μm). Images were taken as soon as the grain samples came out from the chamber. The field of view of the infrared lens was $24^{\circ}\times18^{\circ}$ and the thermal sensitivity of the camera was 0.07°C at 30°C. While taking thermal images, the emissivity (ϵ) of the grain was set as 0.98 in all the experiments. The camera was fixed at 60 cm above the grain. With three replications, five power levels, two exposure times, and four moisture contents for barley and wheat and five moisture contents for canola, a total of 390 (3×5×2×4×2+3×5×2×5×1) thermal images were taken and analyzed.

From each thermal image, average, maximum, and minimum temperatures were extracted using ThermaCAM Researcher 2001 software (FLIR systems, Burlington, ON, Canada) and then the difference between maximum and minimum temperatures (ΔT) on the surface of the grain was also calculated for each thermal image. The temperature details within the region of interest on a thermal image were obtained using the area tool option available in the software (Fig. 3.2). Since the fan was set on all the time throughout the experiments, both ends of the sample were slightly displaced from the original position when it came out from the microwave chamber. Therefore, during the data extraction process, the area was selected in such a way that the selected region was completely filled with grains.

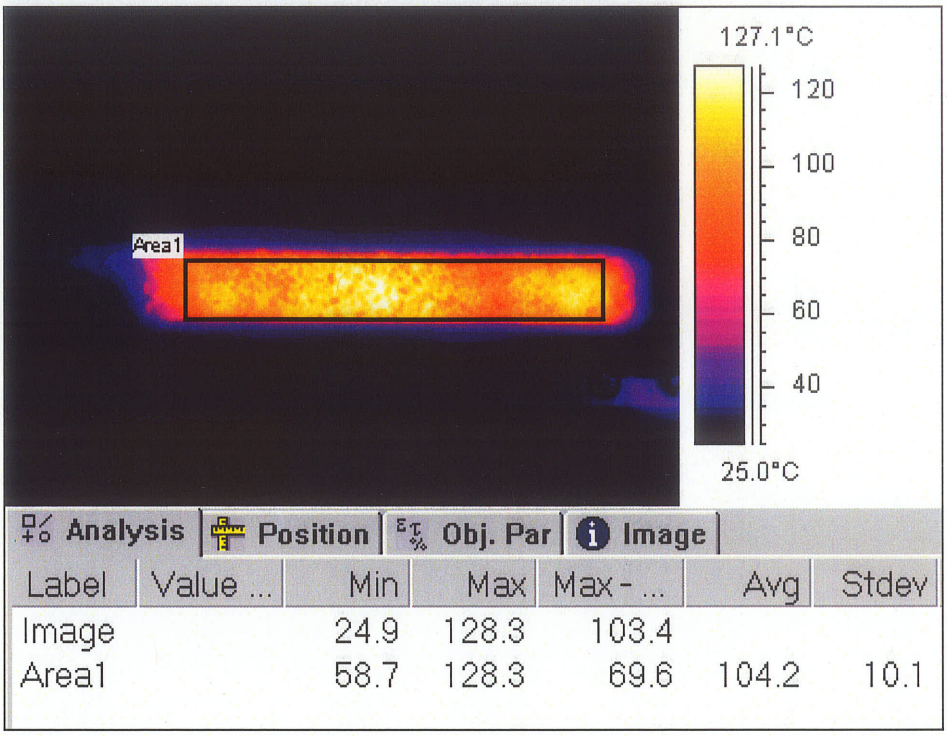

Figure 3.2 Data extraction method from a selected region ('Area 1' in this image) of a thermal image.

3.3.1 Statistical analysis

The effect of moisture content, microwave power, and exposure time on the average surface temperature, maximum temperature, and ΔT for each grain type, was studied by analysis of variance (ANOVA) using a three factorial design model (4 moisture content × 5 power × 2 exposure time). Similarly, the effect of different grain types on surface temperatures at each moisture level was analyzed using a three factorial design model (3 grains × 5 power × 2 exposure time). In both analyses, the differences within the levels under each variable were tested at 95% confidence interval (type I error, $\alpha = 0.05$) using the least significant difference (LSD) method of comparison of means. General linear models (GLM) procedure in Statistical Analysis System software (SAS, version 9.1, SAS Institute, Inc., Cary, NC) was used for all the above-mentioned statistical tests.

3.4 Results and Discussion

Non-uniform heating patterns were observed for all three grain types at all moisture contents, power levels, and exposure times. Figure 3.3 explains the temperature profiles of grains after microwave treatment. In general, hot and cold regions appeared alternatively in each image, however there was no regular pattern observed. The size and locations of hot and cold regions varied in the replications. The final moisture content of the samples was not measured; however, it was assumed that applied microwave energy was used mainly to raise the grain temperature and a small quantity of moisture might have been removed because of the short exposure time (<60 s). Fanslow and Saul (1971) determined that moisture removal was small in the first 60 s during microwave drying of corn. They also reported that around 31 to 56% of microwave power was consumed for moisture removal and the remaining power served to raise the temperature of the grain and air.

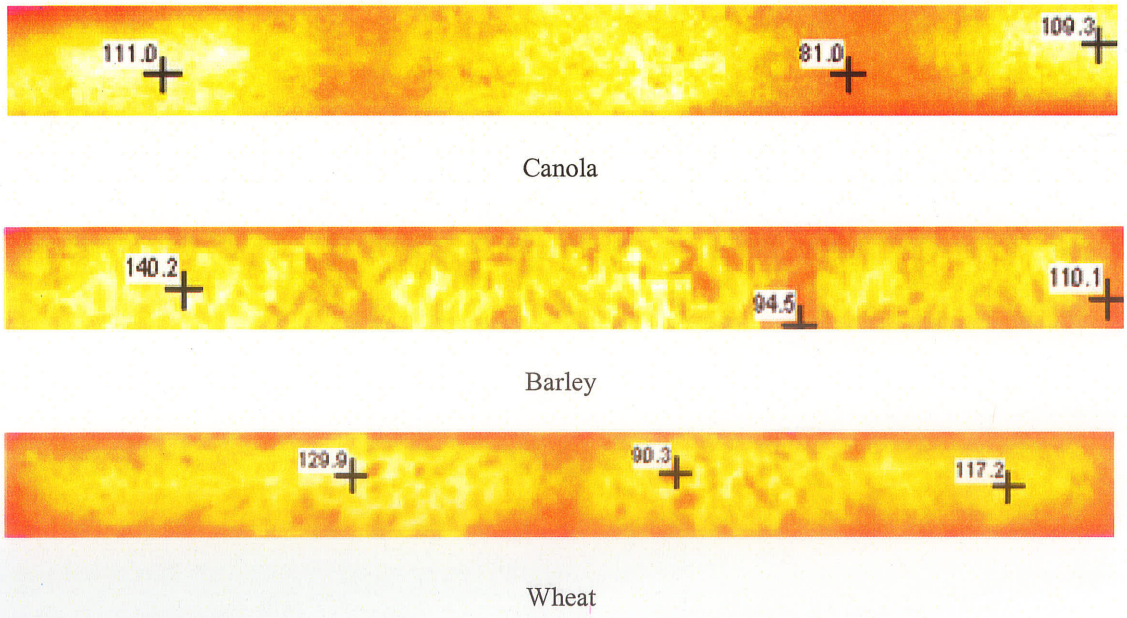

Figure 3.3 Thermograms of grains (12% MC wet basis) after microwave treatment (500 W, 56 s exposure) (values are temperature in °C at the pointed locations)

3.4.1 Effect of power and moisture content on ΔT

The difference between maximum and minimum temperatures (ΔT) on the surface of barley, canola and wheat after microwave treatment is given in Fig. 3.4. When the applied microwave power and exposure time were 500 W and 28 s, the ΔT was in the range of 55.5 to 67.8°C, 57.7 to 69.4°C, and 25.9 to 40.1°C for wheat, barley, and canola, respectively. Similarly, when the exposure time was increased to 56 s at 500 W, the ΔT was in the range of 62.9 to 69.5°C, 64.3 to 75.6°C, and 39.5 to 59.2°C for wheat, barley, and canola, respectively. Since the value of ΔT is very large, for disinfestation applications, the power and exposure time should be selected in such a way that the minimum temperature must be the lethal temperature to the target insects. Among the tested three grains, the ΔT was lower for canola at all moisture contents, microwave powers, and exposure times, which means relatively more even heating occurred in canola than in wheat and barley after microwave treatment. This may be due to the spherical shape (more surface area exposed to microwaves) and small size of canola as opposed to the other two grain types. Oliveira and Franca (2002) also reported that microwave heating is significantly dependent on sample size and shape. Fakhouri and Ramaswamy (1993) stated that temperature uniformity in food materials was dependent on product composition; higher fat content improved the temperature uniformity and the protein content had the opposite effect. Higher temperature differences were also observed in other food products while heating in domestic microwave ovens. Burfoot et al. (1988) measured the ΔT up to 66°C in packs of spaghetti bolognaise after heating in a domestic microwave oven (2450 MHz).

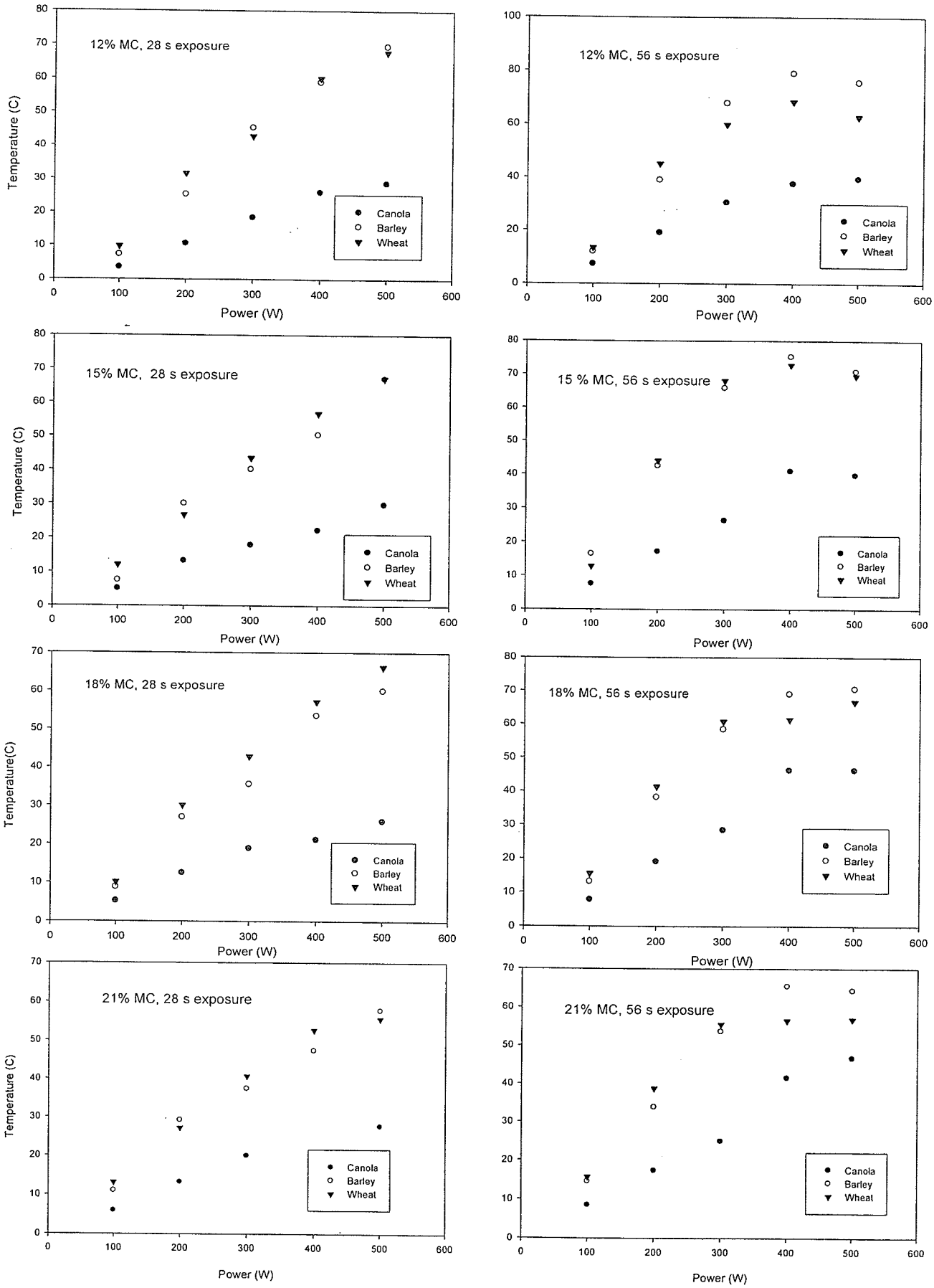

gure 3.4 Difference between maximum and minimum temperatures (ΔT) on the surface of grains with different moisture contents after microwave treatment.

At each moisture level, grain type had a significant effect on ΔT; however, there were no significant differences on ΔT between wheat and barley except at 18% moisture content. At 18% moisture content, the ΔT for each grain type was significantly different from each other. In general, at all moisture levels, the ΔT was higher at higher power levels for all grain types. The ΔT was significantly higher when the grain was exposed to microwaves for 56 s than 28 s, for all three grain types. Similarly, the effect of moisture content on ΔT was significant for all three grain types. However, there were no significant differences in ΔT between 12 and 15% moisture levels in barley, between 12 and 15%, and 12 and 18% in wheat, and 12 and 15 and 18 and 21% in canola.

3.4.2 Effect of power and moisture content on maximum temperature

To retain the original quality, the grain temperature should not exceed the critical limit while drying or processing. The temperature of wheat or flour should not go beyond 50°C at any stage in milling (Myl Subramaniam, Personal communication, Technical Specialist - Milling Technology, Canadian International Grains Institute (CIGI), Winnipeg, Manitoba, Canada). Hence, in grain drying by microwaves, the maximum temperature will be the crucial factor in determining the quality deterioration of the grain. The maximum temperature on the surface of grains after exposing to microwaves is shown in Fig. 3.5. When the wheat samples were exposed to 500 W for 56 s, the maximum temperature was 130.9, 126.4, 117.2, and 108°C at 12, 15, 18 and 21% moisture contents, respectively, and when the exposure time was reduced to 28 s, it was 117.6, 114.2, 107.6, and 98.3°C at 12, 15, 18, and 21% moisture contents, respectively.

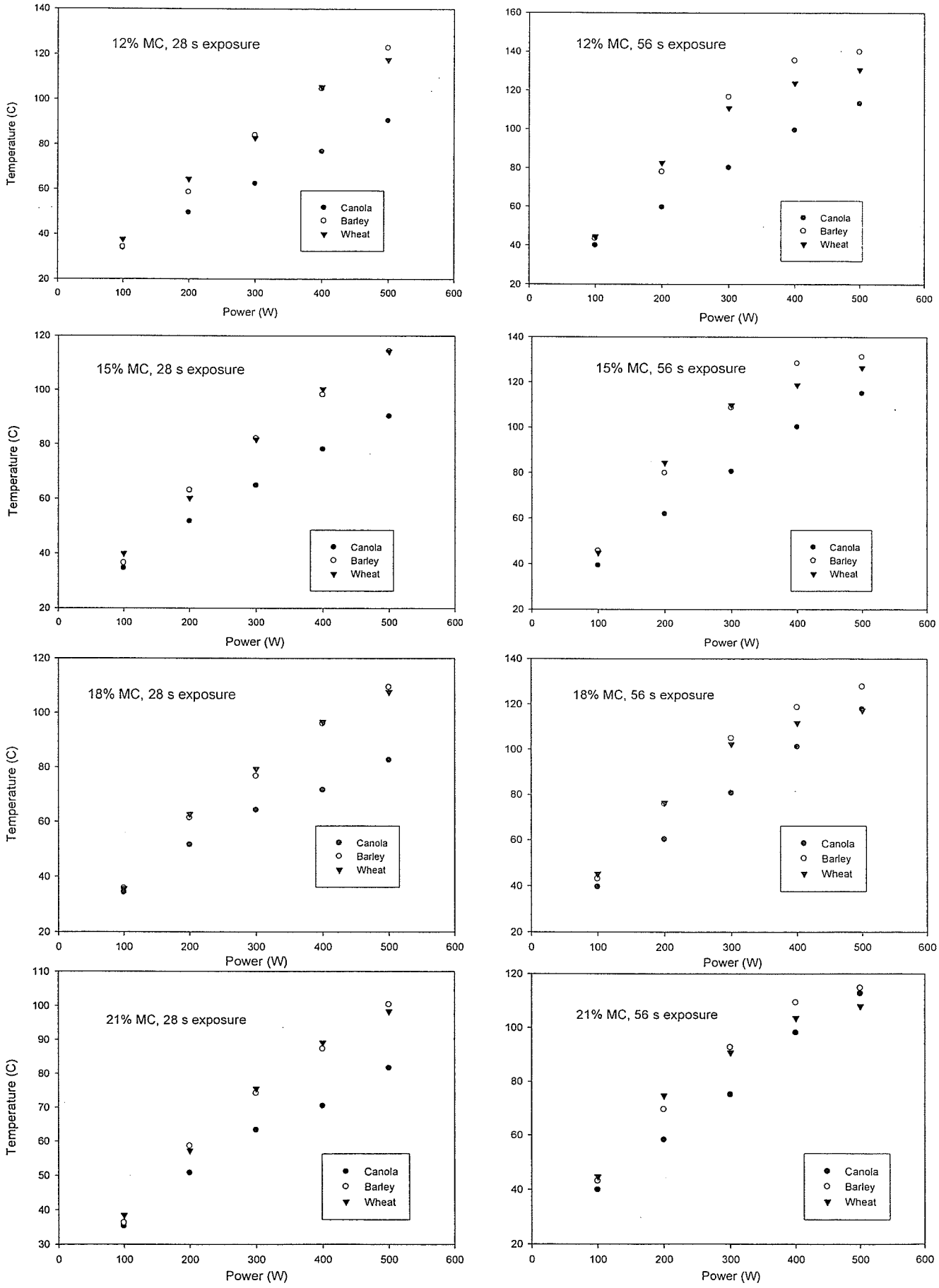

Figure 3.5 **Maximum temperature of grains with different moisture contents after microwave treatment.**

Similarly, when the barley was exposed to 500 W for 56 s, the maximum temperature was 140, 131.2, 127.6, and 114.7°C at 12, 15, 18, and 21% moisture contents, respectively, and 122.8, 114.3, 109.4, and 100.3°C at 12, 15, 18, and 21% moisture contents, respectively, when it was exposed for 28 s. The maximum temperature of canola was 110, 113.3, 115, 118, and 112.6°C at 8, 12, 15, 18, and 21% moisture content, respectively, when 500 W was applied for 56 s and 77.8, 90.4, 90.2, 82.5, and 81.5°C at 8, 12, 15, 18, and 21% moisture content, respectively, when the same power was applied for 28 s.

At all moisture levels, grain type had a significant effect on the maximum temperature. However, there were no significant differences on the maximum temperature between barley and wheat at 15 and 21% moisture contents, whereas at 12 and 18% moisture levels, the maximum temperature of all three grain types was significantly different from each other. The maximum temperature of barley, canola, and wheat increased with microwave power and exposure time at all moisture levels. This confirms the results obtained by Borchers et al. (1972); they reported that the temperature increased with exposure time while treating soybeans by dielectric heating (43 MHz). In their experiment 180 g of soybeans attained 127 and 168°C after heating 0.83 and 2.0 min, respectively. The maximum temperature of barley and wheat decreased with increasing moisture content, and it was different in each moisture level. However, in canola, there were no significant differences on the maximum temperature between 12 and 18% moisture content.

3.4.3 Effect of power and moisture content on average temperature

The average surface temperatures of three grain types when exposed to different power levels are shown in Fig. 3.6.

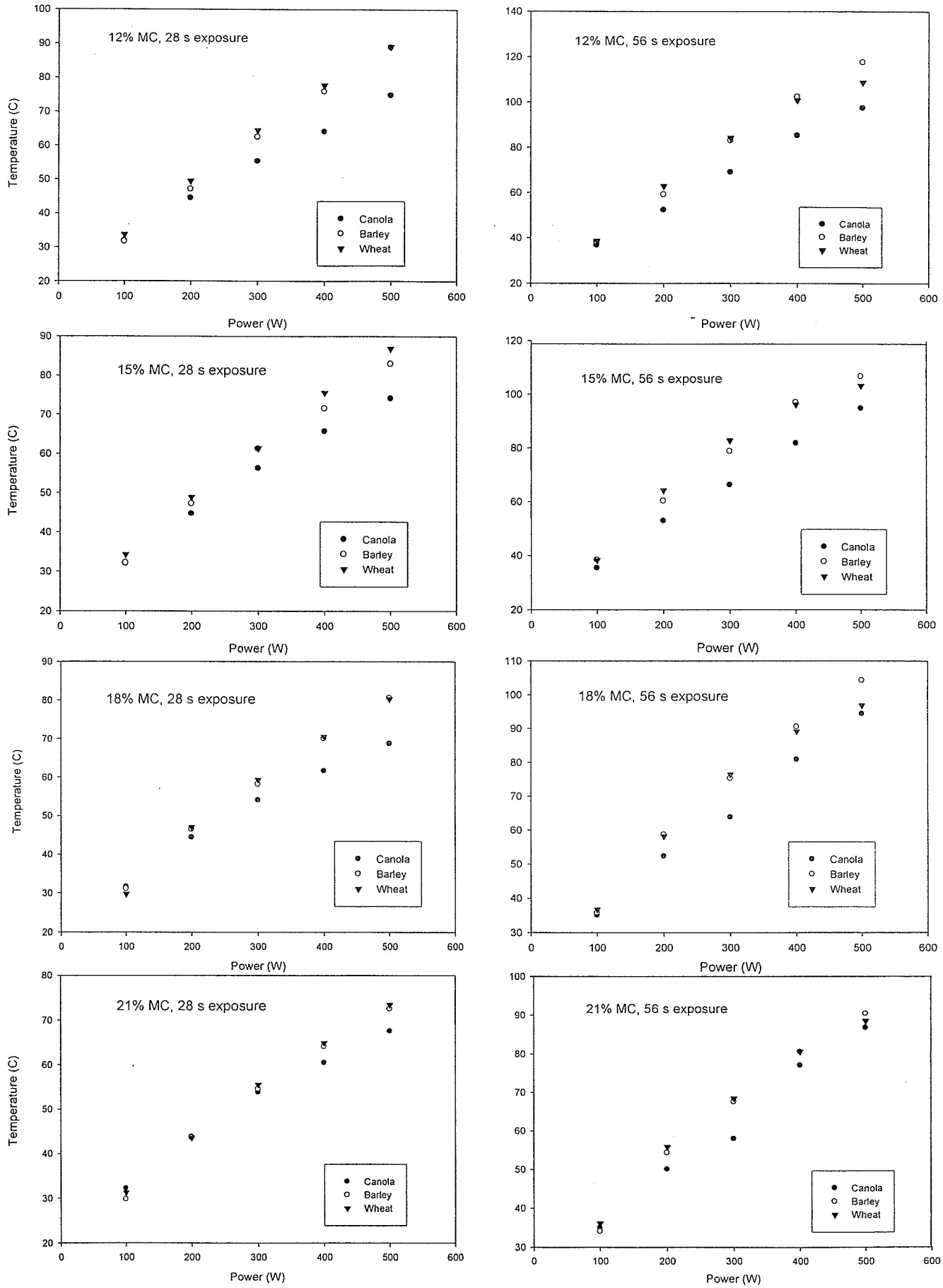

igure 3.6 Average temperature of grains with different moisture contents after microwave treatment.

When wheat was exposed to 500 W for 56 s, the average temperatures were 108.8, 103.1, 96.9, and 88.5°C for the grains with moisture content 12, 15, 18, and 21%, respectively. At the same conditions, the average surface temperatures for barley were 117.5, 106.6, 104.2, and 90.4°C and for canola were 97.5, 94.7, 94.1, and 86.7°C. The average surface temperature of canola was the lowest among the tested three grain types at all moisture, power, and exposure levels. This fact may be due to the presence of more oil content in canola.

Grain type had significant effect on the average temperature, and at all moisture levels, the average temperatures of all three grain types were significantly different from each other. The average temperature increased with microwave power and exposure time for all three grain types. This was in agreement with the results reported by Shivhare et al. (1992b); the temperature of the kernel and drying rate increased with microwave power level while drying corn using microwaves. In our study, the average temperature of barley and wheat decreased with increasing moisture content. When the amount of moisture present in the grain is low, the temperature rise will be more due to the volumetric heating. The same results were also obtained by Nelson (1976); while alfalfa seeds with different moisture contents were treated to radio frequency (RF), the final temperature increased with decreasing moisture content and ranged from 49°C for the highest moisture content to 110°C for extremely dry seeds. Therefore, while developing microwave treatment systems for low moisture grains, the temperature rise should be given top priority in selecting the power and exposure time in order to avoid adverse effect on the quality due to elevated temperature.

Shivhare et al. (1992b) reported that drying rate increased with power level while drying corn using microwaves. Even though a higher power level may lead to a faster drying rate, the quality deterioration due to increased temperature should be considered when developing microwave grain drying systems. However, for some other agricultural materials, quality degradation due to temperature may not be significant. For instance, while drying parsley leaves using microwaves, Soysal (2004) determined that when working at 900 W instead of 360 W, the drying time was reduced by 64% with a good quality product. Another way to maximize the drying rate is by selecting the right combination of microwave power-on and power-off times. Since power-off time provides the rest time required for moisture redistribution within the kernels making it available throughout the grain mass in the subsequent power-on time, therefore the drying would be more efficient (Gunasekaran 1990). Shivhare et al. (1992c) also stated that the time required for drying increased with intermittent operation but that the total duration of power application was less than for drying in the continuous mode.

Many researchers have suggested various methods to minimize the non-uniformity of temperature during microwave treatment of agricultural materials. In a simulation study, Oliveira and Franca (2002) reported that an on-off operating system coupled with sample rotation could produce more uniform heating. A pulsed supply of microwave energy which was combined with a continuous flow of air over the material being dried will avoid over-heating of the product and offers an effective use of the applied energy (Gunasekaran 1990). Fanslow and Saul (1971) reported that popping and cracking damage to corn during microwave drying was due to rapid heating, and suggested that air should be used at a higher flow rate to cool the grain and prevent

damage. During grain drying by microwaves, the temperature of the kernel can be reduced by 20 to 30°C by passing air over it at different flow rates (Fanslow and Saul 1971). Despite several recommendations available to reduce temperature anomalies during microwave treatments, there is no published work on a microwave grain drying system with uniform heating to retain the original quality of grains. The location of hot and cold regions may vary in different driers based on the position of magnetron and other components, but almost similar non-uniform heating pattern is expected in all microwave driers. Therefore, this non-uniformity must be taken into consideration while developing microwave systems for grains. Innovative methods must be tried to minimize the temperature variations on the grain during microwave treatments. While developing systems for heating and drying of grains without deteriorating its original quality by maintaining uniform grain temperature, microwaves have great potential for use in the grain industry.

3.5 Acknowledgements

We thank the Canada Research Chairs Program and the Natural Sciences and Engineering Research Council of Canada (NSERC) for their financial assistance and Ms. G. Sathya and Ms. R. Vadivambal for their help in sample preparation and data extraction processes.

4. GERMINATION AND FREE-FATTY-ACID VALUES OF WHEAT GRAINS FROM HIGH TEMPERATURE AND NORMAL TEMPERATURE REGIONS AFTER MICROWAVE TREATMENT IN A PILOT-SCALE MICROWAVE DRIER

4.1 Summary

Various quality changes of grain after microwave treatment have been reported by several researchers, however the actual reason for these changes is not fully understood. Non-uniformity of heating pattern produces hot spots (localized elevated temperature region) on the grain surface that may be one of the important factors which will determine the quality changes in the grain during microwave treatment. The objective of this research was to determine the germination percentage and fat acidity value (FAV) of wheat samples collected from high temperature and normal temperature regions after microwave treatment. Canada hard red spring wheat samples at four moisture levels (12, 15, 18 and 21% wet basis) were subjected to microwave treatment at five power levels (100, 200, 300, 400 and 500 W) and two exposure times (28 and 56 s) in a continuous type, pilot-scale microwave drier. After microwave treatment, the samples were collected from the high temperature and normal temperature regions by viewing the live thermal images on the monitor of the data-acquisition computer of a thermal-imaging system. At all moisture and power levels, germination percentages were significantly (α=0.05) lower for samples collected from high temperature regions than those from the normal temperature regions. Almost all seeds in the high temperature region became non-germinated seeds at 500 W for 28 s exposure whereas at the same conditions, 4 to 33% germination was observed for samples collected from the normal temperature region. The germination percentage was close to zero at 300 W for the samples collected from the high temperature region, when the exposure time was increased to 56 s and the initial

moisture content was 18 and 21%. At 400 and 500 W power, and 56 s exposure, the germination percentage was almost zero for samples collected from both high temperature and normal temperature regions. The FAV was significantly different for the samples collected from the high temperature and normal temperature regions. An irregular pattern of FAV was observed at different power levels and moisture contents. In general, the FAV increased with moisture content after microwave treatment.

4.2 Introduction

When any food material is subjected to microwave treatment, heat is produced due to molecular friction resulting from dipolar rotation of polar molecules (mainly water molecules) and from conducive migration of dissolved ions (Oliveira and Franca 2002). This heat may be utilized for drying or to obtain other desired changes within the product. Several researchers have investigated potential uses of microwaves for drying and other applications in grains and oilseeds (Anthony 1983; Borchers et al. 1972; Campana et al. 1993; Nelson 1976). Borchers et al. (1972) reported that dielectric heat treatment improved the nutritive value of soybeans in less than two minutes. Microwave drying of rice and soybeans under partial vacuum improved the product quality (Gardner and Butler 1981 cited by Nelson 1987). Anthony (1983) determined that microwave and vacuum drying of cotton improved the marketing qualities of cotton seed oil. In some situations, microwave treatment can be used in combination with other applications. For example, the throughput of a continuous flow grain drier can be increased by pre-heating high moisture grain with a microwave heating system at the inlet (Radajewski et al. 1988). Kadlec et al. (2001) determined that the hot-air drying (80°C) of germinated

yellow pea, after microwave treatment, decreased the α-galactooligosaccharides content (desired quality change) and improved the nutritional quality.

Seed treatment is one of the important applications of microwaves in agricultural operations (Nelson 1987). Nelson and Stetson (1985) reviewed the germination responses of seeds to radio frequency (RF) dielectric treatment. Seed dormancy due to hard seed coats or causes of a biochemical nature may be overcome by microwave or RF treatment for a short time. Treatment time should be in the range of a few seconds to a minute based on the dielectric properties and moisture content of the seeds, and on the frequency and electric-field intensity. Dielectric-heat treatment has increased or accelerated the germination of small-seeded legumes (alfalfa, red clover, arrowleaf clover). Alfalfa-seed germination was improved by dielectric heating at frequencies of 5, 10, 39 and 2450 MHz when proper exposures were used (Nelson 1976). However, seeds of several vegetable and ornamental plants, grasses, and woody plants, not exhibiting dormancy, did not respond to RF-electric treatment on germination (Nelson and Stetson 1985).

Although microwaves have potential for many applications in the grain industry, its complete utilization is restricted because of the adverse effect on various quality parameters during treatment. Campana et al. (1993) investigated the effect of microwave drying (2450 MHz) on the physical, chemical and baking properties of wheat. Total protein content was not changed by microwave treatment but functionality was affected. The wet-gluten content was decreased with increasing microwave power. Baking quality of the wheat dough and loaf volume were decreased by the treatment. Walde et al. (2002) reported that microwave drying can reduce the power consumption in wheat milling industries, but is not suitable where the final products made from that flour need to be

soft in textural characteristics. Velu et al. (2006) determined that protein and starch content of maize were not affected after drying with microwaves. However, viscosity of the flour was decreased with increasing microwave drying time. Doty and Baker (1977) investigated the effect of microwave conditioning (625 W) of wheat on the effect of flour and wheat quality. It was reported that increased ash content, increased dough strength, decreased β-amylase activity, increased flour viscosity, decreased loaf volume and decreased external and internal loaf characteristics were the important degradation qualities due to microwave conditioning and that quality parameters were affected after 270 s of microwave conditioning. The effect of microwave radiation and storage on the quality of wheat flour was studied by MacArthur and Appolonia (1981) who reported that the total sugar content and starch intrinsic viscosity were decreased in the microwave-treated samples after storing for six months.

Although several quality changes of grains during microwave treatment have been measured by many researchers, the reason for the quality deterioration is not understood. Non-uniformity of heating during microwave treatment may be one reason for the quality deterioration of grains. The degradation in bread-making quality of microwave-treated wheat was similar to the effect produced by improper drying of grain (Hamid and Boulanger 1969).

Surface temperatures of wheat samples after microwave treatment are non-uniform (Manickavasagan et al. 2005). The difference between maximum and minimum temperatures (ΔT) was in the range of 56.8 to 69.5°C after grain was exposed to 500 W for 56 s. Investigations on quality deterioration of the grain samples in the high temperature and the remaining regions after microwave treatment would reveal the

causes of quality deterioration of bulk grain from microwave treatment. The objective of this research was to determine the germination percentage and fat acidity value (FAV) for wheat samples collected from the high temperature and normal temperature regions of bulk grain after microwave treatment.

4.3 Materials and Methods

A continuous type pilot-scale microwave drier operated at 230 VAC, 60 Hz, 23 A (Model No: P24YKA03, Industrial Microwave Systems, Morrisville, NC) was used in this study. The microwave drier consisted of a conveyer-belt assembly, microwave applicator, fan and a control panel. The speed of the conveyor and the power output of the microwave generator could be adjusted to the desired level. The fan was on at all times during the experiments and the air inlet temperature was set at 30°C.

Canada hard red spring wheat (obtained from the Cereal Research Centre, Agriculture and Agri-Food Canada, Winnipeg, Canada) was conditioned to four different moisture levels (12, 15, 18 and 21% wet basis) and used in this study. In each experiment, a 50 g sample was spread on the conveyor and the top surface was made flat. Then the grain was allowed to enter the chamber where it was subjected to microwave treatment. The approximate volume of the grain sample on the conveyor during treatment was 300×30×10 mm (length of the belt × width of the belt × depth of grain on the belt). Two microwave exposure times were achieved by changing the speed of the conveyor. Microwave treatment was given at five power levels (100, 200, 300, 400 and 500 W) and two exposure times (28 and 56 s). A thermal camera (Model: ThermaCAM ™ SC500 of FLIR systems, Burlington, ON, Canada; spectral range: 7.5 to 13.0 μm) was set to view the grain sample on the conveyor as soon as it came out from the microwave chamber

after treatment. Samples from the high temperature and normal temperature regions were collected using a spoon while viewing the live thermal images on the monitor of the data acquisition computer and the grain samples were stored in polyethylene bags separately for further analysis. The final moisture content after microwave treatment was measured for the high moisture (18 and 21%) wheat samples (bulk).

Germination tests and fat acidity values (FAV) analyses were conducted for the wheat samples collected from the high temperature and normal temperature regions. It was not possible to conduct baking quality tests since the quantity of sample collected from the high temperature region was small (about 10 to 15 g from 50 g of the microwave-treated sample). However, to detect quality degradation of grain due to high temperature, a germination test can be used because it is a sensitive, simple and reproducible test and the results are reasonably correlated with baking tests (Ghaly and Taylor 1982).

Wheat kernels (25 seeds) were placed on Whatman no. 3 filter paper in a 90 mm diameter Petri-dish saturated with 5.5 mL of distilled water. The Petri-dishes were covered with a polyethylene bag and kept at 25°C for 7 d. The germinated seeds were counted on the seventh day and germination percentage was calculated. For FAV analysis, the wheat samples were dried at 130°C for 19 h and ground in a Stein mill (Seedburo Equipment Company, Chicago, IL). Five grams of ground sample were folded in a Whatman no. 5 filter paper and 30 mL of petroleum ether was used as a solvent to extract the oil from the ground sample. The solvent was boiled continuously in a Soxhlet condensation solvent recovery system (Labconco Corporation, Kansas City, MO) and after 6 h of extraction, the extracted oil was separated from the solvent by heating in

uncovered beakers. Then 25 mL of TAP solution (50% toluene and 50% ethanol with phenolphthalein indicator) were added to the oil and titrated with a potassium hydroxide (KOH) solution (normality = 1.1979 mg/mL of solution) until it turned light pink. Finally, the FAV was expressed as mg of KOH/100 g of dry grain.

Wheat samples were subjected to the germination test on the next day after microwave treatment and the FAV was tested after storing for 6 wk at room temperature (approximately 25°C). Control samples (without microwave treatment) at all moisture levels were also stored for the same period and then subjected to FAV analysis. The entire experiment was replicated three times.

4.3.1 Statistical analysis

The effect of moisture content, microwave power and sample location in 50 g bulks on the germination percentage and FAV at each exposure time was analyzed by the ANOVA method using a factorial experimental design (4 moisture content × 6 power levels (control, 100, 200, 300, 400 and 500) × 2 sample locations (high temperature region and normal temperature region)). The differences within the levels under each variable were tested using the least significant difference (LSD) method of comparison of means. General linear models (GLM) procedure in SAS (version 9.1) was used for all statistical analysis. For the germination percentage and the FAV, the statistical significance between the samples collected from the high temperature and the normal temperature regions at each power level was tested using an independent t test (α=0.05).

4.4 Results and Discussion

4.4.1 Thermal image

In thermal imaging, the radiation pattern of an object (temperature) is converted into a visible image. The color of each pixel in a thermal image represents a temperature value which is given on the temperature scale (right side of Fig. 4.1). Generally, in a thermal image, bright and dark colors represent high and low temperatures, respectively. Because of non-uniform heating, high temperature regions were observed (as patches) at one or two locations on the surface of wheat samples after microwave treatment. Samples were collected from the high temperature zone and the remaining region, and subjected to quality evaluation.

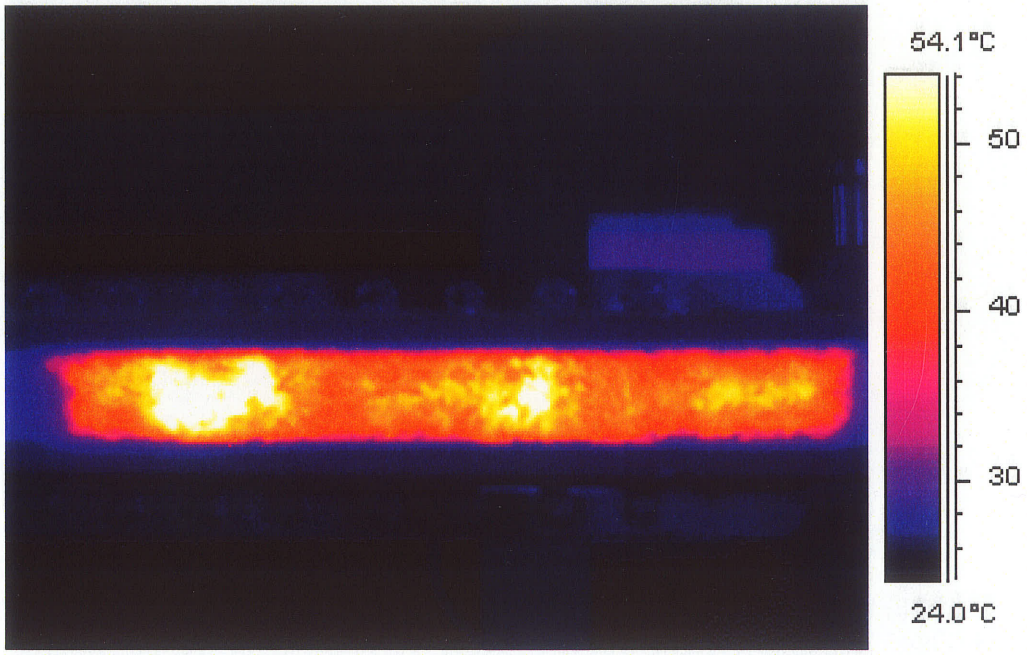

Figure 4.1 Typical thermogram of wheat sample showing high temperature region after microwave treatment.

4.4.2 Germination

Although microwaves have been used for seed treatment to accelerate the germination and increase the germination percentage of various seeds, Nelson and Stetson (1985) reported that RF electric treatment did not improve the seed germination of wheat.

Hence in this research, mainly the effect of high temperatures on the germination percentage of wheat was examined. Germination percentages of samples collected from the high temperature and normal temperature regions after microwave treatments are shown in Figs. 4.2 and 4.3. Sample location (high temperature region vs normal temperature region) had a significant effect on the germination percentage. The germination percentage was lower for the samples which were collected from the high temperature region than those from the normal zone, except for two treatments: 21% moisture content grain at 100 W power and 28 s exposure time, and for 18% moisture content grain at 100 W and 56 s exposure time. In these two treatments, there were no significant differences on the germination percentages of samples collected from the normal and high temperature regions. In general, the difference in germination between samples from the high temperature and normal temperature regions was less at lower power levels and increased as power level increased. When the exposure time was 28 s at 500 W, almost all seeds in the high temperature region became non-germinated seeds except for 12% moisture content grain, whereas at the same conditions, 4 to 33% germination was observed for samples collected from the normal zone. The germination percentage was almost zero at 300 W for the samples collected from the high temperature region, when the exposure time was increased to 56 s and the initial moisture content was 18 and 21%. At 400 and 500 W power levels when the exposure time was 56 s, the germination percentage was almost zero for samples collected from both normal and high temperature regions (except for 12% moisture content).

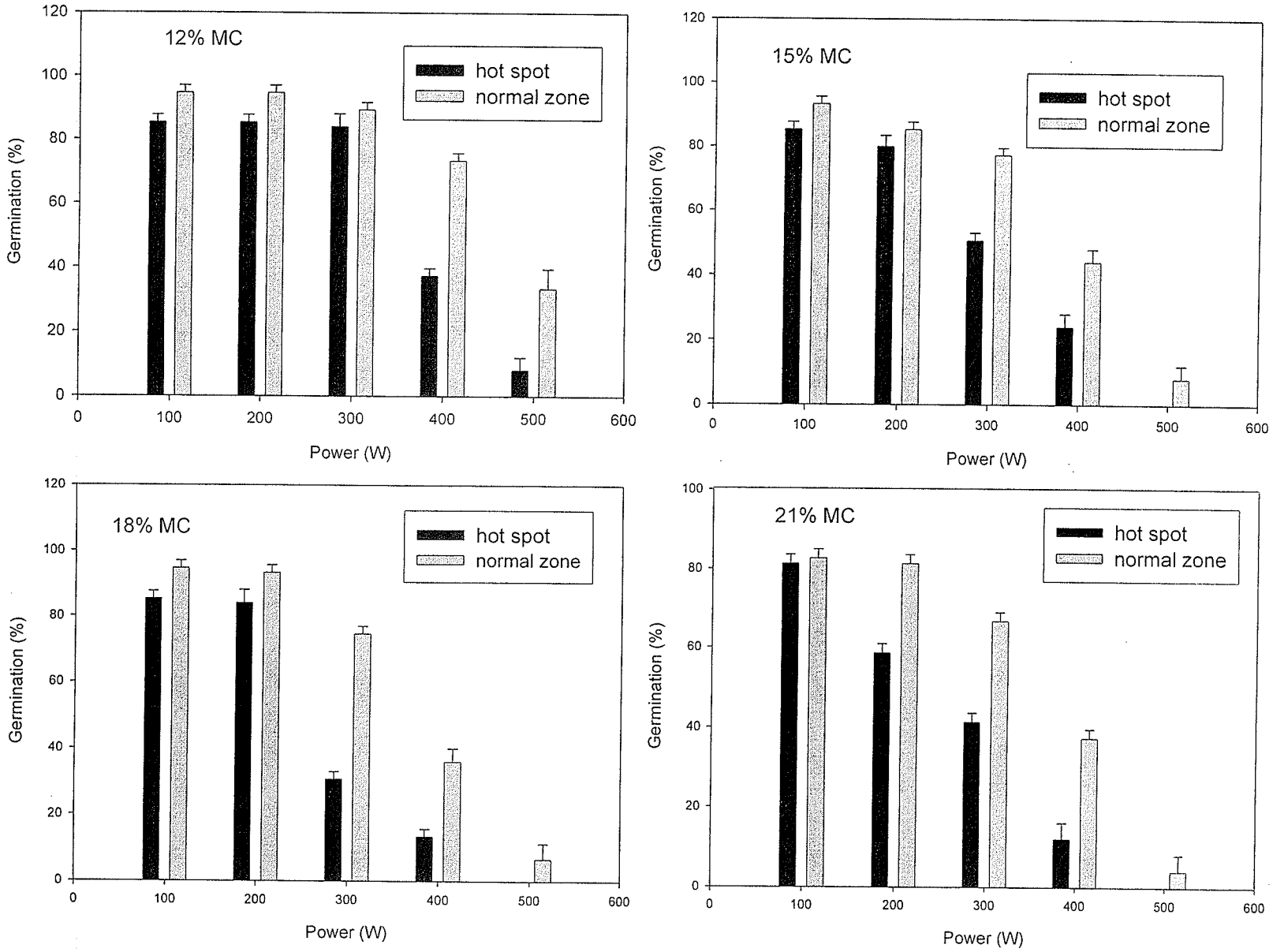

Figure 4.2 **Germination percentages of wheat samples collected from the high temperature (hot spot) and the normal temperature zones after heating for 28 s in a pilot-scale microwave drier.**

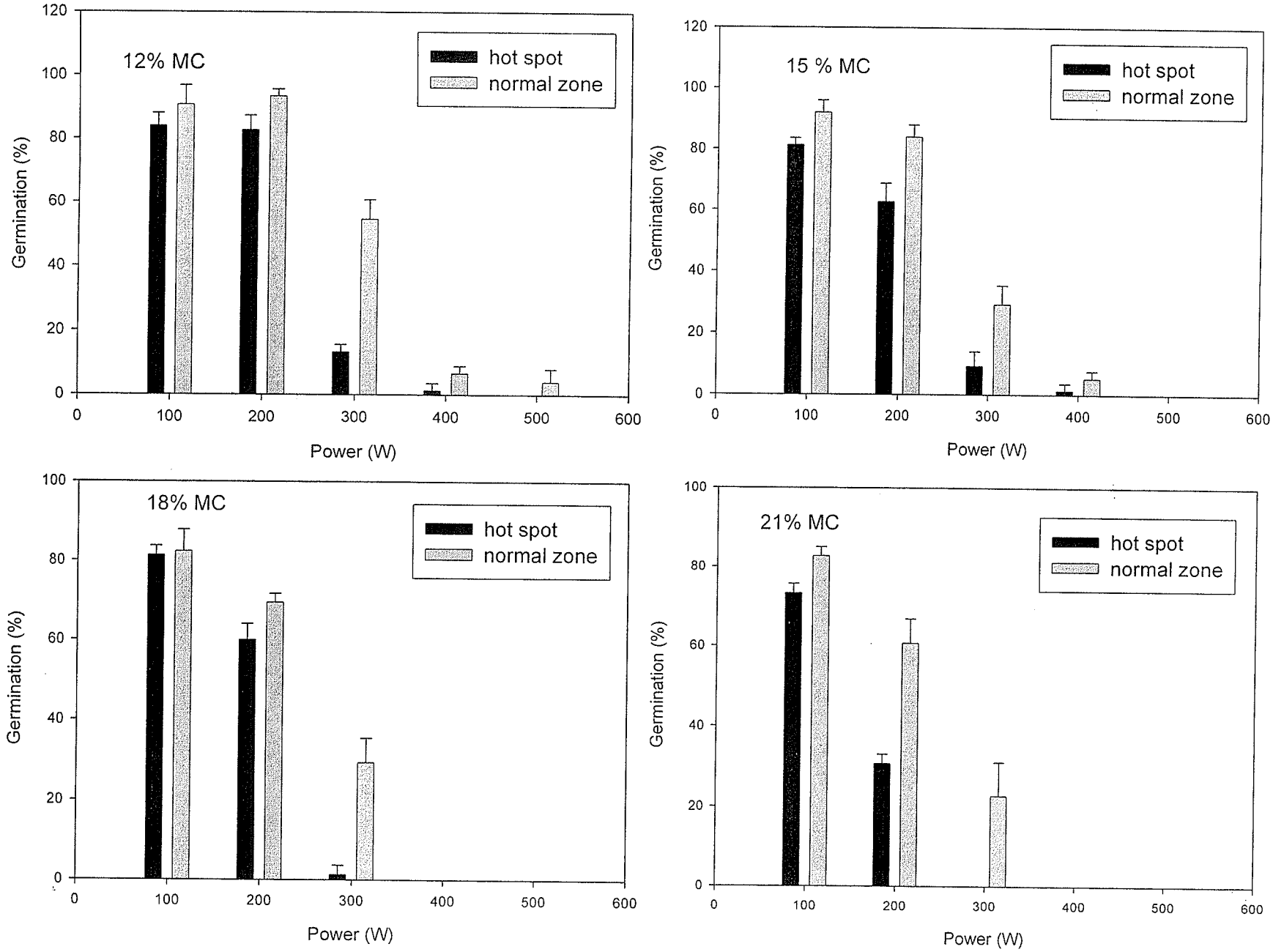

Figure 4.3 **Germination percentages of wheat samples collected from the high temperature (hot spot) and the normal temperature zones after heating for 56 s in a pilot-scale microwave drier.**

Microwave exposure time and power level had a significant effect on the germination percentage of wheat. Germinability decreased with increasing power level and exposure time. While evaluating the level of heat damage to wheat samples in a small batch fluidized-bed rig, Ghaly and Touw (1982) found that the effects of temperature and initial moisture content were highly significant. However they determined that exposure time had little effect on quality deterioration of wheat. But in our experiments using microwave heating, the exposure time had a significant effect on the germination percentage. This is because of the continuous increase in temperature during microwave treatment. The grain temperature during microwave treatment increased with exposure time and power. The germination percentage was essentially determined by grain temperature. Nelson (1976) also reported that optimum germination response was related to elevation of seed temperature during dielectric-heating and was about 75°C for alfalfa seed of 6 to 7% moisture content. If the temperature exceeded this optimum level, the high temperatures damaged seed viability and therefore increased the percentage of non-germinated seeds. Shivhare et al. (1992b) determined that germination of corn was inversely related to microwave power and increased with air velocity. They recommended a power level less than 0.25 W/g for seed-drying purposes. Hence, the microwave power and exposure time would be the important factors while using microwaves for seed processing. In our experiments, the reason for lower germination percentages in the high temperature region was mainly due to the elevated temperature. So, while using microwaves for seed-drying or

processing purposes with wheat, arrangements must be made to reduce the temperature in the high temperature locations to retain the germinability even at lower power levels.

Initial moisture content had a significant effect on germination percentage of wheat after microwave treatment. In general, germinability decreased with increasing moisture content. Although the temperature generated in the high moisture wheat was less than that in the low moisture wheat, the high moisture grain was more susceptible to heat and hence a lower germination percentage was observed in high moistures at all power levels. Moisture content determines the rate at which seed can absorb energy from RF electric fields and the capability of seed to retain its viability at higher temperature (Nelson 1976). Campana et al. (1993) also stated that germination capacity was inversely related to initial moisture content of wheat and final temperature during microwave treatment.

4.4.3 Fat acidity value (FAV)

After storing for six weeks, visible moulds were observed on control samples with 18 and 21% moisture content. Similarly, visible moulds were observed on the wheat samples with 18 and 21% moisture content that had been subjected to microwave treatment at low power levels.

Fats are esters of glycerol with three molecules of fatty acids. Because of hydrolysis caused by fungal secretions, these free fatty acids are liberated and therefore the determination of free fatty acids may be used as an index of quality (CIGI 1993). Fat acidity value can also be used as a measure of deterioration and storability of grains (Zeleny and Coleman 1939 cited by Christensen and Kaufmann 1968). The FAV of

wheat samples collected from the high temperature and the normal temperature regions after microwave treatment are shown in Tables 4.1 and 4.2. The FAV increased with moisture content in both the microwave-treated and control samples. This study confirms the results reported by Wallace et al. (1983); the FAV was positively correlated with moisture. In our experiments, an irregular pattern of FAV was observed at different power levels within all moisture contents. The location of the sample (high temperature region vs normal temperature region) had a significant effect on the FAV. In general, the FAV was higher for the samples collected from the high temperature region than from normal zones when the exposure time was 28 s and this trend was reversed when the exposure time was increased to 56 s. When the exposure time and the initial moisture content were 28 s and 12%, there were no significant differences between the FAV of samples collected from the high temperature and normal temperature regions at all power levels. In contrast, the FAV was significantly different for the samples collected from the high temperature region and the normal temperature regions at all power levels when the exposure time and the moisture content were 56 s and 21%. Considerable amounts of water evaporated from 18 and 21% moisture content samples (Fig. 4.4) due to elevated temperatures at higher power levels and the samples attained a safe storage condition. No visible moulds were seen on these samples, but a high FAV was obtained for samples at 21% moisture content (except at 500 W and 56 s exposure time). Microflora is basically responsible for the production of free fatty acids in grains during storage (Christensen et al. 1949).

Table 4.1 **Fat acidity value (mg of KOH /100 g of dry grain) of wheat samples collected from normal and high temperature regions after microwave treatment for 28 s.**

Power (W)	Moisture content (%)							
	12		15		18		21	
	Normal	High temperature	Normal	High temperature	Normal	High temperature	Normal	High temperature
Control	8.89±0.08		12.34±1.18		27.68±1.17*		35.07±0.23*	
100	7.38±1.28	7.37±1.28	12.51±4.62	10.27±1.31	22.80±1.30	22.09±2.23	35.74±1.67*	34.97±2.25*
200	7.35±1.29	7.37±1.29	9.57±1.30	9.54±1.22	20.62±1.28$^{\Psi}$	16.20±1.29$^{\Psi}$	29.08±1.66*	30.60±2.33*
300	8.07±1.27	8.09±1.28	7.33±1.23$^{\Psi}$	9.57±1.28$^{\Psi}$	14.01±1.26	13.25±0.02	28.38±2.27*$^{\Psi}$	22.47±2.28$^{\Psi}$
400	7.38±1.28	8.09±1.26	10.26±1.28	8.08±2.53	13.13±2.02	11.79±1.25	24.68±3.19$^{\Psi}$	46.09±0.62$^{\Psi}$
500	7.36±1.26	7.36±1.29	8.09±1.29$^{\Psi}$	10.29±1.28$^{\Psi}$	11.80±1.28	12.54±1.27	40.89±2.97$^{\Psi}$	52.76±2.78$^{\Psi}$

* Visible mould observed on the grain.
$^{\Psi}$ Significant difference exists between high temperature and normal temperature regions (α=0.05).

Table 4.2 **Fat acidity value (mg of KOH /100 g of dry grain) of wheat samples collected from normal and high temperature regions after microwave treatment for 56 s.**

Power (W)	Moisture Content (%)							
	12		15		18		21	
	Normal	High temperature	Normal	High temperature	Normal	High temperature	Normal	High temperature
Control	8.89±0.08		12.34±1.18		27.68±1.17*		35.07±0.23*	
100	7.36±1.25	8.10±1.28	10.28±1.24	11.02±0.06	14.01±0.64$^{\Psi}$	22.11±1.91$^{\Psi}$	36.87±1.30*$^{\Psi}$	29.46±1.28*$^{\Psi}$
200	8.10±1.27	7.38±1.28	10.28±1.23$^{\Psi}$	8.84±0.01$^{\Psi}$	13.26±1.88	14.75±2.78	24.29±2.19*$^{\Psi}$	35.34±2.24$^{\Psi}$
300	8.10±1.28	7.37±1.27	9.56±1.30	8.82±2.20	12.51±0.60	11.80±1.69	41.25±3.34$^{\Psi}$	56.75±1.22$^{\Psi}$
400	6.63±0.02$^{\Psi}$	7.38±1.28$^{\Psi}$	9.58±1.29	8.09±1.28	9.59±1.69	8.85±1.92	53.83±2.53$^{\Psi}$	13.24±2.21$^{\Psi}$
500	6.62±0.01$^{\Psi}$	8.11±1.28$^{\Psi}$	8.82±2.18	8.85±0.01	11.79±1.67$^{\Psi}$	8.09±2.75$^{\Psi}$	11.05±2.22$^{\Psi}$	7.37±1.27$^{\Psi}$

* Visible mould observed on the grain.

$^{\Psi}$ Significant difference exists between high temperature and normal temperature regions (α=0.05).

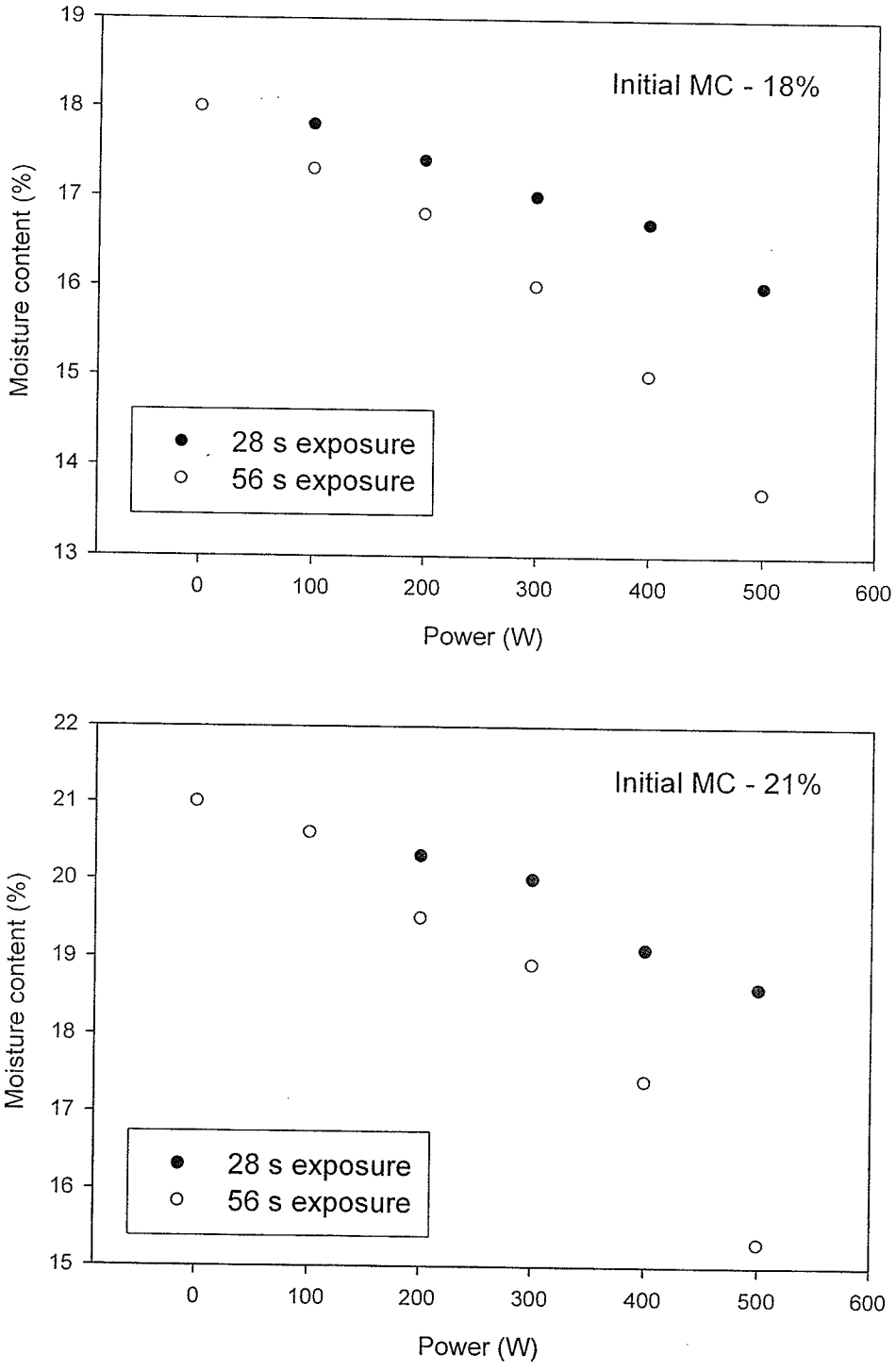

Figure 4.4 **Final moisture content of bulk wheat samples (18 and 21% MC, wet basis) after microwave treatment.**

Karunakaran et al. (2001) determined that FAV increased with storage temperature and storage time when the percentage of seeds infected by microflora was high. They measured FAV of 19% moisture content wheat as 65 mg KOH/100 g dry grain when the wheat was infected by various species of microflora and stored at 35°C for 10 d. In our experiment, when the sample with 21% moisture content was subjected to 500 W for 56 s, it was dried to 15.3%, and the FAV was similar to the low moisture grains.

It is difficult to explain the exact reason for the changes in the FAV after microwave treatment, as already many controversial discussions have been published on this subject. In general, the increase in mould populations of the stored seed was closely correlated with increased production of FAV and CO_2 (Christensen et al. 1949). However, the individual mould species differed significantly with regard to the amount of FAV produced (Nagel and Semeniuk 1947 cited by Christensen and Kaufmann 1968). Furthermore, a given species may produce a relatively large quantity of fatty acids and then consume portions of them. In contrast, it was also reported that the microflora was not responsible for the rancidity (oxidation) development in cotton seed (Christensen and Kaufmann 1968). Therefore, the use of FAV as a measure of deterioration of a given grain sample may encounter some problems and complications (Christensen and Kaufmann 1968). Sinha et al. (1985) reported that wheat with FAV of 5.9 to 9.7 mg KOH/100 of dry grain may be considered as sound seeds. While considering these limits, in general the FAV of high moisture grains (18 and 21%) did not attain the safe limits even after the microwave treatments for a short time of 28 and 56 s.

The germination percentage of wheat samples present in the high temperature region was significantly lower than that of the normal region for almost all moisture and power levels. Microwaves may not be suitable for the drying of wheat which has to be used as seeds,

even at low power levels, unless some provisions are made for uniform heating. Apart from germination, the other quality parameters which are sensitive to heat are also expected to be affected more in the high temperature region than the remaining bulk grain. An irregular pattern was observed on the FAV of high moisture wheat after exposure to microwaves for 28 and 56 s and 6 wk storage. However, to study the effect of microwave drying on the FAV, high moisture grains must be dried to safe storage moisture levels and the changes in FAV should be analyzed during the storage period. While evaluating the quality changes of grain after microwave treatment, testing grain in the high temperature region would yield more realistic information about the damage due to microwave treatment rather than mixing and testing the whole bulk grain.

4.5 Acknowledgements

We thank the Canada Research Chairs Program and the Natural Sciences and Engineering Research Council of Canada (NSERC) for their financial assistance and Mr. Colin J Demianyk, Cereal Research Centre, Agriculture and Agri-Food Canada, Winnipeg, Canada, for his help in FAV analysis.

5. THERMAL IMAGING OF A STORED GRAIN SILO TO DETECT A HOT SPOT

5.1 Summary

A hot spot is a localized high temperature zone in a grain bulk and normally spoilage begins in this location. Many sensors need to be installed throughout the bin to detect hot spots by measuring grain temperature. A non-contact method to detect a hot spot in a stored grain silo would be beneficial. The capability of thermal imaging to detect a hot spot in an experimental silo (galvanized steel, 1.5 m diameter and 1.5 m height) filled with barley was studied. An artificial heat source was placed at nine locations inside the grain bulk and set at four temperature level (30, 40, 50 and 60°C) in each location. The outer surface of the silo wall and the top surface of the grain bulk were thermally imaged up to 48 h at each treatment (n=3). The temperature of the top surface of the grain bulk was significantly (α=0.05) higher (0.4°C to 2.6°C) than the atmospheric temperature after 48 h of hot spot establishment. The hot spot was detected from the thermal images of the silo wall and grain bulk (as a high temperature region) when it was located at 0.3 m from the silo wall and 0.3m below the grain surface, respectively. The hot spot was not detected on the thermal images of the silo wall when the wind velocities were 1.0, 1.5 and 2.0 m/s, and immediately after wind (n=3). Similarly, thermal imaging did not detect the hot spot on the grain bulk when the ambient temperature was 1°C (hot spot=30°C), and on the silo wall when the ambient temperature was −8°C (hot spot=60°C) (n=3). The surface temperature of the grain bulk decreased with increasing moisture content. It was 25.8, 24.3, 23.4, 22.8 and 22.4°C for the grains with 8, 12, 16, 20 and 24% moisture content, respectively when the room temperature was 26°C (n=20). Thermal imaging can not be used as an independent method to monitor the grain temperature in a silo.

5.2 Introduction

In western Canada, the storage capacity of grain silos is almost double the average annual production of grains; 80% of these storage structures are located on farms (Muir 1997a). Galvanized steel structures on concrete foundations are the most common storage units for grain in western Canada (Muir and White 2001). Hot spots (localized high temperature zones in a grain bulk) could develop anywhere inside the grain bulk. Hot spots may develop quickly in stored grain under Canadian winter conditions (Sinha 1961). Depending on origin, a hot spot may be classified into two types as a fungi-induced hot spot in damp grain or an insect-induced hot spot in dry grain (Sinha 1967). Loading wet grain on top of the dry old grain, entry of rain through a roof leak, blowing of snow through ventilators, rising of moisture through a cracked floor or moisture migration within the grain bulk may cause damp grain pockets in granaries. In a high moisture zone, moulds begin to grow and produce heat and moisture. *Penicillium* spp., *Aspergillus* spp., and *Absidia* spp. are the commonly associated species in a fungi-induced hot spot (Wallace and Sinha 1962). Sinha and Wallace (1965) described the ecology of a fungus-induced hot spot (created artificially) in a grain bin during five winter months in Manitoba. The microorganisms started appearing after introducing the damp grain, the temperature increased rapidly, reaching a maximum of 64°C in three months, then cooled down immediately in two weeks. Sinha (1961) studied the physical conditions of insect-induced hot spots in 13 farm granaries in Manitoba and Saskatchewan. A high density of insects and mites at all life stages was found within a hot spot and *Cryptolestes ferrugineus* was the most common insect species encountered in heating grain. In an insect-induced hot spot, moulds always grow in the hot spot area,

producing more heat, moisture and carbon dioxide. The generated heat and moisture stimulate the growth of the insects, moulds and respiration of grains, thereby leading to an accelerated chain reaction. The temperature difference between a hot spot and the surrounding cool grain in a grain bulk could range from 10°C to 50°C (Sinha 1961). The temperature of the hot spots may even go up to self-ignition (combustion) temperature in seeds such as soybeans and fababeans where chemical oxidation of the oil in the seed continues even after the cessation of biological respiration (Christensen and Meronuck 1986 cited by Muir and White 2001). In stored-grain ecosystems, temperature and grain moisture content are directly related to the spoilage of grain. The germination ability of wheat at 17% moisture content was reduced to 10% within a month when the storage temperature was 35°C (Schroth 1996).

Periodic inspection is essential to monitor temperature and moisture content of the grain bulk in a silo. In a temperature detection system for stored grain bins, flexible cables fabricated with isolated thermocouples (spaced at desired locations) are hung throughout the grain bulk. Temperatures at various locations are recorded using data logger systems. Thermocouples were used to measure the temperature of wheat bulk (Sinha and Wallace 1965) and rapeseed (Sinha et al. 1981) in farm bins while investigating the ecology of a fungus-induced hot spot and the quality assessment of grain, respectively. Mani (1999) used 40 thermocouples to measure temperature of wheat in an experimental silo (1 m diameter, 1 m height) while validating a computer model for insect-induced hot spot. Muir and White (2001) suggested that weekly temperature measurement is required in the grain bulk at intervals of less than 0.5 m to thermally detect small hot spots. To achieve this target in big farm granaries, large numbers of

sensors would need to be installed throughout the grain bulk. A non-contact temperature measuring method with the capability of detecting at least severe conditions such as hot spots would be helpful to storage managers. The objective of this research was to determine the capability of infrared thermal imaging to detect a hot spot in a grain silo filled with barley.

5.3 Materials and Methods

5.3.1 Experimental setup

A cylindrical galvanized steel (GS) silo (1.5 m diameter, 1.5 m height, top side open) was used in this study. The silo was filled with the commercial grade barley to a depth of 1.2 m. The moisture content of the grain was in the range of 9% to 10% (wet basis). An artificial heat source with a temperature control mechanism was used to represent the hot spot inside the silo. The artificial hot spot was made up of a hollow steel cylinder (0.2 m diameter, 0.2 m height, both ends covered with metal plates) with the outer surface wrapped with a heat tape. The temperature of the heat source was controlled by a PID temperature controller and measured by a thermocouple placed on the outside surface of the steel cylinder.

The hot spot was placed at three different depths (Y=0.3, 0.6, 0.9 m) from the top surface of the grain bulk and three horizontal distances (X=0.3, 0.6, 0.9 m) from the silo wall. In total, there were nine locations for the hot spot (X×Y=0.3×0.3, 0.3×0.6, 0.3×0.9, 0.6×0.3, 0.6×0.6, 0.6×0.9, 0.9×0.3, 0.9×0.6, 0.9×0.9). At each location, the temperature of the hot spot was set at four levels: 30, 40, 50 and 60°C. This experiment was conducted from November 2004 to November 2005 at the Canadian Wheat Board Centre for Grain Storage Research, University of Manitoba, Winnipeg, MB. The room

temperature and relative humidity were not controlled for this experiment. The room temperature was in the range of 20°C to 30°C during the experiments. The hot spot was set at 30°C, whenever the room temperature was less than 30°C. The laboratory contained many research facilities and the experimental silo was placed near a large mechanical grain cleaning system (Fig. 5.1).

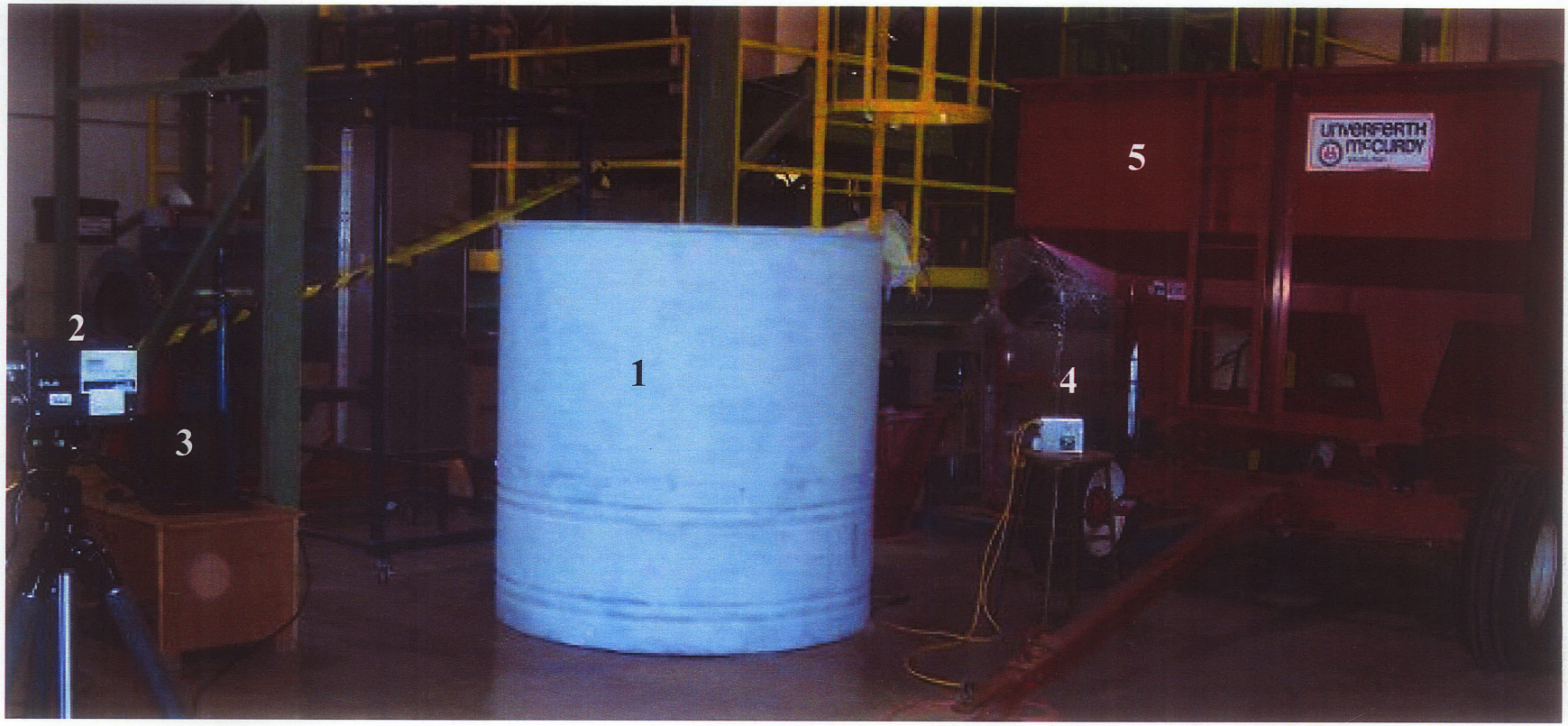

Figure 5.1 Experimental setup of thermal imaging system to detect hot spot in a grain silo.

1. grain silo 2. thermal camera 3. data acquisition computer 4. temperature measurement and control system 5. grain wagon

There are five doors and one large rolling door to this room and they were opened and closed randomly as many people were using this laboratory.

5.3.2 Thermal imaging

All objects with a temperature greater than absolute zero (–273°C) emit infrared radiation. The total radiation emitted from the object is directly related to its temperature. Infrared detectors in a thermal camera receive the radiation (spectral range: 3 to 13 μm) from the surface of the object and convert it into a temperature map called a thermal image. Thermal imaging is a non-contact method to map the surface temperature of the object in two dimensions at a high resolution. This technique is being used for several applications such as detecting hot and cold spots in mechanical and electrical industries (Dani 2005; Motwan and Al-Hussain 2005; VanBree and Wood 2005). In outdoor applications, many factors such as solar radiation, wind, fog, and rain affect the performance of a thermal imaging system (Davis and Lettington 1988). The wind and sun can strongly affect the thermal patterns of objects in field conditions. The wind masks the temperature rise and makes the diagnosis more challenging. Similarly, solar warming and reflection are the two problems associated with solar radiation. The effect of wind and solar radiation must be considered while conducting a thermographic survey in field conditions (Madding and Lyon 2004).

5.3.3 Thermal imaging of silo wall and grain bulk

An un-cooled focal planar array type infrared thermal camera with 320×240 pixels (Model: ThermaCAM ^{TM} SC500 of FLIR systems, Burlington, ON; spectral range: 7.5 to 13.0 μm) was used to take the thermal images of the experimental silo and grain bulk. The thermal sensitivity of the camera was 0.07°C at 30°C. At every location of the hot

spot and each temperature level, the outside surface of the silo wall and the top surface of the grain bulk were imaged at 0, 2, 4, 6, 8, 24, 32 and 48 h (day 1 – 8:00 am, 10:00 am, 12:00 pm, 2:00 pm, 4:00 pm; day 2 – 8:00 am, 4:00 pm; day 3 – 8:00 am) after starting the hot spot.

While taking the thermal images of the empty silo at the beginning of the experiments, many nearby objects were reflected on the image of the silo as thermal emissivity of a GS sheet is very low (ϵ=0.25). Therefore, to increase the emissivity of the silo, the outside surface was coated with a high emissivity paint (Krylon flat white #1502, ϵ=0.98). After coating with high emissivity paint, the surface temperatures of the silo were clearly mapped by thermal imaging. In real time situations, painting the bins with white color has its advantage (reduce undesirable solar heating in warm climates) and disadvantage (feasibility in a big silo). High emissivity paints need not be white, other types of paints can be selected.

After completing the experiments at one temperature, the grain was allowed to cool for 24 h and the next experiment was started at another temperature. When the experiments with four temperature levels at one location were completed, the grain was transferred to a wagon, then the silo was refilled after changing the heat source to the next location. For each treatment (position and temperature of hot spot) three images were taken at 5 min intervals while imaging at each incremental time up to 48 h (n=3). There were no abrupt changes in the weather conditions during the replication time. The temperature of the silo wall and the top surface of the grain bulk after 48 h of hot spot establishment were compared with the ambient temperature during that time by student's t test at 95% confidence interval.

While imaging, the distance was 5 m between the silo and camera, and 4 m between the top surface of the grain bulk and camera. The thermal emissivity of the target object was set at 0.98. All thermal images were analyzed with ThermaCAM Researcher 2001 software (FLIR systems, Burlington, Ontario, Canada). In a thermal image, the color of each pixel represents a temperature value which is given on the temperature scale (right side of each image). Average temperature ($T_{average}$), maximum temperature (T_{max}) and the difference between maximum and minimum temperatures (ΔT), of the silo wall and top surface of the grain bulk were extracted using the area tool option available in the software.

5.3.4 Effect of wind

The effect of wind on the temperature profiles of the silo wall was studied. A domestic fan (blade diameter 0.5 m) was used and the desired wind velocities (approximately 1.0, 1.5 and 2.0 m/s) were developed by adjusting the speed of the fan and the distance between the fan and the silo. The fan was focused on the high temperature region caused by the hot spot and the cooling effect of the wind on the silo appeared on the thermal image of the silo wall. The wind velocity was measured near the silo using an anemometer (Florite 800, Bacharach, UK). The fan was switched on after 48 h of hot spot establishment. Thermal images were taken at 30 min while the fan was on (n=3). After taking images, the fan was turned off and the silo was viewed continuously through the thermal camera until the hot spot reappeared on the silo wall.

5.3.5 Effect of cold weather

Preliminary investigation to study the effect of cold weather on the temperature profiles of the silo and grain bulk was conducted by opening the large rolling door (3.6×3.6 m) to

the building, which was located 8 m away from the experimental silo. The door was kept completely open (after 48 h of the hot spot establishment) which allowed cold ambient air from the outside atmosphere to enter the lab and cool the grain and silo. In this study, two experiments were conducted when the hot spot was placed at 0.9×0.3 m location with 30 and 60°C to test the effect on the top surface of the grain bulk. Similarly, one experiment was carried out when the hot spot was located at 0.3×0.6 m and 60°C to study the effect on the silo wall. These trials were conducted on three different days and the outside weather conditions during these experiments are given in Table 5.1. Thermal images were taken at 30 min intervals up to 3 h (n=3).

Table 5.1 Hot spot location and outside weather conditions while testing effect of cold weather.

Trial	Date	Hot spot		Outside weather conditions*		
		Location m	Temperature (°C)	Temperature (°C)	Wind velocity (m/s)	RH (%)
1	Oct. 7, 2005	0.9×0.3	30	1	9.7	83
2	Oct. 13, 2005	0.9×0.3	60	4	1.4	100
3	Nov. 17, 2005	0.3×0.6	60	-8	8.3	89

* Obtained from Environment Canada (Meteorological Service of Canada)

5.3.6 Effect of moisture content of grain

The capability of thermal imaging to detect high moisture pockets in a grain bulk was also tested. The surface temperature of barley samples with five moisture contents (8, 12, 16, 20 and 24%) was measured by thermal imaging (n=20).

5.4 Results and Discussion

5.4.1 Thermal imaging of the silo wall

The grain level inside the silo was clearly visible on thermal images of the experimental silo, even before starting the hot spot. Generally the temperature of the silo region filled

with grain was slightly cooler (around 1°C) than that of the region without grain (top region). Temperature profiles of the silo wall after 48 h of hot spot establishment are shown in Tables 5.2 to 5.4. Since the ambient conditions were not changed abruptly during replications, the variation among the replications was small. When the hot spot was located at 0.3 m from the silo wall there were no significant differences between the $T_{ambient}$ and the $T_{average}$ of the silo wall in some treatments (at 30°C and 50°C in 0.3×0.3 m location, 30°C in 0.3×0.6 m location, and 30, 40 and 50°C in 0.3×0.9 m location) even after 48 h of hot spot establishment. However, the hot spot was identified on the thermal images of the silo wall (as a high temperature region) when it was located at 0.3×0.6 and 0.3×0.9 m except at 30°C. The high temperature region (due to hot spot) identified on the thermal images of the silo wall had slightly higher temperature (0.8°C to 1.0°C) than the surrounding region.

Table 5.2 **Temperature profile of silo and top surface of grain bulk when hot spot was at 0.3 m from silo wall (after 48 h)** (n=3).

Hot spot location m (X×Y)*	$T_{hot\ spot}$ °C	$T_{ambient}$ °C	Silo wall			Grain surface		
			$T_{average}$ °C	T_{max} °C	ΔT (max–min)	$T_{average}$ °C	T_{max} °C	ΔT (max– min)
0.3×0.3	30	20.0^{Ψ}±0.2	19.9±0.2	21.6±0.1	2.0±0.3	20.5^{Ψ}±0.1	21.0±0.2	0.8±0.1
	40	$22.3^{\Phi\Psi}$±0.2	21.7^{Φ}±0.1	22.6±0.2	1.5±0.3	23.0^{Ψ}±0.2	23.4±0.2	0.9±0.1
	50	19.2^{Ψ}±0.7	18.7±0.5	19.7±0.4	2.0±0.2	20.4^{Ψ}±0.6	20.9±0.6	0.9±0.1
	60	$21.7^{\Phi\Psi}$±0.1	21.5^{Φ}±0.2	22.5±0.2	1.8±0.0	23.2^{Ψ}±0.1	23.7±0.1	0.9±0.1
0.3×0.6	30	26.4^{Ψ}±0.3	26.5±0.4	27.1±0.2	1.2±0.1	27.3^{Ψ}±0.1	27.5±0.1	0.5±0.1
	40	$27.1^{\Phi\Psi}$±0.1	27.6^{Φ}±0.1	28.0±0.1	0.9±0.1	27.6^{Ψ}±0.1	27.8±0.1	0.5±0.0
	50	$26.7^{\Phi\Psi}$±0.1	26.9^{Φ}±0.1	27.4±0.0	1.3±0.0	27.7^{Ψ}±0.3	28.0±0.3	0.6±0.2
	60	$24.2^{\Phi\Psi}$±0.1	24.8^{Φ}±0.2	25.3±0.1	1.3±0.1	25.7^{Ψ}±0.3	26.0±0.3	0.7±0.1
0.3×0.9	30	21.3^{Ψ}±0.7	21.0±0.7	22.4±0.3	2.4±0.4	23.3^{Ψ}±0.1	23.7±0.1	1.0±0.1
	40	20.7^{Ψ}±0.3	20.6±0.3	22.0±0.3	2.7±0.2	22.7^{Ψ}±0.0	23.1±0.1	1.1±0.1
	50	20.1^{Ψ}±0.4	20.2±0.1	21.3±0.1	2.4±0.2	22.1^{Ψ}±0.1	22.5±0.1	1.1±0.1
	60	$21.6^{\Phi\Psi}$±0.0	21.4^{Φ}±0.1	22.7±0.1	2.4±0.0	23.2^{Ψ}±0.1	23.6±0.1	1.1±0.2

* X- horizontal distance from silo wall, Y- vertical distance from top surface of grain bulk

$^{\Phi}$ $T_{ambient}$ and $T_{average}$ of silo wall are significantly different (α=0.05)

$^{\Psi}$ $T_{ambient}$ and $T_{average}$ of top surface of the grain bulk are significantly different (α=0.05)

Table 5.3 **Temperature profile of silo and top surface of grain bulk when hot spot was at 0.6 m from silo wall (after 48 h)** (n=3).

Hot spot location m (X×Y)*	$T_{hot\ spot}$ °C	$T_{ambient}$ °C	Silo wall			Grain surface		
			$T_{average}$ °C	T_{max} °C	ΔT (max– min)	$T_{average}$ °C	T_{max} °C	ΔT (max– min)
0.6×0.3	30	$24.0^{\Phi\Psi}$±0.1	24.3^{Φ}±0.1	24.8±0.1	1.1±0.1	24.5^{Ψ}±0.1	24.8±0.1	0.8±0.1
	40	$25.9^{\Phi\Psi}$±0.1	26.1^{Φ}±0.1	26.4±0.1	0.8±0.1	26.5^{Ψ}±0.3	26.8±0.3	0.8±0.1
	50	$24.9^{\Phi\Psi}$±0.0	25.2^{Φ}±0.1	25.7±0.1	1.0±0.1	26.2^{Ψ}±0.1	26.7±0.1	1.0±0.2
	60	25.3^{Ψ}±0.2	25.5±0.3	26.1±0.2	1.2±0.1	26.8^{Ψ}±0.1	27.3±0.1	0.9±0.1
0.6×0.6	30	$23.6^{\Phi\Psi}$±0.3	24.3^{Φ}±0.1	25.1±0.1	1.9±0.1	25.7^{Ψ}±0.1	26.2±0.1	1.2±0.2
	40	$26.1^{\Phi\Psi}$±0.1	26.3^{Φ}±0.1	27.4±0.1	1.8±0.1	27.5^{Ψ}±0.1	27.8±0.1	0.6±0.1
	50	$22.8^{\Phi\Psi}$±0.1	23.1^{Φ}±0.1	23.8±0.1	1.2±0.1	23.8^{Ψ}±0.2	24.1±0.2	0.6±0.1
	60	24.8^{Ψ}±0.4	25.2±0.5	26.4±0.4	2.0±0.2	26.8^{Ψ}±0.1	27.1±0.1	0.7±0.1
0.6×0.9	30	$25.2^{\Phi\Psi}$±0.0	25.4^{Φ}±0.1	25.9±0.1	1.0±0.1	26.0^{Ψ}±0.1	26.3±0.1	0.5±0.1
	40	29.6^{Ψ}±0.8	29.3±0.5	30.5±0.4	2.7±0.0	31.1^{Ψ}±0.1	31.1±0.4	0.7±0.3
	50	$25.5^{\Phi\Psi}$±0.2	26.3^{Φ}±0.1	26.8±0.1	1.0±0.1	26.5^{Ψ}±0.2	26.7±0.1	0.7±0.1
	60	27.7^{Ψ}±0.4	27.5±0.4	29.0±0.4	3.1±0.1	29.4^{Ψ}±0.1	29.9±0.2	0.9±0.3

* X- horizontal distance from silo wall, Y- vertical distance from top surface of grain bulk

$^{\Phi}$ $T_{ambient}$ and $T_{average}$ of silo wall are significantly different (α=0.05)

$^{\Psi}$ $T_{ambient}$ and $T_{average}$ of top surface of the grain bulk are significantly different (α=0.05)

Table 5.4 **Temperature profile of silo and top surface of grain bulk surface when hot spot was at 0.9 m from silo wall (after 48 h)** (n=3).

Hot spot location m (X×Y)*	$T_{hot\ spot}$ °C	$T_{ambient}$ °C	Silo wall			Grain surface		
			$T_{average}$ °C	T_{max} °C	ΔT (max– min)	$T_{average}$ °C	T_{max} °C	ΔT (max– min)
0.9×0.3	30	$22.1^{\Phi\Psi}$±0.1	22.4^{Φ}±0.1	23.2±0.2	1.9±0.1	22.5^{Ψ}±0.1	23.1±0.1	1.0±0.1
	40	24.1^{Ψ}±0.1	24.1±0.2	24.9±0.1	1.6±0.3	24.7^{Ψ}±0.1	25.1±0.1	0.9±0.1
	50	23.0^{Ψ}±0.0	23.2±0.4	24.0±0.4	1.6±0.2	24.2^{Ψ}±0.2	24.7±0.2	1.0±0.2
	60	$22.3^{\Phi\Psi}$±0.1	22.7^{Φ}±0.2	23.6±0.1	1.7±0.3	23.8^{Ψ}±0.2	24.2±0.2	1.0±0.1
0.9×0.6	30	27.8^{Ψ}±0.2	27.9±0.2	28.6±0.2	1.5±0.1	29.2^{Ψ}±0.1	29.5±0.1	0.5±0.1
	40	$29.5^{\Phi\Psi}$±0.1	29.7^{Φ}±0.1	31.0±0.1	2.8±0.1	31.1^{Ψ}±0.2	31.4±0.1	0.6±0.1
	50	$26.9^{\Phi\Psi}$±0.1	27.5^{Φ}±0.1	27.8±0.1	1.0±0.1	27.6^{Ψ}±0.1	28.0±0.1	0.7±0.1
	60	30.8^{Ψ}±0.2	31.0±0.2	32.0±0.1	2.1±0.2	32.0^{Ψ}±0.3	32.2±0.3	0.6±0.1
0.9×0.9	30	28.0^{Ψ}±0.1	27.9±0.1	28.4±0.1	1.1±0.1	28.7^{Ψ}±0.2	28.9±0.3	0.5±0.1
	40	$24.5^{\Phi\Psi}$±0.3	25.2^{Φ}±0.4	25.5±0.4	0.7±0.2	26.3^{Ψ}±0.1	26.7±0.1	0.6±0.1
	50	$27.3^{\Phi\Psi}$±0.2	27.5^{Φ}±0.1	28.1±0.1	1.3±0.1	28.0^{Ψ}±0.1	28.2±0.1	0.5±0.1
	60	$27.9^{\Phi\Psi}$±0.1	28.4^{Φ}±0.1	28.9±0.1	1.3±0.1	28.6^{Ψ}±0.1	28.9±0.1	0.7±0.1

* X- horizontal distance from silo wall, Y- vertical distance from top surface of grain bulk

$^{\Phi}$ $T_{ambient}$ and $T_{average}$ of silo wall are significantly different (α=0.05)

$^{\Psi}$ $T_{ambient}$ and $T_{average}$ of top surface of the grain bulk are significantly different (α=0.05)

When the hot spot was located at 0.3×0.3 m, the high temperature region was merged with the region without grain, and a typical hot spot was not observed. Whereas at 0.3×0.6 and 0.3×0.9 m locations, the hot spots were clearly identified on the thermal images of the silo wall (Fig. 5.2). At the 0.3×0.6 m location, the hot spot started appearing on the thermal images of the silo wall after 48 h, when temperature was 40°C and 50°C, and after 32 h when the temperature was 60°C. When the hot spot was positioned at 0.3×0.9 m, it started appearing on the thermal images after 48 h at 40°C and after 24 h at 50°C and 60°C. At locations greater than 0.3 m from the silo wall, no spots appeared on the thermal images of the silo even after 48 h and at higher temperature levels. However, the boundary between the silo regions, with and without grain, was disturbed and an irregular temperature pattern was observed. This might be caused by the combined effect of heat conduction through the grain and the silo wall. Therefore, if the hot spot is located much farther than 0.3 m from the silo wall, it appears unlikely to be detected on the thermal images of the silo wall.

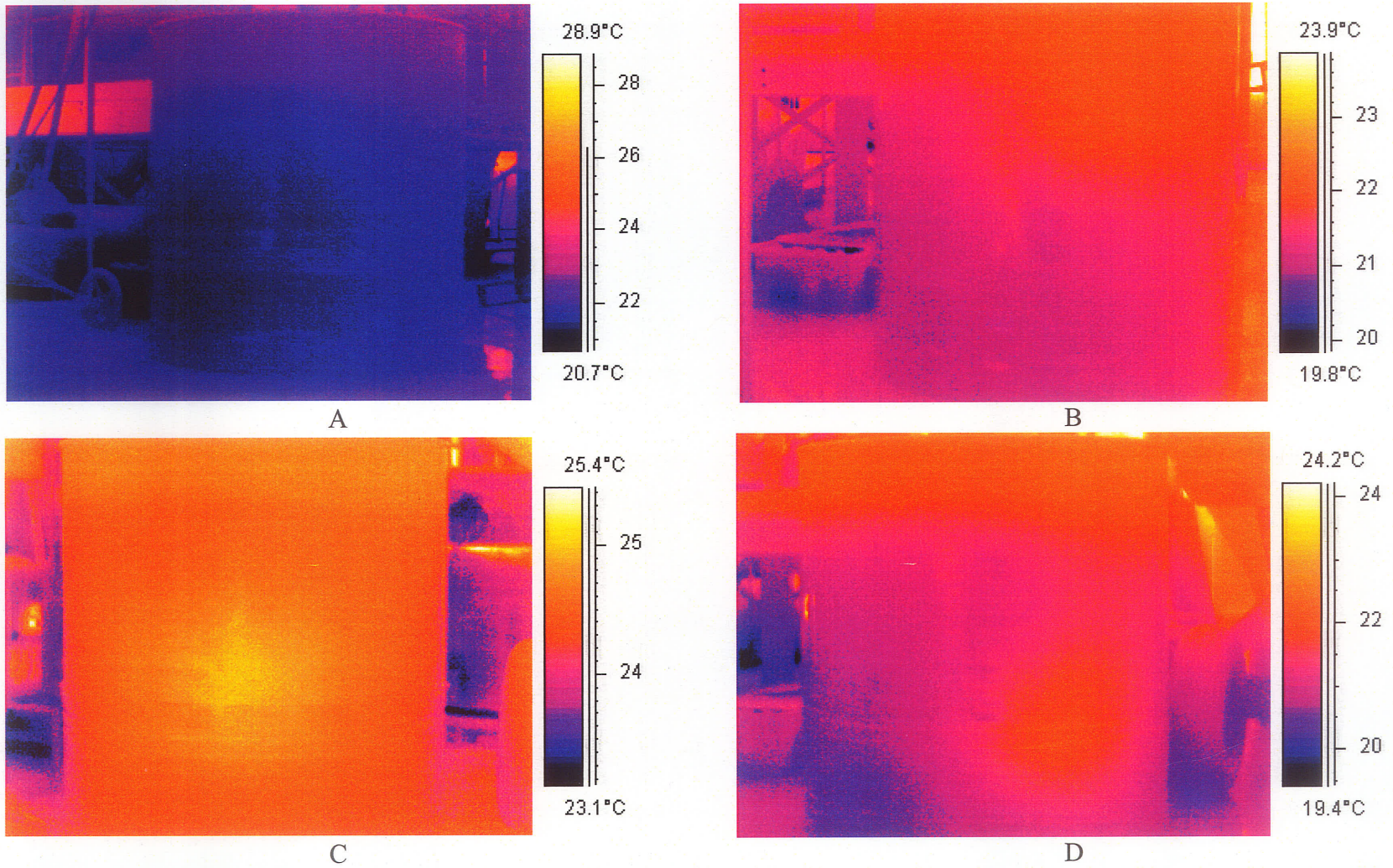

Figure 5.2 **Thermal images of the silo wall when the hot spot was at 0.3 m from the silo wall at different depths and 60°C (after 48 h).**
a. without hot spot; b. 0.3×0.3 m; c. 0.3×0.6 m; d. 0.3×0.9 m

5.4.2 Thermal imaging of top surface of the grain bulk

The temperature profiles on the top surface of the grain bulk after 48 h of hot spot establishment are given in Tables 5.2 to 5.4. In all experiments, the average temperature ($T_{average}$) at the top surface of the grain bulk was significantly (α =0.05) higher (0.4°C to 2.6°C) than the ambient temperature after 48 h of hot spot establishment. The temperature profile on the surface of the grain bulk was almost uniform at all temperatures of hot spots, in which ΔT was in the range of 0.5°C to 1.2°C. But the ΔT was higher (0.8°C to 3.1°C) for the silo wall, as temperature profile was easily affected by the environmental conditions due to the high thermal conductivity of the GS material.

The hot spot was identified on the thermal images of the grain bulk, when it was located 0.3 m below the surface (0.3×0.3, 0.6×0.3 and 0.9×0.3 m). At all these locations, hot spots started appearing on the thermal images after 48 h when the hot spot temperature was 30°C and 40°C, and after 24 h when the temperature was 50°C and 60°C. The difference between the high temperature region (due to the hot spot) and the surrounding cool grain on the thermal images of the top surface of the grain bulk was 0.4°C to 0.8°C even when the hot spot was at 60°C. Therefore, a slight rise in temperature on the surface of the bulk indicates that a high temperature region is located inside the bulk (Malvik 2002). Even though the average temperature of the grain surface was higher than the ambient temperature, when the hot spots were positioned at deeper locations (>0.3 m), there were no distinguishable spots or high temperature regions on the thermal images of the grain bulk. In a cereal grain bulk, natural air convection does not greatly influence the heat transfer mechanism and conduction is the main form of heat transfer (Smith and Sokhansanj 1989). When the hot spot was positioned at deeper locations it

was not possible to detect it on the thermal images of the top surface of the grain bulk because grain is a good insulator.

5.4.3 Effect of wind

The hot spot was kept at 0.3×0.6 m and 60°C (wherein it was detected on the thermal images of the silo wall at room conditions without wind and cold air) to test the effect of wind on the silo wall. After 48 h of the hot spot establishment, the fan was turned on and the silo was viewed continuously through the thermal camera. Thermal imaging did not detect the hot spot on the silo wall during the tested windy conditions (1.0, 1.5 and 2.0 m/s). However, when the fan was turned off (after blowing air for 30 min) the hot spot reappeared on the thermal images of the silo wall after 5 min when the wind velocity was 1.0 m/s and after 15 min when the wind velocities were 1.5 and 2.0 m/s. Madding (2004) suggested that thermographic survey must be carried out when the wind speed is less than 4.4 m/s. But in our experiments it was observed that thermal imaging was not suitable to detect a hot spot in a grain silo at low wind velocities such as 1 m/s and immediately after wind has died down. In our experiments, the wind was perpendicularly hitting the centroid of the hot spot. Further investigations are required to study the impact of wind while hitting the hot spot at different angles (for example 15, 30, 45, 60, 75, 105, 120, 135 and 180°).

5.4.4 Effect of cold weather

The effect of cold weather on the grain surface and silo wall was studied when the hot spot was kept 0.3 m below the grain surface and 0.3 m from the silo wall. In the first trial, the hot spot was set at 30°C and the outside temperature was 1°C. The hot spot on the thermal images of the grain surface disappeared in the first 30 min and after that the hot

spot was not observed. During the second trial (hot spot = 60°C, outside temperature = 4°C), the hot spot was clearly visible on the thermal images of the grain bulk even after 3 h. With these two preliminary trials, it may not be possible to summarize the effect of cold weather on the grain. However, in general, if the ambient condition is cold and the temperature of the hot spot is slightly higher than the grain temperature, it may not be possible to detect the hot spot on the thermal images of the top surface of the grain bulk. Furthermore, farm silos are always kept closed, whereas our experimental silo was completely kept open and the variations due to this factor must be studied. In the third trial (hot spot = 60°C, outside temperature = −8°C), the hot spot disappeared on the thermal images of the silo wall within 10 min after allowing cold air into the laboratory. Given that the thermal conductivity of GS metal is high, and the temperature difference between the high temperature region due to the hot spot and the surrounding regions on the silo wall was small, it was not possible to detect the hot spot on the thermal images of the silo wall even when the hot spot was located 0.3 m from the silo wall. The combined effect of wind and cold weather must be studied to determine the feasibility of this method for field conditions.

5.4.5 Effect of moisture content of grain

The mean surface temperature of the barley samples was decreased with increasing moisture content. The surface temperature was 25.8, 24.3, 23.4, 22.8 and 22.4°C for the grains with 8, 12, 16, 20 and 24%, respectively when the room temperature was 26°C. The probable reason for low surface temperatures in high moisture grains is due to the increased evaporative cooling. Hand-held thermal imaging devices may be useful to locate the high moisture pockets on or near the surface of the grain bulk in bins.

5.5 Conclusions

Thermal imaging of GS silo was possible only after coating with high emissivity paint. Under laboratory conditions without wind, thermal imaging of a silo wall and the top surface of the grain bulk detected the hot spots located close (0.3 m) to the silo wall or the grain surface or both. If the hot spot is located at greater depths (> 0.3 m), thermal imaging will not detect the hot spots directly. The temperature profile of the silo wall was easily affected by the atmospheric weather variations. Therefore, imaging the surface of the grain bulk might require more information about the grain condition. Preliminary effects of wind velocity were studied using wind directly applied to the hot spot, and the effects of wind from variable directions away from the hot spot wall location were not tested. Hot spots were not detected on the thermal images of the silo wall when the wind velocity was even at 1.0 m/s. Future research could benefit by studying wind effects with the center of wind impact targeted radially at selected distances along the silo wall away from the centroid of the hot spot. When the ambient temperature was low (4 and -8^{o}C) thermal imaging did not detect the hot spot on the silo wall and grain bulk even when the hot spot was positioned at 0.3 m distance. Further study is required to study the combined effect of cold weather and wind on the hot spot detection by thermal imaging. Follow-up research could be beneficial to develop practical applications of thermal image monitoring of grain silos, bins and flat storages for hot spots that are moisture leak or moisture migration related.

5.6 Acknowledgements

We thank the Canada Research Chairs Program and the Natural Sciences and Engineering Research Council of Canada (NSERC) for their financial assistance and Mr.

Matt MacDonald, Department of Biosystems Engineering, University of Manitoba for his help in the fabrication of the heat source.

6. WHEAT CLASS IDENTIFICATION USING THERMAL IMAGING

6.1 Summary

Wheat classes and varieties are determined by trained professionals in the laboratory. Several approaches have been made using machine vision technology for non-destructive and online identification of wheat classes, but the performance has been poor and inconsistent. An infrared thermal imaging system was developed to identify eight western Canadian wheat classes. Samples of 20 g of wheat at 14% moisture content (wet basis) spread in a 100 mm × 100 mm monolayer were heated by a plate heater (90°C) placed at a distance of 10 mm from the grain bulk. The surface temperature of the top surface of the grain bulk was imaged before heating, after heating for 180 s and after cooling for 30 s using an infrared thermal camera (n=100). Temperature rise (after heating) and drop (after cooling) were significantly different for wheat classes (α=0.05). The temperature rise ranged from 14.94 (Canada Western Red Spring) to 17.80°C (Canada Prairie Spring Red) and the drop ranged from 3.67 (Canada Western Extra Strong) to 4.42°C (Canada Prairie Spring Red) after heating for 180 s and cooling for 30 s, respectively. The rate of heating and cooling was negatively correlated with protein content of wheat ($r = -0.63$ for heating, $r = -0.65$ for cooling) and positively correlated with grain hardness ($r = +0.41$ for heating, $r = +0.53$ for cooling). Overall classification accuracies of a quadratic discriminant analysis model while 8 classes mixed, red classes mixed (4 classes), white classes mixed (4 classes) and pairwise (2 classes) comparison were 76, 87, 79 and 95%, and 64, 87, 77 and 91% using bootstrap and leave-one-out validation methods, respectively. To evaluate the suitability of a thermal imaging system in grain handling

facilities, the effect of moisture content of grain bulk on temperature profiles must be studied.

6.2 Introduction

In Canada, wheat class is determined by hardness (hard versus soft), color (red versus white), and growing season (spring versus winter) whereas varieties represent different breeding lines within a class. There are eight major classes of wheat in western Canada and several varieties under each class. Since wheat from each class has different end use, mixing of classes at any stage in handling operations is not allowed. At present, wheat classes and varieties are identified by trained personnel in the laboratory. Polyacrylamide gel electrophoresis (PAGE) and high performance liquid chromatography (HPLC) are two common methods used for the measurement of variety-specific proteins in the laboratory (Canadian Grain Commission 2005a). In routine grain handling operations, most of the grading factors including varietal purity are determined by trained human inspectors (visual inspection). This subjective method of inspection leads to error in several circumstances (Majumdar and Jayas 2000a). A reliable and rapid method is required for online testing of wheat classes. In many situations, quick identification, within a few minutes, is required especially in cases where the load of grain is delivered to a mill or storage facility (Wrigley and Batey 1995).

Several attempts have been made with machine vision technology for online classification of wheat classes and varieties (Neuman et al. 1987; Symons and Fulcher 1988a, 1988b; Zayas et al. 1986). Neuman et al. (1987) used shape features and Fourier descriptors of kernel perimeter to classify western Canada wheat classes. They obtained a classification accuracy of 41.7 to 58.4% for Canada Western Soft White Spring

(CWSWS), 50% for Canada Western Red Winter (CWRW), 54.2% for Canada Prairie Spring (CRS), 75% for Canada Utility (CU) and 100% for Canada Western Red Spring (CWRS) and Canada Western Amber Durum (CWAD) classes of wheat. While discriminating cultivars within classes, they observed a classification accuracy of 15 to 96%. Neuman et al. (1989) classified three Canadian wheat classes (Hard Red Spring (HRS), CWAD and CWSWS) using color features and achieved 62 to 76% accuracy. Symons and Fulcher (1988a) used morphological variations to classify three eastern Canadian wheat classes and obtained a classification accuracy of 64 to 100%. In another study, Symons and Fulcher (1988b) used whole kernel, crease and bran features to identify cultivars within soft white winter wheat and obtained 36 to 100% accuracy. Varieties in different classes of Canadian wheat tend to be relatively uniform in kernel type because of the limited genetic resources used by the breeders (Sapirstein 1995) and hence the classification efficiencies of imaging methods were poor and inconsistent. Zayas et al. (1986) classified three classes of wheat from the USA (Hard Red Winter, Soft Red Winter and Hard Red Spring) and their varieties using kernel length, width, length ratio, tangent, sine and length of arc of parabolic segment, and obtained 77 to 85% accuracy. Myers and Edsall (1989) classified five Australian wheat varieties using size and shape features and obtained a classification accuracy of 44 to 96%.

Most of the above mentioned approaches used kernel morphological features of a single grain for variety and class identification. In some cases, the images were taken by keeping the grain in a fixed orientation. Classification systems strictly based on morphological features would yield error when the kernel characteristics show plasticity in response to the environment (Symons and Fulcher 1988a). It would be highly desirable

to have an alternative method for online classification of wheat classes and varieties, which may use some characteristics of the kernels other than morphological features. A simple variety identification system with less complexity for bulk sample testing (not single grain analysis) would be most desirable in the grain handling facilities (Lookhart et al. 1995). Therefore, the objective of this study was to develop and evaluate the feasibility of a thermal imaging technique to identify western Canadian wheat classes by bulk sample analysis.

6.2.1 Thermal imaging

Thermal imaging is a method in which the invisible radiation pattern (temperature) of an object is converted into a visible image. The region in the infrared band with wavelengths from 3 to 14 μm is called the thermal infrared region. This band is useful in imaging applications that use heat signatures (Gonzalez and Woods 2002). An infrared thermal imaging system provides the surface temperature (2D mapping) of any object and these data may be used directly or indirectly for many applications. This technique has been widely used for various applications in the pre-harvest and post-harvest agricultural operations. Plant, soil, and water relationships by thermal imaging were studied in detail and the outcome of this kind of research would yield valuable information required for the site specific management and precision farming (Egnell and Orlander 1993; Christoph et al. 2002; Jones 1999; Smith et al. 1985). Similarly, the capability of thermal imaging has potential for various post-harvest operations such as identification of fruits on trees for mechanical harvesting, maturity evaluation, detection of bruises in fruits and vegetables, and detection of spoilage by microbial activities (Stajnko et al. 2004; Danno

et al. 1978, 1980; Varith et al. 2003). Thermal imaging has the potential to classify agricultural materials based on various parameters such as rate of heating and cooling.

6.3 Materials and Methods

6.3.1 Grain samples

All major wheat classes cultivated in western Canada were tested in this study. Canada Prairie Spring Red, CPSR (variety: Crystal CPS Red); Canada Prairie Spring White, CPSW (AC Vista); Canada Western Extra Strong, CWES (CDC Rama); Canada Western Hard White Winter, CWHW (Snowbird); CWRS (AC Barrie); CWAD (Strong field durum); CWRW (CDC Falcon); and CWSWS (AC Andrew) classes of wheat were obtained from the seed producers in the provinces of Manitoba and Alberta. Wheat samples from all the classes were reconditioned to 14% moisture content (wet basis) before the experiments.

6.3.2 Image acquisition and analysis

The experimental set up for the developed thermal imaging system is shown in Fig. 6.1. An un-cooled focal plane array type infrared thermal camera (Model: ThermaCAM ™ SC500 of FLIR systems, Burlington, Ontario, Canada) with 320×240 pixels and a spectral range of 7.5 to 13.0 μm was used. The thermal resolution of the camera was 0.07°C at 30°C. Twenty grams of grain sample were taken and spread in a single layer (100 mm × 100 mm) on the base of the copymate camera stand (Model: Copymate II copystand 900-20 SC, Bencher Inc., Antioch, IL) . The temperature of the base was maintained at 30±0.5°C before placing the sample. A plate heater with temperature control mechanism was developed and used in this study. A steel plate (175 mm × 175 mm × 2 mm) was heated by a heat tape and the temperature of the bottom surface of the

plate was measured by a thermocouple and controlled using a PID temperature controller. The plate heater was fixed on a stand using a hinge joint which provided a swing motion. The wheat sample was heated by the plate heater, set at 90°C, for 180 s. Then the heater was swung away from the grain surface and the grain was allowed to cool for the next 30 s. The distance between the top surface of the grain bulk and the bottom surface of the heater was 10 mm during heating. Three thermal images were taken for each sample: 1. before heating, 2. after heating (for 180 s), 3. after cooling (for 30 s). With 100 replications, in total 2400 thermal images (3 images per sample × 100 replications per class × 8 classes) were taken and analyzed.

The size of the original image was 320×240 pixels, in which the grains occupied 205×182 pixels. Algorithms were developed in Matlab 7.1 to extract temperature data (205×182=37,310 temperature values) of the grain region from all images automatically. Mean, maximum, minimum, median, mode and standard deviations of the surface temperatures of the grain bulk were extracted from the thermal images.

6.3.3 Model development for classification

A quadratic discriminant analysis (QDA) model was developed to classify the western Canadian wheat classes based on temperature data. The details of the feature set (derived data) used in the classification model are explained in Table 6.1.

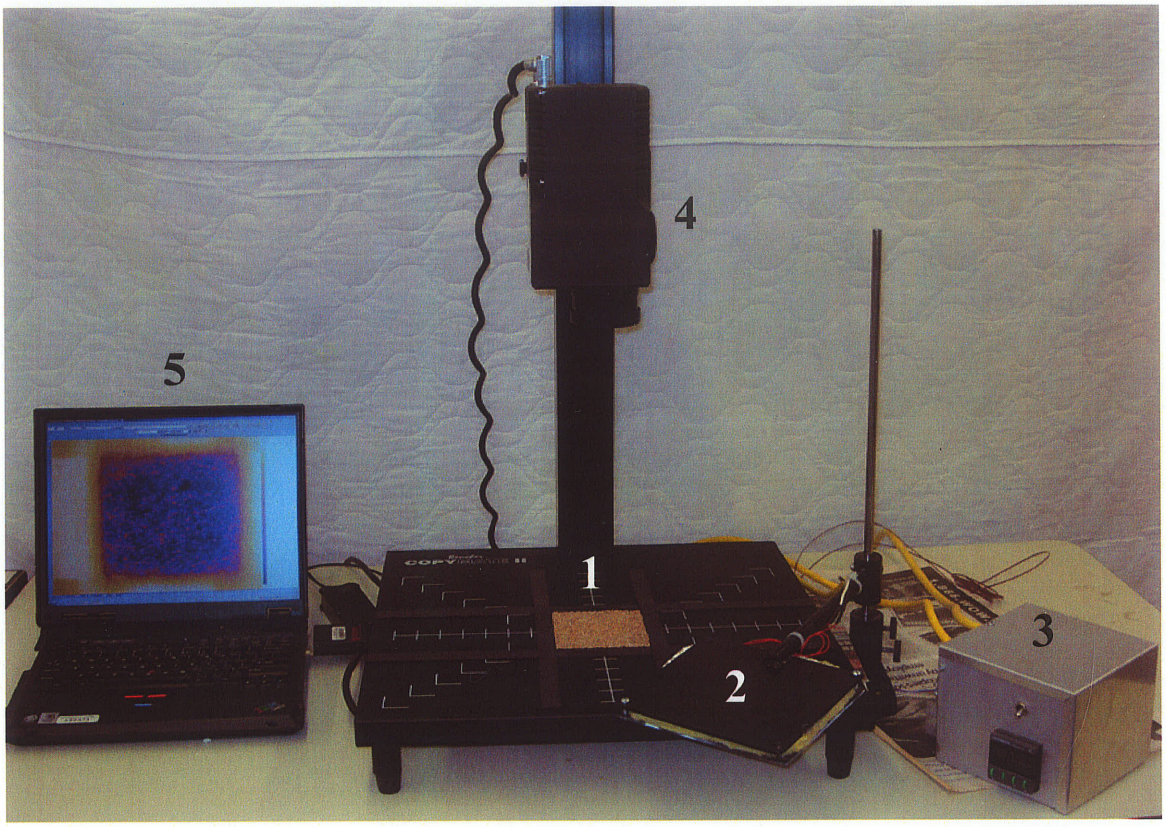

Figure 6.1 **Experimental setup of a thermal imaging system to identify wheat classes.**
1. wheat sample 2. heater 3. temperature control system 4. thermal camera 5. data acquisition system

Table 6.1 Derived features (from thermal data) used for classification model.

Name	Description
ΔT_{Hmean}	(mean surface temperature of grain bulk after heating) – (mean surface temperature of grain bulk before heating)
$\Delta T_{Hmedian}$	(median of surface temperatures of grain bulk after heating) – (median of surface temperatures of grain bulk before heating)
ΔT_{Hmode}	(mode of surface temperatures of grain bulk after heating) – (mode of surface temperatures of grain bulk before heating)
ΔT_{Hmax}	(maximum surface temperature of grain bulk after heating) – (maximum surface temperature of grain bulk before heating)
ΔT_{Hmin}	(minimum surface temperature of grain bulk after heating) – (minimum surface temperature of grain bulk before heating)
ΔT_{Hsd}	(standard deviation of surface temperatures of grain bulk after heating) – (standard deviation of surface temperatures of grain bulk before heating)
ΔT_{Cmean}	(mean surface temperature of grain bulk after heating) – (mean surface temperature of grain bulk after cooling)
$\Delta T_{Cmedian}$	(median of surface temperatures of grain bulk after heating) – (median of surface temperatures of grain bulk after cooling)
ΔT_{Cmode}	(mode of surface temperatures of grain bulk after heating) – (mode of surface temperatures of grain bulk after cooling)
ΔT_{Cmax}	(maximum surface temperature of grain bulk after heating) – (maximum surface temperature of grain bulk after cooling)
ΔT_{Cmin}	(minimum surface temperature of grain bulk after heating) – (minimum surface temperature of grain bulk after cooling)
ΔT_{Csd}	(standard deviation of surface temperatures of grain bulk after heating) – (standard deviation of surface temperatures of grain bulk after cooling)

The PROC DISCRIM procedure in SAS (version 9.3, SAS Institute Inc., Cary, NC) was used for the development of QDA models. The PROC DISCRIM calculates the generalized squared distance and then each observation is assigned a probability of belonging to a given group based on the generalized squared distance from the group mean. In a quadratic discriminant function, the classification criterion is based on the individual within-group covariance matrices. Leave-one-out and bootstrap methods were used for the validation of the developed discriminant function. In bootstrap analysis, 1000 bootstrap samples, each with 50 observations were created. Further details about these two methods of validation have been explained by Balasubramanian et al. (2004).

Three types of discriminant analyses were conducted using a QDA model: (i) 8 classes mixed; (ii) red and white classes separately (4 classes mixed); and (iii) pairwise comparison in red and white classes (2 classes mixed).

6.4 Results and Discussion

Generally, agricultural materials reach thermal equilibrium with respect to environment within a short time. While developing classification systems by thermal imaging, it is essential to create a suitable thermal environment for better classification. For instance, the rate of heating or cooling may be used to classify objects, or to identify the abnormality within an object. Varith et al. (2003) used heating and cooling treatments with forced air to detect the bruises in apples. Vanlinden et al. (2003) used microwave heating to detect bruises in tomato. Danno et al. (1978) used heating and cooling treatments before thermal imaging to determine the maturity of fruits and vegetables.

In the preliminary trials for this study, super heated steam and microwave heating was tested for their capability to identify the wheat classes. After heating with super heated steam (temperature=150°C, pressure=7 kPa, velocity=1 m/s) for 60 s, the grain temperature increased to 130°C, but still there were several overlaps between various classes. Non-uniform pattern of heating within a sample due to the nature of microwaves was the major problem associated with microwave heating. So in view of practical feasibility at grain handling facilities, a simple plate heater with a temperature control mechanism was fabricated and used.

6.4.1 Rate of heating and cooling

Temperature rise, drop and other temperature features after heating and cooling of different wheat classes are given in Tables 6.2 and 6.3.

Table 6.2 Temperature features (°C) in different classes of wheat after heating for 180 s.

Class†	ΔT_{Hmean}	ΔT_{Hmax}	ΔT_{Hmin}	$\Delta T_{Hmedian}$	ΔT_{Hmode}	ΔT_{Hsd}
CWAD	16.28^{a}* ±0.67**	16.94^{a} ±1.02	13.22^{a} ±0.80	16.46^{a} ±0.69	16.74^{a} ±0.75	0.50^{a} ±0.16
CWES	15.35^{b} ±1.08	16.52^{b} ±1.06	12.14^{bd} ±1.38	15.51^{b} ±1.10	15.79^{b} ±1.20	0.53^{ab} ±0.23
CWHW	15.77^{c} ±0.41	16.65^{b} ±0.75	12.46^{c} ±0.45	15.95^{c} ±0.42	16.25^{c} ±0.49	0.57^{b} ±0.10
CPSW	16.21^{a} ±1.23	18.32^{c} ±2.33	12.45^{bc} ±0.74	16.35^{a} ±1.25	16.63^{a} ±1.30	0.81^{c} ±0.25
CWRS	14.94^{d} ±0.75	15.95^{d} ±0.66	12.08^{d} ±1.12	15.08^{d} ±0.76	15.32^{d} ±0.79	0.54^{ab} ±0.21
CWRW	15.68^{c} ±1.13	16.86^{ab} ±1.77	12.46^{c} ±0.81	15.80^{bc} ±1.13	16.00^{b} ±1.15	0.56^{b} ±0.16
CPSR	17.80^{e} ±0.80	19.80^{e} ±2.29	13.86^{e} ±0.78	17.95^{e} ±0.80	18.26^{e} ±0.92	0.84^{c} ±0.28
CWSWS	16.39^{a} ±0.44	17.54^{f} ±1.83	12.92^{f} ±0.69	16.56^{a} ±0.45	16.78^{a} ±0.55	0.68^{d} ±0.31

† CWAD-Canada Western Amber Durum, CWES-Canada Western Extra Strong, CWHW-Canada Western Hard White Winter, CPSW-Canada Prairie Spring White, CWRS-Canada Western Red Spring, CWRW-Canada Western Red Winter, CPSR-Canada Prairie Spring Red, CWSWS-Canada Western Soft White Spring

* values with same letters in a column are not significantly different (α=0.05) by t test, ** standard deviation (n=100)

Table 6.3 Temperature features (°C) in different classes of wheat after cooling for 30 s.

Class†	ΔT_{Cmean}	ΔT_{Cmax}	ΔT_{Cmin}	$\Delta T_{Cmedian}$	ΔT_{Cmode}	ΔT_{Csd}
CWAD	3.87^{a}* ±0.24**	5.28^{ad} ±0.54	2.32^{a} ±0.28	3.90^{ae} ±0.25	3.93^{a} ±0.35	0.41^{a} ±0.07
CWES	3.67^{b} ±0.25	5.13^{ac} ±0.61	2.08^{b} ±0.36	3.68^{b}±0.25	3.70^{b} ±0.39	0.38^{b} ±0.09
CWHW	3.71^{b} ±0.18	5.15^{a} ±0.48	2.35^{a} ±0.28	3.70^{b} ±0.18	3.66^{b} ±0.32	0.35^{c} ±0.04
CPSW	3.91^{ad} ±0.47	5.68^{b} ±1.16	2.18^{c} ±0.28	3.91^{ae} ±0.48	3.87^{ac} ±0.59	0.45^{de} ±0.13
CWRS	3.71^{b} ±0.21	5.00^{c} ±0.51	2.24^{ce} ±0.28	3.73^{bc} ±0.21	3.70^{b} ±0.34	0.37^{bc} ±0.10
CWRW	3.83^{a} ±0.43	5.36^{df}±0.94	2.34^{a} ±0.34	3.81^{ac} ±0.43	3.73^{bc} ±0.48	0.35^{bc} ±0.08
CPSR	4.42^{e} ±0.34	6.28^{e} ±1.00	2.78^{d} ±0.36	4.41^{d} ±0.35	4.40^{d} ±0.51	0.46^{df} ±0.11
CWSWS	3.95^{d} ±0.27	5.48^{bf} ±0.71	2.28^{ae} ±0.29	3.95^{e} ±0.28	3.86^{a} ±0.39	0.45^{ef} ±0.11

† CWAD-Canada Western Amber Durum, CWES-Canada Western Extra Strong, CWHW-Canada Western Hard White Winter, CPSW-Canada Prairie Spring White, CWRS-Canada Western Red Spring, CWRW-Canada Western Red Winter, CPSR-Canada Prairie Spring Red, CWSWS-Canada Western Soft White Spring

* values with same letters in a column are not significantly different (α=0.05) by t test, ** standard deviation (n=100)

Temperature profiles of different wheat classes after heating for 180 s and cooling for 30 s were significantly different (α=0.05). The mean value of the temperature rise ranged between 14.94 (CWRS) to 17.80°C (CPSR). However, there were overlaps between some classes. For instance, there were no significant differences in mean temperature rise between CWAD, CPSW and CWSWS; and CWHW and CWRW. But the ΔT_{Hmax} was significantly different for CWAD, CPSW and CWSWS, and ΔT_{Hmode} was different for CWHW and CWRW. The temperature rise of CPSR was unique and did not overlap with any other wheat class by all parameters except ΔT_{Hsd}. There were many overlaps in ΔT_{Hsd} and resulted in least number of clusters by t test statistics.

Temperature drop (ΔT_{Cmean}) after cooling for 30 s was in the range of 3.67 (CWES) to 4.42°C (CPSR). There were many overlaps in derived cooling features between various classes of wheat. In temperature drop analysis, ΔT_{Csd} and ΔT_{Cmax} formed maximum number of clusters by t test statistics. In all features, the number of clusters was higher (or equal) in temperature rise data set than in temperature drop data set except ΔT_{Csd}. It may not be possible to determine the exact reason for the variations in temperature profiles among different classes, because several constituents are present in the seed coat, endosperm and germ of a wheat kernel. We analyzed the reasons for the variations in temperature profiles using three approaches: (i) specific heat of wheat; (ii) wheat quality; and (iii) starch distribution.

6.4.2 Relationship between specific heat and temperature rise

In non-biological materials, the temperature rise due to an external heating source can be easily calculated using empirical equations as thermal properties are well defined, whereas it is not easy for biological materials. In general, the temperature rise (ΔT) in

wheat samples after heating is mainly dependent on the specific heat (C_p) of different classes as the heat gained (Q) and the mass (M) of the sample are constant (Eqn. 6.1).

$$\Delta T = \frac{Q}{M(C_p)} \tag{6.1}$$

Singh and Heldman (1993) suggested the following formula (Eqn. 6.2) to determine the specific heat for the products with known composition.

$$C_p = 1.424m_c + 1.549m_p + 1.675m_f + 0.837m_a + 4.187m_m \tag{6.2}$$

where C_p is specific heat, m is mass fraction, and the subscripts are: c, carbohydrate; p, protein; f, fat; a, ash; and m, moisture content. The specific heat of different wheat classes were determined by substituting the measured values in Eqn. 6.2. The calculated specific heat of samples from 8 classes at 14% moisture content was in the range of 1.8213 to 1.8309 kJ/kg °C. This result was within the range of the specific heat of different Canadian and American wheat varieties at 14% moisture content listed by Mohsenin (1980) which was between 1.6652 and 2.092 kJ/kg °C. The temperature rise of each class after heating for 180 s was compared with its specific heat. As expected, the temperature rise was inversely proportional to the specific heat and the correlation coefficient was −0.64. The probable reason for not obtaining high correlation is due to the complex structure in protein and other constituents within various classes as explained in the following section.

6.4.3 Relationship between quality and temperature rise

Some common quality parameters were measured for the wheat samples taken from the same lots used in this study. The correlation between rate of heating and cooling, with different quality parameters are given in Table 6.4. Among the tested parameters, the correlation coefficients between the temperature variations and quality ranged between

0.17 and 0.65. Many qualities of wheat are mainly determined by the amount of protein. Similarly, in this study also, the rate of heating and cooling had the highest correlation with the flour protein ($r = -0.63$ and -0.65 for temperature rise and drop, respectively). However, it is difficult to define the exact relationship between the temperature variations and protein content as there are several types of protein present in each class. For example, in a recent study, Mark et al. (2006) have characterized 612 types of protein in wheat germ of an Australian cultivar. Out of this, 347 individual proteins were identified from protein sequence database and the remaining 265 proteins gave no matches to the protein in the databases.

All over the world, researchers have been working to characterize the wheat protein for different cultivars. In general, based on solubility wheat protein can be broadly classified into four types namely, glutenin (soluble in dilute acid or alkali), gliadin (soluble in 70% ethanol), globulin (soluble in salt solution), and albumins (soluble in water) (Sun 2002). Glutenin and gliadin are the major constituents in wheat protein. Gliadins are made of single-chained protein with intermolecular disulfide bond linkages, whereas glutenins are multi-chained polymers (Daniels and Frazier 1976). The variations in wheat properties are basically determined by the structure, amount and the proportion of different gluten protein (glutenin and gliadin), amount and types of sub-units of glutenin and gliadin, molecular weight distribution and the ratio of gliadin/glutenin polymers (Kasarda 1989).

Table 6.4 **Relationship (correlation coefficients) between rate of heating (ΔT_{Hmean}) and cooling (ΔT_{Cmean}), and different quality parameters of wheat.**

to → / from ↓	PSI	FPRO	LECOG	WSV	FASH	FC-L	FC-A	FC-B	MDT	ETP	PBW	SAP
ΔT_{Hmean}	0.41	−0.63	−0.59	−0.39	0.38	−0.34	0.26	0.2	−0.57	−0.54	0.27	−0.48
ΔT_{Cmean}	0.53	−0.65	−0.65	−0.38	0.19	−0.2	−0.2	−0.2	−0.37	−0.41	0.17	−0.36

PSI =Particle size index (a measure of kernel hardness)
FPRO =Flour protein
LECOG =Leco protein
WSV =Sodium dodecyl sedimentation
FASH =Flour ash
FC-L =Flour color L (minolta, light-dark)
FC-A =Flour color a (minolta, red-green)
FC-B =Flour color b (minolta, yellow-blue)

Mixograph parameters
MDT = Mixo development time
ETP = Energy to peak
PBW = Peak band width
SAP = Slope 1 min after peak

The detailed protein characterization for all wheat varieties used in this study is not available. Sapirstein and Fu (1998) reported different types of glutenin in six Canadian wheat classes. It was stated that soluble and insoluble glutenin were significantly different for different classes. We obtained a correlation coefficient of −0.82 while comparing the temperature rise with the ratio of soluble to insoluble glutenin of four classes (CWRS, CWES, CPSW and CWSWS) taken from Sapirstein and Fu (1998). Hence in addition to total protein content, the types of protein might have contributed for the variations in temperature profiles among different classes.

6.4.4 Relationship between starch distribution and temperature rise

The microscopic images (taken using an optical microscope, model SMZ 10, Nikon Inc., Tokyo, Japan) of the cross sectional views of eight wheat classes used in this study are given in Fig. 6.2. In general, if the starch accumulation was observed near the seed coat, then the temperature rise was high. In CPSR wheat, the starch granules were evenly distributed almost all over the cross sectional surface and its temperature rise was maximum amongst all classes. Even though the starch granules were densely packed in the lower end of the crease in CWSWS, sparse packing was observed evenly all over the cross section. In CWAD wheat, dense distribution of starch was found as a layer along the seed coat, and hence might have recorded a temperature rise of 16.28°C. On the lower end, the ΔT_{Hmean} for CWES and CWRS was 15.35 and 14.94, respectively. The packing was different in CWES than the rest of the classes and starch granules were randomly found in small patches across the cross section.

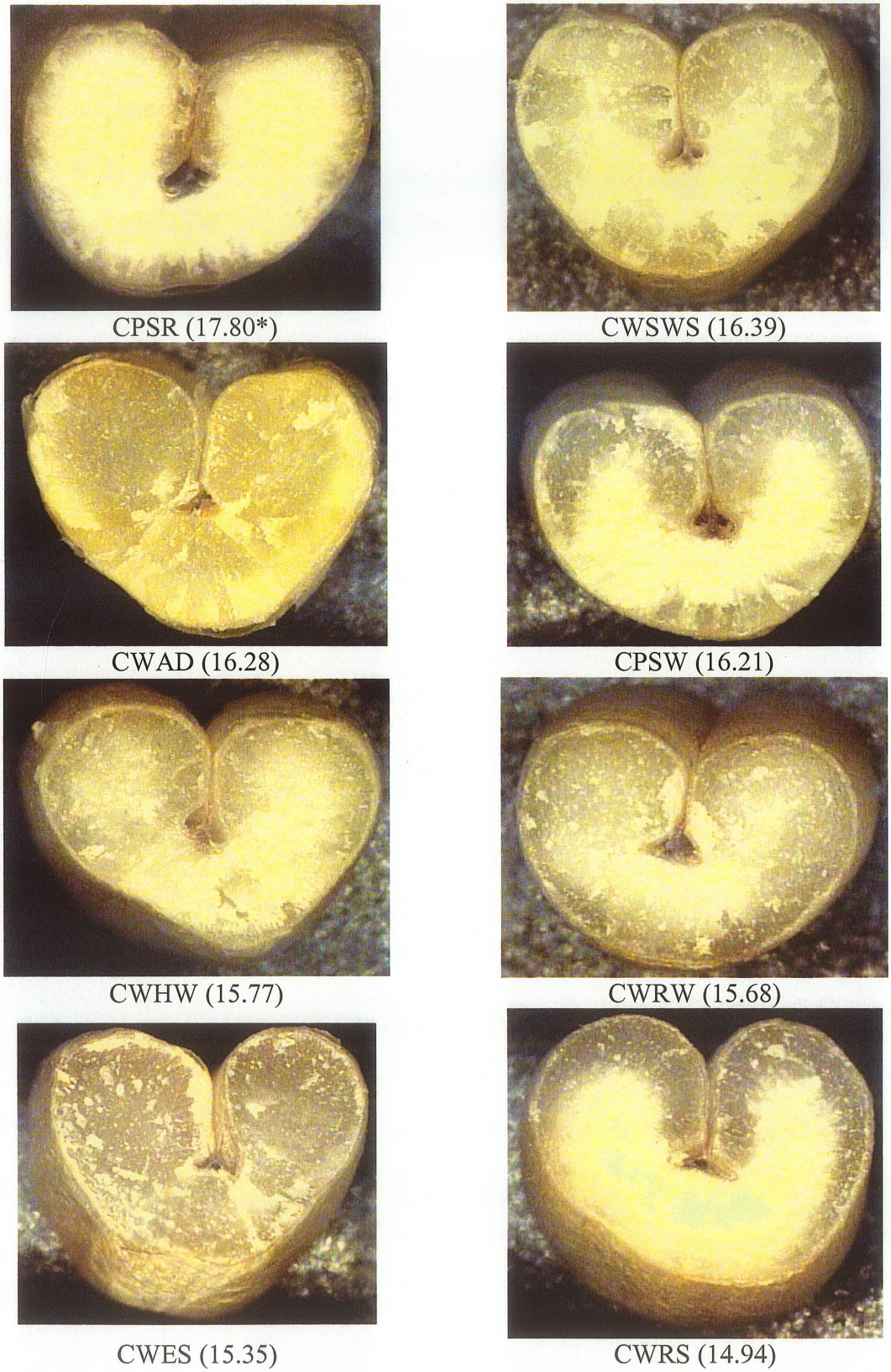

Figure 6.2 Cross sectional view of different classes of wheat kernels.
* mean temperature rise (ΔT_{Hmean}) °C

In spite of a dense layer of starch in the middle of the cross section of CWRS wheat, no spread was noticed near the seed coat especially at the crease end. However in all classes, it was not possible to quantify the temperature rise with respect to starch distribution. Among the compared parameters, none of the single factors had good correlation with the temperature rise. So the temperature rise may be due to the combined effect of various factors with major contribution from protein.

6.4.5 Classification using QDA

For the classification of agricultural and food materials, statistical (parametric and non-parametric) and artificial neural network (ANN) classifiers have been widely used (Visen et al. 2004; Majumdar and Jayas 2000b; Balasubramanian et al. 2004). The selection of the best classifier for a particular application generally involves some degree of experimentation (Jayas et al. 2000; Luo et al. 1999). In this paper the classification performance of a quadratic discriminant function with two validation techniques is discussed.

6.4.5.1 ***Ranking of features*** The ranking of the temperature features based on their contribution to the classification model is given in Table 6.5. This ranking was made using PROC STEPDISC in SAS (version 9.3, SAS Institute Inc., Cary, NC). In STEPDISC analysis, the ranking of various features are determined by correlation coefficients and average squared canonical correlation (Majumdar and Jayas 2000a). Even though overlapping was observed in ΔT_{Hsd} by t test statistics, it obtained the second rank after ΔT_{Hmean}. Out of the top 6 most important features, four were from the derived features after cooling. As indicated in Table 6.3, more variation among classes was obtained in ΔT_{Csd} and it came first in derived cooling features.

6.4.5.2 ***Classification of eight classes*** The classification accuracies of a QDA using bootstrap and leave-one-out validations are given in Tables 6.6 and 6.7. When eight classes were mixed, the classification accuracy of a QDA model ranged from 54 to 88% by bootstrap validation and 40 to 84% by leave-one-out validation. For all classes, the bootstrap validation yielded higher accuracy. In both methods, the classification accuracy was the highest for CPSR and the lowest for CPSW classes. The temperature profiles of CPSR after heating was different from other classes of wheat (Table 6.2) and hence classified with the highest accuracy. The quality of CPSW has been inconsistent due to the availability of limited varieties and variations in biotypes. In some growing regions, the color of this class varies between white and red (Myl Subramaniam, Personal communication, Technical Specialist - Milling Technology, Canadian International Grains Institute, Winnipeg, Manitoba, Canada). The quality of this '3-medium' category (medium protein, medium gluten strength and medium kernel hardness) overlaps with other classes and might have yielded the lowest classification accuracy.

While classifying four Canadian wheat classes using shape characteristics, Neuman et al. (1987) observed significant confusions (more than 50%) between CWSWS and CWRW. Even when they attempted to classify these two classes by pairwise discrimination, satisfactory classification was not achieved. But in our study, there was no misclassification from CWRW to CWSWS and CWSWS to CWRW even when 8 classes were mixed in both validation methods. Thermal imaging has the potential to yield better classification in situations where other machine vision approaches have yielded significant confusions. However, in our eight classes discrimination,

misclassification from one class to several other classes was observed. For instance, CWHW was misclassified to all other 7 classes in leave-one-out validation.

Table 6.5 Ranking of temperature features of wheat classes on the basis of their level of contribution to the classifier using STEPDISC analysis.

No.	Temperature features	Partial r^2
1	ΔT_{Hmean}	0.47
2	ΔT_{Hsd}	0.16
3	ΔT_{Csd}	0.21
4	ΔT_{Cmean}	0.17
5	$\Delta T_{Cmedian}$	0.21
6	ΔT_{Cmin}	0.09
7	ΔT_{Hmin}	0.10
8	ΔT_{Hmax}	0.09
9	$\Delta T_{Hmedian}$	0.04
10	ΔT_{Hmode}	0.02
11	ΔT_{Cmax}	0.02
12	ΔT_{Cmode}	0.006

Table 6.6 **Classification accuracies (%) for wheat (8 classes mixed) using QDA by bootstrap validation.**

Class to from → ↓	CWAD	CWES	CWHW	CPSW	CWRS	CWRW	CPSR	CWSWS
CWAD	**85**	2	4	1	2	0	1	5
CWES	11	**57**	14	1	10	4	0	3
CWHW	1	4	**81**	1	4	6	0	3
CPSW	0	1	4	**54**	9	16	4	12
CWRS	4	9	6	0	**81**	0	0	0
CWRW	3	4	4	6	2	**76**	5	0
CPSR	2	0	3	3	0	4	**88**	0
CWSWS	4	5	2	3	2	0	0	**84**

Table 6.7 **Classification accuracies (%) for wheat (8 classes mixed) using QDA by leave-one-out validation.**

Class to from → ↓	CWAD	CWES	CWHW	CPSW	CWRS	CWRW	CPSR	CWSWS
CWAD	**67**	6	6	2	5	0	3	11
CWES	14	**45**	15	4	14	4	0	4
CWHW	3	7	**65**	2	6	12	2	3
CPSW	0	5	4	**40**	12	16	6	17
CWRS	4	13	6	2	**72**	2	0	1
CWRW	3	8	4	8	4	**66**	7	0
CPSR	4	0	3	4	0	5	**84**	0
CWSWS	8	9	2	8	2	0	1	**70**

6.4.5.3 ***Classification of four classes*** The overall classification accuracy was improved in both validation methods while red and white classes where analyzed separately (4 classes mixed in red wheat and 4 classes mixed in white wheat). The classification accuracy was between 78 and 90% for white wheat and, 76 and 95% for red wheat by bootstrap validation and, 72 and 79% for white wheat and 69 and 94% for red wheat by leave-one-out validation (Tables 6.8 to 6.11). In both validation techniques, significant confusion existed between CWRS and CWES classes. Even though the total protein content of these two classes was different, overlapping in thermal behavior might be due to the similarities in protein types or structures. Sun (2002) reported that there were no significant differences in soluble glutenin and ratio of insoluble to soluble glutenin between CWES and CWRS classes of wheat. The CPSR was the most correctly classified class in red wheat analysis. Significant misclassification of CPSW to CWHW and CWSWS was observed in both validation techniques during white class discrimination. Furthermore, all white classes were misclassified to all other 3 classes (at least 1) in both validation methods. Symons and Fulcher (1988a) observed significant misclassification from hard red spring (similar to CWRS) to hard red winter of eastern Canada (similar to CWRW) while classifying using kernel morphological variations. But in our four classes discrimination (red wheat) by bootstrap validation, only 1% CWRS was misclassified to CWRW and 2% CWRW was misclassified to CWRS.

6.4.5.4 ***Classification of two classes*** In pairwise discrimination, two classes were mixed and analyzed (within red and within white classes). The classification accuracy of a QDA model ranged from 80 to 100% by bootstrap validation and 74 to 100% by leave-one-out validation (Fig. 6.3). CWRS and CWES were correctly classified (100%

accuracy) while comparing with CPSR in both validation methods. The pair with maximum misclassification was CWES and CWRS. In pairwise discrimination, the classification accuracy of all classes was more than 80% except for CWES. Wrigley and Batey (1995) described three scenarios associated with the need for variety identification method: (i) is this variety A?; (ii) is this variety A or variety B?; and (iii) what is it?. The thermal imaging approach has potential to find the answer to question (ii).

Table 6.8 **Classification accuracies (%) for red wheat (4 classes mixed) using QDA by bootstrap validation.**

Class to from → ↓	CWES	CWRS	CWRW	CPSR
CWES	**76**	18	6	0
CWRS	10	**89**	1	0
CWRW	6	2	**87**	5
CPSR	1	0	4	**95**

Table 6.9 **Classification accuracies (%) for red wheat (4 classes mixed) using QDA by leave-one-out validation.**

Class to from → ↓	CWES	CWRS	CWRW	CPSR
CWES	**69**	24	7	0
CWRS	17	**77**	6	0
CWRW	11	4	**77**	8
CPSR	1	0	5	**94**

Table 6.10 **Classification accuracies (%) for white wheat (4 classes mixed) using QDA by bootstrap validation.**

Class to from → ↓	CWAD	CWHW	CPSW	CWSWS
CWAD	**90**	4	1	5
CWHW	3	**93**	1	3
CPSW	1	9	**78**	12
CWSWS	6	3	3	**88**

Table 6.11 **Classification accuracies (%) for white wheat (4 classes mixed) using QDA by leave-one-out validation.**

Class to from → ↓	CWAD	CWHW	CPSW	CWSWS
CWAD	**79**	8	2	11
CWHW	6	**79**	10	5
CPSW	1	10	**72**	17
CWSWS	10	4	9	**77**

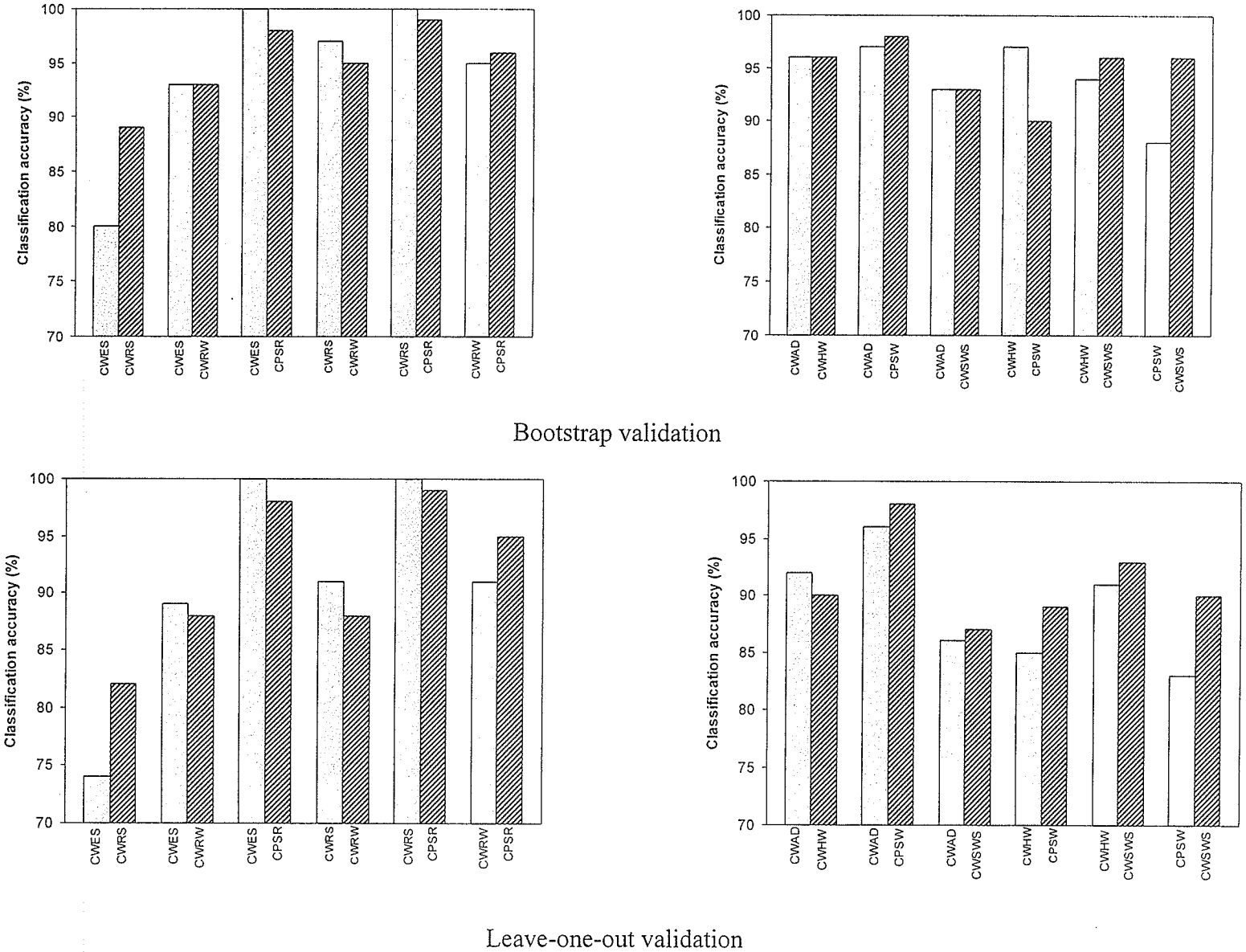

Figure 6.3 Pairwise discrimination of wheat classes (red and white) by bootstrap and leave-one-out validations.

6.5 Potential Applications

Non-registered varieties do not qualify for the top grades of Canadian wheat. Their presence in top grades in excess of grade tolerances can result in the downgrading of shipments. For example, Alsen is a non-registered wheat variety in Canada and would be eligible for feed grades only. Since Alsen looks like other CWRS varieties, it is visually indistinguishable from registered varieties which are eligible for the CWRS class (Canadian Grain Commission 2003). Because some non-registered varieties are indistinguishable from eligible varieties, monitoring relies on the use of protein or DNA-based variety identification methods. For example, the protein electrophoresis method used at the Canadian Grain Commission, can identify one of two biotypes of the non-registered variety Alsen; the second biotype is indistinguishable from the electrophoretic pattern of a registered CWRS variety, it needs further testing by a DNA-based microsatellite method (Brigitte Dupuis, Personal communication, Program Manager, Variety Identification Monitoring, Grain Research Laboratory, Canadian Grain Commission, Winnipeg, Manitoba, Canada). Thermal imaging has the potential to resolve such aforementioned scenarios (indistinguishable by visual inspection and challenges in biochemical methods).

There were significant misclassifications when eight classes were mixed together. However, this kind of situation is not common in grain handling facilities. Under many circumstances, grain inspectors have difficulty in identifying the non-registered varieties which look like a registered variety. Since higher accuracies (90 to 95%) were obtained in pairwise discriminations, specific procedures can be developed for the confusing varieties (studies are currently underway in our lab).

6.6 Further Work

In this study, one common variety from each class was selected to represent that class. Thermal behavior (during heating and cooling) of other varieties within a class must be studied. All wheat classes were conditioned to a constant moisture content (14%) before the experiments. The temperature rise and drop with respect to moisture content should also be analyzed before developing thermal imaging system for grain handling facilities. In addition to quality of wheat, the temperature rise and drop in wheat bulk would be determined by several other parameters such as heating methods, heating time and temperature of the heat source. It may not be possible to develop universal methods to identify different wheat varieties and classes. Wheat grown in various regions might require different protocols for identifications.

6.7 Acknowledgements

We thank the Canada Research Chairs Program and the Natural Sciences and Engineering Research Council of Canada (NSERC) for their partial financial assistance and Ms. Kelly Griffiths and Ms. Caroline Shields for their help in sample preparation and data collection processes.

7. THERMAL IMAGING TO DETECT INFESTATION BY *CRYPTOLESTES FERRUGINEUS* INSIDE WHEAT KERNELS

7.1 Summary

Canada's zero tolerance for live grain-feeding insects in grain received from farmers, and shipped to domestic and export buyers, has necessitated the development of an accurate insect detection method. An infrared thermal imaging system was developed to detect infestation by six developmental stages of *Cryptolestes ferrugineus* under the seed coat on the germ of wheat kernels. Canada Western Red Spring (CWRS) wheat was artificially infested with *C. ferrugineus* eggs and incubated at 30°C and 70% RH (n=283). The infested kernels were removed from the incubation room and thermally imaged using an infrared thermal camera to identify each developmental stage (four larval instars, pupae and adults). Before imaging, each kernel was refrigerated (5°C) for 60 s and then kept at the ambient condition for 20 s. The uninfested (control) kernels were also stored in the incubation room and thermally imaged along with the infested kernels in a similar manner. Algorithms were developed to extract the temperature values of the grain surface automatically from all thermal images. The mean of the highest 5 and 10% temperature values on the surface of the grain was significantly higher (α=0.05) for grains having young larvae inside and lower for grains having pupae inside. Temperature distribution on the surface of the infested kernels with different stages of *C. ferrugineus* was highly correlated with the respiration efficiency of each developmental stage (r = 0.83 to 0.91). Twenty five thermal features were obtained from thermal data of the grain, and classified using quadratic and linear discriminant functions with leave-one-out validation. In pairwise discrimination (each developmental stage vs control), the overall classification accuracy for a quadratic discriminant analysis method was 83.5 and 77.7% for infested and sound kernels, respectively, and for a linear discriminant analysis method, it was 77.6

and 83.0% for infested and sound kernels, respectively. Thermal behavior of infested kernels with other insect species must be studied before developing a broadly based insect detection method using thermal imaging for grain handling facilities.

7.2 Introduction

Canada produces an average of 25 Mt of wheat every year, which is 49% of the nation's total grain production, and about 74% of the produced wheat is exported (Canadian Wheat Board 2005). *Cryptolestes ferrugineus* (Stephens) (Coleoptera: Cucujidae), the rusty grain beetle is the most common and serious insect of stored grain in western Canada (Agriculture and Agri-Food Canada 2002). An adult female lays 2 to 3 eggs per day and about 400 eggs in its life time (Smith 1965). If the storage environment is favorable, the insect population can multiply 60-fold in a month. In some storage seasons, the infestation by this species is severe in Canada. For example, during 1983, up to 45% of farm granaries in Manitoba were infested by *C. ferrugineus* (Agriculture and Agri-Food Canada 2002). If the grain is infested with one or more detectable live stored-product insects, then it is not allowed to enter the Canadian grain handling system. To meet this high standard, there is a need to develop a quick and reliable insect detection method. Though many researchers have investigated the capabilities of several techniques such as, acoustic monitoring (Adams et al. 1954), chemicals (Dennis and Decker 1962), near infrared spectroscopy (Dowell et al. 1998; Paliwal et al. 2004), and X-ray (Karunakaran et al. 2004b) to detect infestation in grains, the "Berlese funnel" method is still commonly used in Canadian grain handling facilities (Canadian Grain Commission 2005) where 1 kg of grain is placed under a heat source for 6 h.

Smith (1977) reported that a Berlese funnel recovered 3.4 to 35% of first and second instar larvae (free living), 52.5 to 85% of fourth instar larvae (free living), and 31.2 to 90% of adults of *C. ferrugineus.* Minkevich et al. (2002) determined that the

extractions efficiencies of Berlese funnel were 34 to 44% for implanted larvae, 66 to 86% for free living larvae and 96% for adults of *C. ferrugineus*. The Berlese funnel approach takes a long time to extract the insects from a grain sample and the accuracy of this method is low for the developing life stages. Furthermore, it is not possible to extract the pupa by Berlese funnel method, as there is no movement at this stage. An alternative method is required to detect the developing life stages inside wheat kernels. Hence the objective of this research was to determine the efficiency of a thermal imaging technique to detect the presence of *C. ferrugineus* inside wheat kernels at six developmental stages (four larval, pupal and adult).

7.2.1 Thermal imaging

Thermal imaging is a technique to convert the invisible radiation pattern (temperature) of an object into a visible image. By this method, the surface temperature of any object can be mapped at a high resolution in two dimensions. These thermal data may be used directly or indirectly for many applications. Thermal imaging has been used by many researchers for various applications in agriculture such as plant physiology, irrigation scheduling (Jones 1999), yield forecasting (Smith et al. 1985; Stajnko et al. 2004), maturity evaluation of fruits (Danno et al. 1980), detection of bruises in fruits (Danno et al. 1978; Varith et al. 2003), and detection of spoilage by microbial activity (Hellebrand et al. 2002). However, there is little application of this technology in grain storage.

7.3 Materials and Methods

7.3.1 Insect culture

The procedure described by Karunakaran et al. (2004b) was followed for the development of *C. ferrugineus* cultures and artificial infestation of wheat grains. Canada Western Red Spring (CWRS) wheat was conditioned to 14% moisture content (wet basis) and 400 kernels (n=400) were artificially infested with *C. ferrugineus* eggs and incubated

at 30°C and 70% RH. The kernels were thermally imaged on days 4, 8, 11, 15, 22, and 27 to represent the infestation by four larval (L_1, L_2, L_3, L_4), pupal and adult stages, respectively.

7.3.2 Image acquisition

For each life stage, the kernel was moved from a 30°C incubator to a refrigerator (5±2°C) for 60 s and then to ambient conditions for 20 s, before being thermally imaged (Fig. 7.1). After imaging, the kernel was transferred back to the incubator. The control samples (uninfested wheat) were also placed in the same environment as the infested grains and thermally imaged similarly. An un-cooled focal plane array type infrared thermal camera was used in this study (Model: ThermaCAM^{TM} SC500, FLIR systems, Burlington, Ontario, Canada). A 50 µm close-up lens was attached to the original lens of the camera (FOV 24° × 18°) to get the magnified thermal image of a kernel. The thermal resolution of the camera was 0.07°C at 30°C.

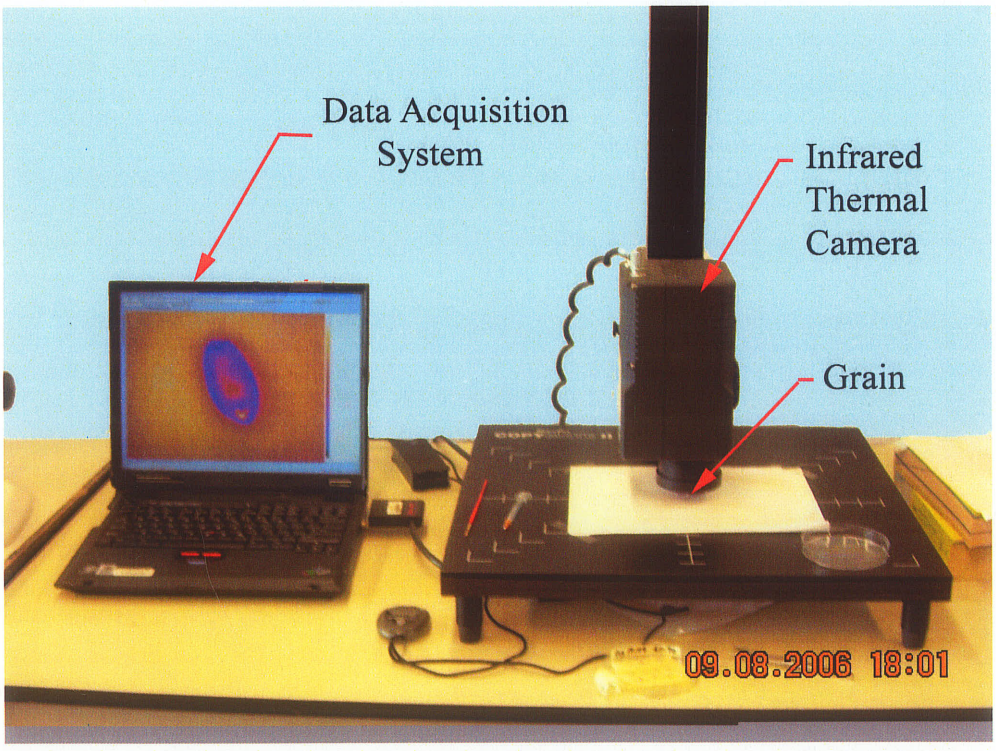

Figure 7.1 Experimental setup to detect insect infestation inside a wheat kernel.

7.3.3 Data analysis

Algorithms were developed in Matlab software (Version 7.1, The Mathworks Inc., Natick, MA) to segment the kernel from the background (using global image threshold technique) (Fig. 7.2) and extract the temperature values of the grain. The size of the original image was 240×320 pixels (240×320 = 76,800 temperature values) in which grain occupied approximately 10,000 temperature values. After extracting the temperature values of the grain, five data sets were formed: (i) all temperature values on the grain surface, (ii) the highest 5% temperature values on the grain surface, (iii) the highest 10% temperature values on the grain surface, (iv) the highest 20% temperature values on the grain surface, and (v) the highest 30% temperature values on the grain surface. Five features (mean, minimum, maximum, standard deviation (SD) and difference between maximum and minimum temperatures (ΔT)) from the data set i and five features (mean, minimum, SD, ΔT, ΔT_{mean}) from the data sets ii to v were extracted. ΔT_{mean} was calculated by subtracting the mean of the highest values with the remainder mean of the grain. For example, in dataset ii, ΔT_{mean} was calculated as: mean of the highest 5% temperature values of the grain surface - mean of remaining 95% temperature values of the grain surface. Thus, in total 25 temperature features were obtained from each thermal image and used for classification. The means of six developmental stages and control under each temperature feature were compared by least significance difference method (LSD) at 95% confidence interval.

A quadratic and linear discriminant analyses (QDA and LDA) with the leave-one-out method of validation were conducted using the PROC DISCRIM in SAS (version 9.3, SAS Institute Inc., Cary, NC). Three types of analyses were carried out: (i) seven classes (four instars larvae, pupae, adults and control) mixed and treated separately, (ii) each

developmental stage vs control (pairwise discrimination), and (iii) all developmental stages mixed and treated as infested (one class) vs control (pairwise discrimination).

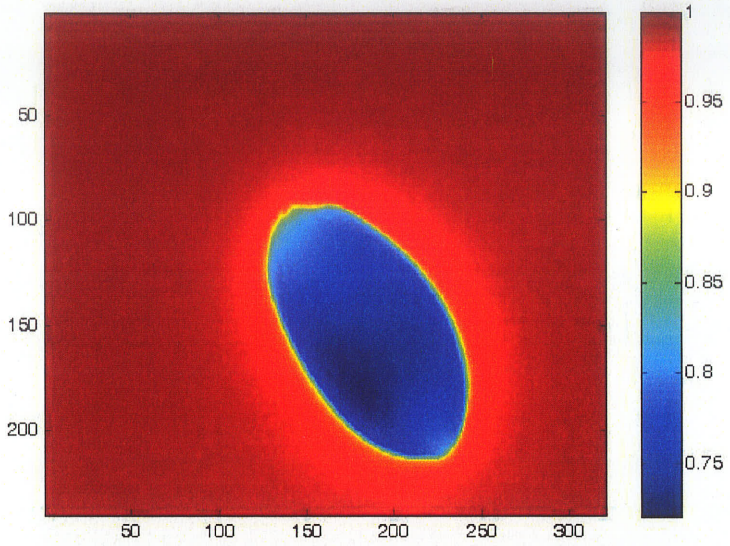

Normalized image

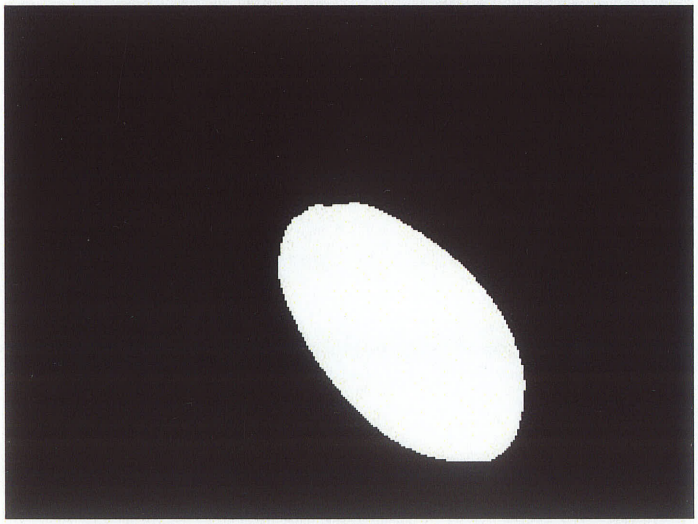

Segmented image

Figure 7.2 Segmentation of a thermal image by global thresholding technique to obtain temperature values from the surface of grain.

7.4 Results and Discussion

Out of 400 artificially infested kernels with *C. ferrugineus* eggs, only 283 eggs developed into adults. In a study with *C. ferrugineus* eggs by Karunakaran et al. (2004b), about 20% mortality was encountered. The damage to eggs during handling in the artificial infestation process, and the whole wheat kernel as a food source (rather than ground wheat) might have caused the higher mortality of eggs (Karunakaran et al. 2004b). Thermal images of the kernels with actual infestation (n=283) were alone considered for further analysis.

It is hypothesized that the temperature distribution on the surface of the grain would be different for infested and uninfested kernels. This is due to the variations in the respiration pattern of an uninfested kernel from the kernel having a live insect. The respiration of insects (at all life stages) and resulting heat production are higher than that of the grain (Cofie-Agblor et al. 1995a, 1995b, 1996a, 1996b; Emekci et al. 2002, 2004; Damcevski et al. 1998). The heat production by respiration of any grain is around 0.01W/t (Muir 1997b). The heat production of adults by respiration in 10 h was 66 to 81 μW per insect for the granary weevil, *Sitophilus granarius* (Coleoptera: Curculionidae) 46 to 56 μW per insect for the rice weevil, *Sitophilus oryza* (Coleoptera: Curculionidae) 18 to 40 μW per insect for the red flour beetle, *Tribolium castaneum* (Coleoptera: Tenebrionidae) and 13 to 35 μW per insect for the lesser grain borer, *Rhyzopertha dominica* (Coleoptera: Bostrychidae) (Cofie-Agblor et al. 1995b). To magnify the difference in the temperature profile of infested and uninfested grains, the kernels were cooled for 60 s and kept at ambient condition for 20 s (chosen based on preliminary trials) before imaging.

The germ of an uninfested kernel cooled slower than the endosperm. The variation in chemical constituents between endosperm and germ within a kernel might be

causing the dissimilarity in cooling pattern. Furthermore, the germ end is less dense and usually there is a small air pocket between the germ and seed coat. Another probable reason is non-uniform distribution of moisture within a kernel even at the equilibrium state as shown by magnetic resonance images of wheat kernels (Ghosh et al. 2004).

Carbon dioxide (CO_2) production or oxygen (O_2) consumption may be used as an index to represent the respiration rate and heat of respiration by insects (Cofie-Agblor 1995b; Emekci et al. 2002). In this study no attempts were made to accelerate the respirations of developing insects. Cofie-Agblor (1995b) reported that *C. ferrugineus* is a weak feeder of whole grain (prefers broken kernels), and the respiration of *C. ferrugineus* increased with initial grain temperature (among tested levels: 15 to 35°C), moisture content (among tested levels: 12 to 18%) and the degree of damage to kernels. In our experiments, we used undamaged kernels and the grain temperature was around 20°C during thermal imaging, and therefore respiration of insects might have been relatively low during the imaging time.

The mean of the highest 5% temperature values were 20.56, 26.25, 26.23, 24.83, 24.46, 19.71 and 21.52°C for control, L_1, L_2, L_3, L_4, pupae and adults, respectively. Similarly the mean of the highest 10% temperature values were 20.09, 25.91, 25.83, 24.52, 24.17, 19.51 and 21.31°C for control, L_1, L_2, L_3, L_4, pupae and adults, respectively. In both cases, the temperature was the highest for the kernels infested with early larval stages (no difference between L_1 and L_2) and then for the late larval stages (no difference between L_3 and L_4). The mean of the highest 5 and 10% temperatures followed the pattern of respiration rate of different developmental stages. Campbell and Sinha (1978) reported that larvae of *C. ferrugineus* had a high respiration rate that decreased steadily from 149 $\mu l\ O_2\ mg^{-1}h^{-1}$ for first instar larva to 27.5 $\mu l\ O_2\ mg^{-1}h^{-1}$ during the adult stage. *Cryptolestes ferrugineus* larvae were mobile (faster than larvae of some other species)

and the energy utilization of larvae was very high when compared to the later developmental stages (Campbell and Sinha 1978). This might have caused the higher value of the highest 5 and 10% temperatures in larvae than pupae and adults.

The kernels infested with pupae had the lowest values in both means of the highest 5% and 10%, and there were no significant differences between pupae and control in the highest 10% temperature values. The respiration of the pupal stage was the lowest among all the developmental stages, and this was previously observed in *C. ferrugineus* (Campbell and Sinha 1978) and *Tribolium castaneum* (Emekci et al. 2002). This might have caused the lowest mean of the highest 5 and 10% temperature values on the kernels infested with pupae.

The temperature distribution patterns on the surface of the infested and uninfested kernels are shown in Table 7.1. Temperature features were significantly different (α=0.05) for the uninfested (control) and infested grains with various developmental stages. SD and ΔT of the highest 5 and 10% temperature values formed a maximum number of clusters by statistical grouping. In these four features, all developmental stages and control were significantly different from each other except L_3 and L_4. In the highest 5 and 10% temperature values, SD and ΔT were the lowest for the kernels infested with pupae. No physical movement coupled with low respiration rate of pupae might have caused the lowest SD and ΔT of the highest 5 and 10% temperature values.

Table 7.1 Temperature distribution on grain surface after cooling for 60 s at 5°C.

Life stage	All temperature values		Highest 5% temperature values			Highest 10% temperature values			Highest 20% temperature values			Highest 30% temperature values		
	ΔT	SD	ΔT	SD	ΔT_{mean}	ΔT	SD	ΔT_{mean}	ΔT	SD	ΔT_{mean}	ΔT	SD	ΔT_{mean}
Control	5.37^{a*} ±1.03**	1.21^{a} ±0.25	0.99^{a} ±0.49	0.29^{a} ±0.15	3.39^{a} ±0.66	1.82^{a} ±0.69	0.55^{a} ±0.22	3.06^{a} ±0.61	2.86^{a} ±0.75	0.85^{a} ±0.22	2.54^{ab} ±0.55	3.44^{ac} ±0.76	1.00^{a} ±0.21	2.20^{a} ±0.50
Instar 1 (L_1)	5.11^{b} ±0.75	1.23^{ab} ±0.20	0.68^{b} ±0.23	0.20^{b} ±0.07	3.23^{b} ±0.50	1.39^{b} ±0.38	0.41^{b} ±0.12	3.03^{a} ±0.49	2.50^{b} ±0.51	0.75^{b} ±0.16	2.60^{be} ±0.45	3.14^{b} ±0.55	0.95^{b} ±0.18	2.26^{a} ±0.40
Instar 2 (L_2)	5.62^{c} ±0.86	1.36^{c} ±0.26	0.78^{c} ±0.28	0.23^{c} ±0.08	3.61^{c} ±0.60	1.58^{c} ±0.43	0.47^{c} ±0.14	3.37^{bc} ±0.61	2.78^{a} ±0.53	0.84^{a} ±0.16	2.89^{c} ±0.57	3.51^{a} ±0.59	1.06^{c} ±0.20	2.51^{b} ±0.51
Instar 3 (L_3)	5.64^{c} ±1.22	1.44^{d} ±0.37	0.59^{d} ±0.19	0.17^{d} ±0.06	3.60^{c} ±0.83	1.24^{d} ±0.36	0.37^{d} ±0.11	3.46^{b} ±0.84	2.50^{b} ±0.59	0.75^{b} ±0.19	3.09^{d} ±0.80	3.35^{c} ±0.77	1.03^{ac} ±0.25	2.71^{c} ±0.72
Instar 4 (L_4)	5.43^{a} ±1.20	1.39^{c} ±0.36	0.59^{d} ±0.39	0.18^{d} ±0.12	3.40^{a} ±0.82	1.19^{d} ±0.56	0.35^{d} ±0.17	3.27^{c} ±0.82	2.30^{c} ±0.73	0.68^{c} ±0.22	2.95^{c} ±0.78	3.15^{b} ±0.80	0.95^{b} ±0.26	2.62^{c} ±0.71
Pupa	4.78^{d} ±0.98	1.28^{b} ±0.29	0.36^{e} ±0.12	0.11^{e} ±0.04	2.95^{d} ±0.64	0.81^{e} ±0.27	0.24^{e} ±0.08	2.90^{d} ±0.63	1.77^{d} ±0.51	0.53^{d} ±0.16	2.69^{e} ±0.61	2.57^{d} ±0.60	0.79^{d} ±0.20	2.43^{b} ±0.57
Adult	4.50^{e} ±1.31	1.18^{a} ±0.38	0.43^{f} ±0.29	0.13^{f} ±0.09	2.77^{e} ±0.85	0.89^{f} ±0.45	0.26^{f} ±0.13	2.69^{e} ±0.84	1.74^{d} ±0.64	0.52^{d} ±0.19	2.47^{a} ±0.80	2.44^{e} ±0.78	0.73^{e} ±0.23	2.24^{a} ±0.75

* values with same letters in a column are not significantly different (α=0.05) by least significant difference (LSD) method, ** standard deviation (n=283)

The temperature distribution pattern on the infested grain surface was highly correlated with "respiration efficiency" (ratio of respiration to assimilation) while testing the bioenergetics indices of *C. ferrugineus* reported by Campbell and Sinha (1978). The correlation coefficient (r) with the respiration efficiency was: 0.91, 0.91, 0.86, 0.83, 0.87 and 0.87 for mean of the highest 5%, mean of the highest 10%, ΔT of the highest 5%, SD of the highest 5%, ΔT of the highest 10%, SD of the highest 10%, respectively. In addition to respiration of the insect, the changes in the structure of the grain (physical damage inside the grain due to infestation) might have contributed to the variations in the temperature distribution on the grain surface.

It is difficult to correlate the temperature distribution on the surface of the infested grain with the metabolism or respiration behavior of developing life stages of *C. ferruginius* because no published work is available for the respiration pattern of a single insect present inside the wheat kernel. In many published reports, around 1000 to 5000 adults and life stages were taken in 100 to 500 g bulks of grain, and then respiration of the grain alone was deducted from the total respiration of the culture to obtain the respiration of insects. The respiration rate of single insect (adult or developing stage) within a kernel may be different from their group responses.

7.4.1 Classification using statistical classifiers

Although statistical and artificial neural network (ANN) classifiers have been widely used for the classification of food materials (Visen et al. 2004; Majumdar and Jayas 2000a; Balasubramanian et al. 2004), the selection of the best one for a particular application generally involves some degree of experimentation (Jayas et al. 2000; Luo et al. 1999). In this paper the classification performance of a QDA and LDA with leave-

one-out validation is discussed. ΔT of the highest 10% temperature values ranked first based on contribution to the classification using PROC STEPDISC in SAS (version 9.3, SAS Institute Inc., Cary, NC).

In the first analysis (all stages mixed and treated separately), there were several misclassification among the developmental stages and control. Karunakaran et al. (2004b) also reported the same trend while classifying the life stages of *C. ferrugineus* using soft X-ray. Hence, invisible imaging techniques might have difficulties in the identification of developmental stages inside wheat kernels. However, in our study, kernels infested by pupae were correctly classified with an accuracy of 88.3% using the QDA method, even when seven classes (6 developmental stages and control) were mixed and treated separately.

The performance of pairwise discrimination of each stage with the control (second analysis) using QDA and LDA methods is shown in Figs. 7.3 and 7.4, respectively. The classification accuracy was the highest for pupae in QDA (95%) and for adults in LDA (89.9%). QDA yielded higher accuracy for infested kernels than uninfested except for L_2 and L_4. Whereas the classification accuracy was higher for uninfested kernels while comparing the larval stages and higher for infested kernels while comparing pupae and adults in LDA. In the third analysis (all stages mixed and treated as infested), the classification was higher in QDA for both infested and uninfested kernels (Fig. 7.5). The classification accuracy was more than 80% for the infested kernels in both QDA and LDA methods.

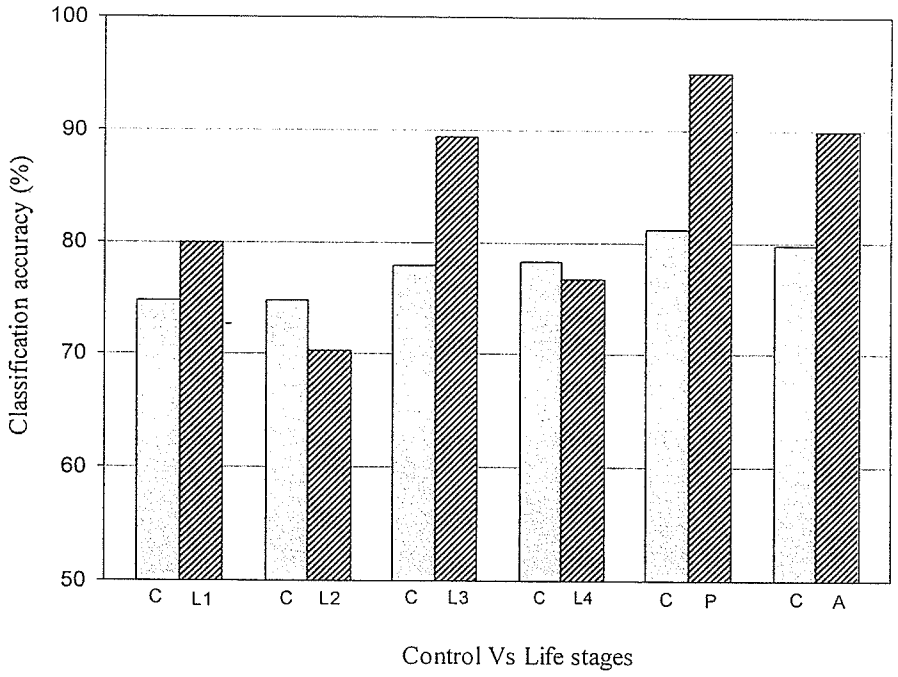

Figure 7.3 **Pairwise comparison of control with *Cryptolestes ferrugineus* life stages using a quadratic discrimination function** (C: control; L1: instar 1; L2: instar 2; L3: instar 3; L4: instar 4; P: pupa; A: adult).

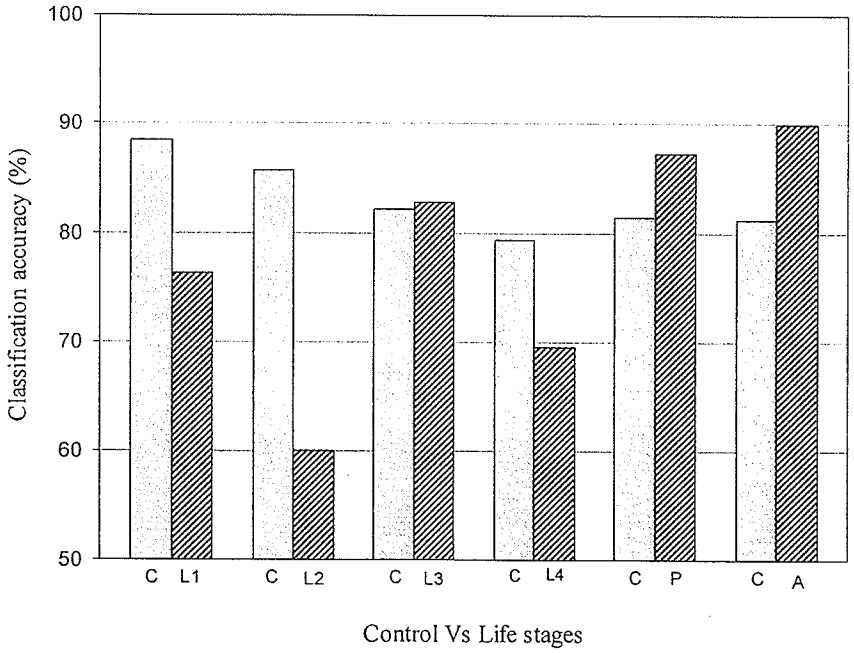

Figure 7.4 **Pairwise comparison of control with *Cryptolestes ferrugineus* life stages using a linear discrimination function** (C: control; L1: instar 1; L2: instar 2; L3: instar 3; L4: instar 4; P: pupa; A: adult).

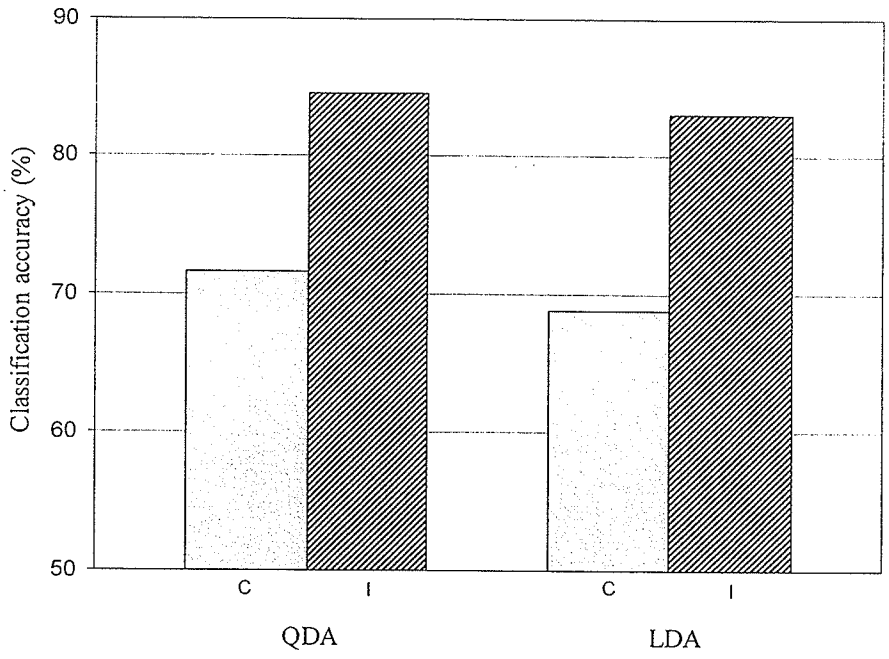

Figure 7.5 **Pairwise comparison of uninfested (control) with infested by *Cryptolestes ferrugineus* (all stages mixed) using quadratic** (QDA) and linear (LDA) discrimination functions (C: control; I: infested).

7.5 Potential Applications and Further Research

Berlese funnel method performs reasonably well for the detection of adult stages, but fails to identify the early developmental stages. Thermal imaging technique yielded around 80% accuracies in pair wise discriminations to detect the infested kernels. It has potential to identify whether the grain is infested or not, rather than detecting the infestation by the exact developmental stage.

In this study, thermal images of the infested kernels with live insects were alone analyzed. During development time, insects consume the grain mass, and the whole germ would be eaten by a *C. ferrugineus* insect while growing inside a kernel. The temperature distribution patterns on the surface of the infested grain are influenced by the combined effect of insect respiration and the changes in the grain mass. To determine the effect of a

live insect alone on the temperature profiles, the kernels without insect (or with a dead insect) and with the same level of physical damage at all developmental stages should be thermally imaged and analyzed (studies are currently underway in our lab). Similarly, thermal behavior of other insect species should be studied before developing thermal imaging system to detect the infestation in grain elevators.

7.6 Acknowledgements

We thank the Canada Research Chairs Program and the Natural Sciences and Engineering Research Council of Canada (NSERC) for their partial financial assistance, Dr. Gabriel Thomas for his partial help in image analysis and Ms. Kelly Griffiths for her partial help in the development of insect culture and image acquisition processes.

8. CONCLUSIONS AND RECOMMENDATIONS FOR FUTURE RESEARCH

8.1 Conclusions

1. The heating patterns (temperature rise, maximum temperature, and the difference between maximum and minimum temperatures) of three grain types with different moisture content while subjecting to microwave treatment in a pilot-scale drier have been reported. The surface temperatures of barely, canola and wheat increased with microwave power levels and exposure times, but decreased with moisture content. The average surface temperatures were between 72.5 and 117.5°C, 65.9 and 97.5°C, 73.4 and 108.8°C, for barley, canola and wheat, respectively, when the applied microwave power was 500 W. The difference between maximum and minimum temperatures (ΔT) was in the range of 7.2 to 78.9°C, 3.4 to 59.2°C and 9.7 to 72.8°C, for barley, canola and wheat, respectively. This information would be useful in developing microwave systems for drying and disinfestations for grain industry.
2. The quality of wheat samples subjected to same microwave treatments, but collected at two different locations (high temperature and normal temperature regions) were significantly different. After microwave treatments, the germination percentages of wheat samples collected from the high temperature region were significantly lower than that of the normal zones at all moisture content and power levels (α=0.05). An irregular pattern was observed in the FAV of wheat samples after microwave treatment. The FAV of wheat samples collected from the high temperature region was significantly different from the normal zone. Since the detrimental effect on quality was severe at the high temperature

locations, the non-uniformity of heating must be reduced before developing microwave systems for various applications in grain industry.

3. The hotspot in a stored grain silo was detected on the thermal images of a silo wall and top surface of the grain bulk when it was located 0.3 m from the silo wall or below the grain surface or both. Since, the temperature of the silo wall and grain surface were easily affected by weather conditions, thermal imaging can not be used as an independent method to monitor grain temperatures in a silo.
4. The rate of heating and cooling of bulk samples of Canadian wheat classes were significantly different (α=0.05) and negatively correlated with protein content (r = -0.63 for heating, r = -0.65 for cooling). The classification accuracy of a quadratic discriminant method was higher during pairwise comparison of wheat classes, and ranged between 80 to 100% for bootstrap validation and 74 to 100% for leave-one-out validation. Thermal imaging method has the potential to classify registered and un-registered varieties which are indistinguishable by visual inspection.
5. Thermal imaging technique has potential to detect early stages of infestation inside wheat kernels. The temperature profiles on the surface of the grain was significantly different for infested and sound wheat kernels (α=0.05). The kernels infested by *C. ferrugineus* were correctly identified with an accuracy of more than 80% by statistical classifiers. However, thermal imaging has potential to identify whether the grain is infested or not, rather than detecting the infestation by the exact developmental stage.

8.2 Recommendations

1. Further study is required to determine the effect of different operational procedures such as supply of pulsed microwave energy, addition of air during microwaving, and microwave treatment under vacuum conditions, on the uniformity of heating of grains.
2. Further research is required to study the changes in FAV of microwave dried grains after long term storage.
3. Further study is required to determine the combined effect of cold weather and wind on the efficiency of the thermal imaging method to detect a hot spot in a stored grain silo.
4. The efficiency of a thermal imaging technique to identify wheat classes with different varieties under each class, and at various moisture contents must be studied.
5. To determine the actual effect of live insects on the thermal profiles of an infested kernel, further research is required with kernels having no live insects inside but the same level of physical damage by developmental stages.

REFERENCES

Adams, R.E., J.E. Wolfe, M. Milner and J.A. Shellenberger. 1954. Detection of internal insect infestation in grain by sound amplification. *Cereal Chemistry* 31(3): 271-176.

Adu, B. and L. Otten. 1996. Microwave heating and mass transfer characteristics of white beans. *Journal of Agricultural Engineering Research* 64(1): 71-78.

Agerskans, J. 1975. Thermal imaging-A technical review. In *Proceedings of Temperature Measurement*, 375-388. London. April 9-11.

Agriculture and Agri-Food Canada. 2002. Predicting rusty grain beetle infestations: Don't let the rusty grain beetle ruin wheat in storage. Report no. Sp06. Winnipeg, MB: Cereal Research Centre, Agriculture and Agri-Food Canada.

Anonymous. 2002. Infrared training: Level 1 course manual. North Billerica, MA: Infrared Training Centre.

Anthony, W.S. 1983. Vacuum microwave drying of cotton: effect on cotton seed. *Transactions of the ASAE* 26(1): 275-278.

Antti, A.L. and P. Perre. 1999. A microwave applicator for on line wood drying: Temperature and moisture distribution in wood. *Wood Science and Technology* 33(2): 123-138.

Baker, V.H., D.E. Wiant and O. Taboada. 1956. Some effects of microwaves on certain insects which infest wheat and flour. *Journal of Economic Entomology* 49(1): 33-37.

Balasubramanian, S., S. Panigrahi, C.M. Logue, M. Marchello, C. Doetkott, H. Gu, J. Sherwood and L. Nolan. 2004. Spoilage identification of beef using an electronic nose system. *Transactions of the ASAE* 47(5): 1626-1633.

Berliner, P., D.M. Oosterhuis and G.C. Green. 1984. Evaluation of the infrared thermometer as a crop stress detector. *Agricultural and Forest Meteorology* 31(3-4): 219-230.

Borchers, R., L.D. Manage, S.O. Nelson, and L.E. Stetson. 1972. Rapid improvement in nutritional quality of soybeans by dielectric heating. *Journal of Food Science* 37(2): 333-334.

Boulanger, R.J., W.M. Boerne and M.A.K. Hamid. 1969. Comparison of microwave and dielectric heating systems for the control of moisture content and insect infestations of grain. *Journal of Microwave Power* 4(3): 194-207.

Burfoot, D., W.J. Griffin and S.J. James. 1988. Microwave pasteurization of prepared meals. *Journal of Food Engineering* 8(3): 145-156.

Campana, L.E., M.E. Sempe and R.R. Filgueira. 1993. Physical, chemical, and baking properties of wheat dried with microwave energy. *Cereal Chemistry* 70(6): 760-762.

Campbell, A. and R.N. Sinha. 1978. Bioenergetics of granivorous beetles, *Cryptolestes ferrugineus* and *Rhyzopertha dominica* (Coleoptera: Cucujidae and Bostrichidae). *Canadian Journal of Zoology* 56(4): 624-633.

Canadian Grain Commission. 2003. Canadian Grain Commission stresses industry approach to handling of Alsen wheat. Available at: http://www.grainscanada.gc.ca/newsroom/news_releases/2003/2003-11-07-e.htm. Accessed on August 8, 2006.

Canadian Grain Commission. 2005a. Available at: http://www.grainscanada.gc.ca/grl/variety_id/variety_id-e.htm. Accessed on August 8, 2006.

Canadian Grain Commission. 2005b. Available at: http://www.grainscanada.gc.ca/entomology/monitor02-e.htm. Accessed on August 8, 2006.

Canadian Wheat Board. 2005. Statistical tables.Available at : http://www.cwb.ca/en/publications/students_researchers/pdf/stats_english_2001-02.pdf. Accessed on October 6, 2006. Accessed on August 8, 2006.

Christensen, C.M., J.H. Olafson, and W.F. Geddes. 1949. Grain storage studies 8: Relation of moulds in moist stored cotton seeds to increased production of carbon dioxide, fatty acid and heat. *Cereal Chemistry* 26(2): 109-128.

Christensen, C.M. and H.H. Kaufmann. 1968. Grain storage - The role of fungi in quality loss, Minneapolis, MN: University of Minnesota Press.

Christensen, C.M. and R.A. Meronuck. 1986. Quality maintenance in stored grains and seeds 138. Minneapolis, MN: University of Minnesota Press.

Christoph, S.G., U. Schurr and B. Jahne. 2002. Thermographic measurements on plant leaves. In *Proceedings of Thermosense XXIV*, 407-416. Bellingham, WA: The International Society for Optical Engineering.

CIGI. 1993. Grains & Oilseeds: Handling, marketing, processing 4th ed., Winnipeg, MB: Canadian International Grains Institute.

Cofie-Agblor, R., W.E. Muir, Q. Zhang and R.N. Sinha. 1995a. CO_2 production by *Cryptolestes ferrugineus* (Stephens) in stored wheat under adiabatic conditions. *Journal of Agricultural Engineering Research* 62(2): 95-104.

Cofie-Agblor, R., W.E. Muir, Q. Zhang and R.N. Sinha. 1995b. Comparative heat of respiration of five grain beetles in stored wheat. *Post Harvest Biology and Technology* 5(1-2): 167-175.

Cofie-Agblor, R., W.E. Muir, R.N. Sinha and P.G. Fields. 1996a. Heat production by adult *Cryptolestes ferrugineus* (Stephens) of different ages and densities. *Post Harvest Biology and Technology* 7(4): 371-380.

Cofie-Agblor, R., W.E. Muir, Q. Zhang and R.N. Sinha. 1996b. Heat of respiration of *Cryptolestes ferrugineus* (Stephens) adults and larvae in stored wheat. *Canadian Agricultural Engineering* 38(1): 37-44.

Damcevski, K.A., P.C. Annis and C.J. Waterford. 1998. Effect of grain on apparent respiration of adult stored-product Coleoptera in an air-tight system: Implications for fumigant testing. *Journal of Stored Products Research* 34(4): 331-339.

Dani, M.A.M. 2005. Infrared inspection on electrical installations in hospitals. In *Proceedings of Inframation 2005* Volume 5, 397-399, N. Billerica, MA: Infrared Training Centre.

Daniels, N.W.R. and P.J. Frazier. 1976. Wheat proteins: Physical properties and baking function. *In Plant Proteins*, ed. G. Norton, 299-315. London, UK: Butterworths and Co. (Publishers) Ltd.

Danno, A., M. Miyazato and E. Ishiguro. 1978. Quality evaluation of agricultural products by infrared imaging method: Grading of fruits for bruise and other surface defects. *Memoirs of the Faculty of Agriculture*, Kagoshima University 14:123-138.

Danno, A., M. Miyazato and E. Ishiguro. 1980. Quality evaluation of agricultural products by infrared imaging method: Maturity evaluation of fruits and vegetables. *Memoirs of the Faculty of Agriculture*, Kagoshima University 16:157-164.

Davis, A.P. and A.H. Lettington. 1988. Principles of thermal imaging. In *Applications of Thermal Imaging,* ed. S.G. Burnay, T.L. Williams and C.H. Jones, 1-34. Bristol, UK: IOP Publishing Ltd.

Dennis, N.M. and R.W. Decker. 1962. A method and machine for detecting living internal infestation in wheat. *Journal of Economic Entomology* 55(6): 199-203.

Doty, N.C. and C.W. Baker. 1977. Microwave conditioning of Hard Red Spring wheat. I. Effects of wide power range on flour and bread quality. *Cereal Chemistry* 54(4): 717-727.

Dowell, E.F., J.E. Throne and J.E. Baker. 1998. Automated nondestructive detection of internal insect infestation of wheat kernels using near-infrared reflectance spectroscopy. *Journal of Economic Entomology* 91(4): 899-904.

Egnell, G. and G. Orlander. 1993. Using infrared thermography to access viability of *Pinus sylvestris* and *Picea abies* seedlings before planting. *Canadian Journal of Forest Research* 23(9): 1737-1743.

Emekci, M., S. Navarro, E. Donahaye, M. Rindner and A. Azrieli. 2002. Respiration of *Tribolium castaneum* (Herbst) at reduced oxygen concentrations. *Journal of Stored Products Research* 38(5): 413-425.

Emekci, M., S. Navarro, E. Donahaye, M. Rindner and A. Azrieli. 2004. Respiration of *Rhyzopertha dominica* (F.) at reduced oxygen concentrations. *Journal of Stored Products Research* 40(1): 27-38.

Epsky, N.D. and D. Shuman. 2001. Laboratory evaluation of an improved electronic grain probe insect counter. *Journal of Stored Products Research* 37(2): 187-197.

Fakhouri, M.O. and H.S. Ramaswamy. 1993. Temperature uniformity of microwave heated foods as influenced by product type and composition. *Food Research International* 26(2): 89-95.

Fanslow, G.E. and R.A. Saul. 1971. Drying field corn with microwave power and unheated air. *Journal of Microwave Power* 6(3): 229-235.

Fargo W.S., D. Epperley, G. W. Cuperus, B.C. Clary and R. Noyes. 1989. Effects of temperature and duration of trapping on four stored grain insect species. *Journal of Economic Entomology* 82(3):970-973.

Gardner, D.R. and J.L. Butler. 1981. Preparing crops for storage with a microwave vacuum (MIVAC) drying system. In *Drying '81, Second International Symposium Drying*, New York, NY: Hemisphere Publishing Company.

Ghaly, T.F. and J.W.V. Touw. 1982. Heat damage studies in relation to high temperature disinfestations of wheat. *Journal of Agricultural Engineering Research* 27(4): 329-336.

Ghaly, T.F. and P.A. Taylor. 1982. Quality effects of heat treatment of two wheat varieties. *Journal of Agricultural Engineering Research* 27(3): 227-234.

Ghosh, P.K., D.S. Jayas, M.L.H. Gruwel and N.D.G. White. 2004. Magnetic resonance image analysis to explain moisture movement in wheat drying. ASAE Paper No. 043118. St. Joseph, MI: ASAE.

Gonzalez, R.C. and R.E. Woods. 2002. *Digital Image Processing*, 2nd edition. 44-45. Delhi, India: Pearson Education private limited.

Gunasekaran, S. 1990. Grain drying using continuous and pulsed microwave energy. *Drying Technology* 8(5): 1039-1047.

Hagstrum, D.W., J.C. Webb and K.W. Vick .1988. Acoustical detection and estimation of *Rhyzopertha dominica* (F.) larval populations in stored wheat. *Florida Entomologist* 71(4): 441-447.

Hamid, M.A.K. and R.J. Boulanger. 1969. A new method for the control of moisture and insect infestations of grain by microwave power. *Journal of Microwave Power* 4(1): 11-18.

Health Canada. 1999. Health protection branch guidelines for the general cleanliness of food-an Overview. http://www.hc-sc.gc.ca/food-aliment/mh-dm/mhe-dme/compendium/volume_1/e_EmoE02.html. Accessed on March 3, 2005.

Hellebrand, H.J., H. Beuche and M. Linke. 2002. Thermal imaging: A promising high-tec method in agriculture and horticulture. In *Physical Methods in Agriculture: Approach to Precision and Quality*, ed. J. Blahovec and M. Kutilek, 411-427. New York, NY: Kluwer Academic/Plenum Publishers.

Hulbert, G.J., J.B. Litchfield and S.J. Schmidt. 1995. Temperature mapping in carrot using T_1 weighted magnetic resonance imaging. *Journal of Food Science* 60(4): 780-785.

Hurlock, E.T., B.E. Llewelling and L.M. Stables.1979. Microwaves can kill insect pests. *Food Manufacture* 54(1): 37-38.

Inoue, Y., B.A. Kimball, R.D. Jackson, P.J. Pinter and R.J. Reginato. 1990. Remote estimation of leaf transpiration rate and stomatal resistance based on infrared thermometry. *Agricultural and Forest Meteorology* 51(1): 21-33.

James, K. and D. Rice. 2002. Finding termites with thermal imaging. Paper No. ITC 035A. North Billerica, MA: Infrared Training Centre.

Jayas, D.S., J. Paliwal and N.S. Visen. 2000. Multi-layer neural networks for image analysis of agricultural products. *Journal of Agricultural Engineering Research* 77(2): 119-128.

John, C.S. and L.Otten. 1989. Thin-layer microwave drying of peanuts. *Canadian Agricultural Engineering* 31(2): 265-270.

Jones, H.G. 1999. Use of infrared thermometry for estimation of stomatal conductance as a possible aid to irrigation scheduling. *Agricultural and Forest Meteorology* 95(3): 139-149.

Kadlec, P., A. Rubecova, A. Hinkova, J. Kassova, Z. Bubnik and V. Pour. 2001. Processing of yellow pea by germination, microwave treatment and drying. *Innovative Food Science and Emerging Technologies* 2(2): 133-137.

Kalma, J.D. and D.L.B. Jupp. 1990. Estimating evaporation from pasture using infrared thermometry: Evaluation of a one layer resistance model. *Agricultural and Forest Meteorology* 51(3-4): 223-246.

Kantt, C.A., A.G. Webb and J.B. Litchfield. 1997. Temperature measurement of foods using chemical shift magnetic resonance imaging as compared with T1- weighted temperature mapping. *Journal of Food Science* 62(5): 1011-1016.

Kantt, C.A., S.J. Schmidt, S.E. Sizer, S. Palaniappan and J.B. Litchfield. 1998. Temperature mapping of particles during aseptic processing with magnetic resonance imaging. *Journal of Food Science* 63(2): 305-311.

Karunakaran, C., W.E. Muir, D.S. Jayas, N.D.G. White and D. Abramson. 2001. Safe storage time of high moisture wheat. *Journal of Stored Products Research* 37(3): 303-312.

Karunakaran, C. 2002. Soft X-ray inspection of wheat kernels to detect infestations by stored-grain insects. Unpublished Ph.D. thesis. Winnipeg, MB: Department of Biosystems Engineering, University of Manitoba.

Karunakaran, C., D.S. Jayas and N.D.G. White. 2003. Soft X-ray inspection of wheat kernels infested by *sitophilus oryzae*. *Transactions of the ASAE* 46(3): 739-745.

Karunakaran, C., D.S. Jayas and N.D.G. White. 2004a. Identification of wheat kernels damaged by the red flour beetle using X-ray images. *Biosystems Engineering* 87(3): 267-274.

Karunakaran, C., D.S. Jayas and N.D.G. White. 2004b. Detection of infestations by *Cryptolestes ferrugineus* inside wheat kernels using a soft X-ray method. *Canadian Biosystems Engineering* 46: 7.1-7.9.

Kasarda, D.D. 1989. Glutenin structure in relation to wheat quality. In *Wheat is Unique: Structure, Composition, Processing, End-use properties, and Products*, ed. Y. Pomeranz, 277-302. St. Paul, MN: American Association of Cereal Chemists, Inc.

Kim, Y.H. and S.H. Lee. 2004. Thermal and visual image characteristics of potato transplants as affected by photosynthetic photon flux and electrical conductivity. ASAE Paper No. 044101. St. Joseph, MI: ASAE.

Ljungberg, S.A. and O. Jonsson. 2002. Infrared thermography: A tool to map temperature anomalies of plants in a green house heated by gas fired infrared heaters. In *Proceedings of Thermosense XXIV,* 399-406. Bellingham, WA: The International Society for Optical Engineering.

Lookhart, G.L, B.A. Marchylo, V.J. Mellish, K. Khan, D.B. Lowe and L. Seguin. 1995. Wheat identification in North America. In *Identification of Food Grain Varieties,* ed. C.W. Wrigley, 91-130. St. Paul, MN: American Association of Cereal Chemists, Inc.

Loschiavo, S.R. and J.M. Atkinson. 1967. An improved trap to detect beetles (Coleoptera) in stored grain. *The Canadian Entomologist* 99: 1160-1163.

Luo, X., D.S. Jayas and S. J. Symons. 1999. Comparison of statistical and neural network methods for classifying cereal grains using machine vision. *Transactions of the ASAE* 42(2): 413-419.

MacArthur, L.A. and B.L.D. Appolonia. 1981. Effects of microwave radiation and storage on hard red spring wheat flour. *Cereal Chemistry* 58(1): 53-56.

Madding, R.P. 2004. Common misconceptions in infrared thermography condition based maintenance applications. In *Utility CD*, North Billerica, MA: Infrared Training Centre.

Madding, R.P. and B.R. Lyon. 2004. Wind effects on electrical hot spots – some experimental IR data. In *Utility CD*, North Billerica, MA: Infrared Training Centre.

Majumdar, S. and D.S. Jayas. 2000a. Classification of cereal grains using machine vision: I. Morphology models. *Transactions of the ASAE* 43(6): 1669-1675.

Majumdar, S.and D.S. Jayas. 2000b. Classification of cereal grains using machine vision: IV. Combined morphology, color and texture models. *Transactions of the ASAE* 43(6): 1689-1694.

Malvik, K. 2002. Report on plant disease. Report no. 119. Chicago, IL: Department of Crop Sciences, University of Illinois.

Mani, S. 1999. Computer modeling of insect-induced hot spots in stored grain. Unpublished M.Sc. thesis. Winnipeg, MB: Department of Biosystems Engineering, University of Manitoba.

Manickavasagan, A., D.S. Jayas, R. Vadivambal and N.D.G. White. 2005. Thermal imaging to study the heating pattern of wheat in an industrial microwave drier. In *Proceedings of Inframation*, 345-353. N. Billerica, MA: Infrared Training Centre.

Mark, Y., D.J. Skylas, R. Willows, A. Connolly, S.J. Cordwell, C.W. Wrigley, P.J. Sharp and L. Copeland. 2006. A proteomic approach to the identification and characterization of protein composition in wheat germ. *Functional and Integrative Genomics* 6(4): 322-337.

Meinlschmidt, P. and V. Margner. 2003. Thermographic techniques and adopted algorithms for automatic detection of foreign bodies in food. In *proceedings of Thermosense XXV, 168*-177. Bellingham, WA: The International Society for Optical Engineering.

Minkevich, J.M., C.J. Demianyk, N.D.G. White, D.S. Jayas and B. Timlick. 2002. A rapid method to detect *Cryptolestes ferrugineus* (Coleoptera: Cucujidae) larvae in stored grain. *Canadian Journal of Plant Science* 82(3): 591-597.

Mohsenin, N.N. 1980. *Thermal Properties of Foods and Agricultural Materials*. New York, NY: Gordon and Beach Science Publishers.

Motwan, T. and A. Al-Hussain. 2005. IR thermography in hydraulic system troubleshooting. In *Proceedings of Inframation 2005* Volume 5, 155-159, N. Billerica, MA: Infrared Training Centre.

Muir, W.E. 1997a. Grain Preservation Biosystems. Unpublished Manual, Winnipeg, MB: Department of Biosystems Engineering, University of Manitoba.

Muir, W.E. 1997b. *Grain Preservation Biosystems.* Preliminary version 2, Unpublished Manual, Winnipeg, MB: Department of Biosystems Engineering, University of Manitoba.

Muir, W. E. and N. D. G. White. 2001. Microorganisms in stored grain. In *Grain Preservation Biosystems*, ed. W.E. Muir, 28-42. Winnipeg, MB: Department of Biosystems Engineering, University of Manitoba.

Myers, D.G. and K.J. Edsall. 1989. The application of image processing techniques to the identification of Australian wheat varieties. *Plant Varieties and Seeds* 2: 109-116.

Nagel, C.M. and G. Semeniuk. 1947. Some mould-induced changes in shelled corn. *Plant Physiology* 22: 20-23.

Nelson, S.O. 1976. Use of microwave and lower frequency RF energy for improving alfalfa seed germination. *Journal of Microwave Power* 11(3): 271-277.

Nelson, S.O. 1987. Potential agricultural applications for RF and microwave energy. *Transactions of the ASAE* 30(3): 818-822.

Nelson, S.O. and L.E. Stetson. 1985. Germination responses of selected plant species to RF electrical seed treatment. *Transactions of the ASAE* 28(6): 2051-2058.

Neuman, M., H.D. Sapirstein, E. Shwedyk and W. Bushuk. 1987. Discrimination of wheat class and variety by digital image analysis of whole grain samples. *Journal of Cereal Science* 6(2): 125-132.

Neuman, M.R., H.D. Sapirstein, E. Shwedyk and W. Bushuk. 1989. Wheat grain color analysis by digital image processing. II. Wheat class discrimination. *Journal of Cereal Science* 10(3): 183-188.

Nott, K.P. and L.D. Hall. 1999. Advances in temperature validation of foods. *Trends in Food Science and Technology* 10(11): 366-374.

Okazaki, K. and S. Ishihara. 1980. Studies on the effect of drying on the quality of high moisture wheat. Research Bulletin 126, 123-134, Hokkaido, Japan: Hokkaido National Agricultural Experiment Station.

Oliveira, M.E.C. and A.S. Franca. 2002. Microwave heating of foodstuffs. *Journal of Food Engineering* 53(4): 347-359.

Paliwal, J., W. Wang, S.J. Symons and C. Karunakaran. 2004. Insect species and infestation level determination in stored wheat using near-infrared spectroscopy. *Canadian Biosystems Engineering* 46: 7.17-7.24.

Perdikou, P., C. Clayton and D. Hadjimitsis. 2002. Use of ETM + thermal band to identify irrigation patterns in the Aral sea basins, Kazakhstan. In *Proceedings of SPIE* 4879, 62-71. Bellingham, WA: The International Society for Optical Engineering.

Perez, M.J., J.E. Throne, F.E. Dowell and J.E. Baker. 2003. Detection of insect fragments in wheat flour by near-infrared spectroscopy. *Journal of Stored Products Research* 39(3): 305-312.

Radajewski, W., P. Jolly and G.Y. Abawi. 1988. Grain drying in a continuous flow dryer supplemented with a microwave heating system. *Journal of Agricultural Engineering Research* 41(3): 211-225.

Reddy, M.V.B., G.S.V. Raghavan, A.C. Kushalappa and T.C. Paulitz. 1998. Effect of microwave treatment on quality of wheat seeds infected with *Fusarium graminearum*. *Journal of Agricultural Engineering Research* 71(2): 113-117.

Ridgway, C., E.R. Davies, J. Chambers, D.R. Mason and M. Bateman. 2002. Rapid machine vision method for the detection of insects and other particulate bio-contaminants of bulk grain in transit. *Biosystems Engineering* 83(1): 21-30.

Sapirstein, H.D. 1995. Variety identification by digital image analysis. In *Identification of Food Grain Varieties,* ed. C.W. Wrigley, 91-130. St. Paul, MN: American Association of Cereal Chemists, Inc.

Sapirstein, H.D. and B.X. Fu. 1998. Intercultivar variation in the quantity of monomeric proteins, soluble and insoluble glutenin, and residue protein in wheat flour and relationships to bread making quality. *Cereal Chemistry* 75(4): 500-507.

Schroth, E. 1996. Modelling allowable storage time of wheat at 17% moisture content. Unpublished M.Sc. thesis. Winnipeg, MB: Department of Biosystems Engineering, University of Manitoba.

Shivhare, U.S., G.S.V. Raghavan and R.G. Bosisio. 1992a. Microwave drying of corn I. Equilibrium moisture content. *Transactions of the ASAE* 35(3): 947-950.

Shivhare, U.S., G.S.V. Raghavan and R.G. Bosisio. 1992b. Microwave drying of corn II. Constant power, continuous operation. *Transactions of the ASAE* 35(3): 951-957.

Shivhare, U.S., G.S.V. Raghavan and R.G. Bosisio. 1992c. Microwave drying of corn III. Constant power, intermittent operation. *Transactions of the ASAE* 35(3): 959-962.

Shuman, D. 2003. Monitoring system counts insects identifies species. *Agricultural Research Magazine* 51(7): 12-13.

Singh, R.P. and D.R. Heldman. 1993. *Introduction to Food Engineering,* 2nd edition. San Diego, CA: Academic Press Inc.

Sinha, R.N. 1961. Insects and mites associated with hot spots in farm stored grain. *The Canadian Entomologist* 8: 609-621.

Sinha, R.N. 1967. Grain storage and associated problems – a report on elevator surveys. Report No. 35. Winnipeg, MB: Canada Department of Agriculture.

Sinha, R.N. and H.A.H. Wallace. 1965. Ecology of a fungi-induced hot spot in stored grain. *Canadian Journal of Plant Science* 45: 48-59.

Sinha, R.N., J.T. Mills, H.A.H. Wallace and W.E. Muir. 1981. Quality assessment of rapeseed stored in ventilated and non-ventilated farm bins. *Sciences Des Aliments* 1(2): 247-263.

Sinha, R.N., W.E. Muir, and D.B. Sanderson. 1985. Quality assessment of stored wheat during drying with near-ambient temperature air. *Canadian Journal of Plant Science* 65: 849-866.

Smith, L.B. 1965. The intrinsic rate of natural increase of *Cryptolestes ferrugineus* (Stephens) (Coleoptera: Cucujidae). *Journal of Stored Products Research* 1(1): 35-49.

Smith L.B. 1977. Efficiency of Berlese-tullgren funnels for removal of the rusty grain beetle, *Cryptolestes ferrugineus*, from wheat samples. *The Canadian Entomologist* 109: 503-509.

Smith, R.C.G., H.D. Barrs, J.L. Steiner and M. Stapper. 1985. Relationship between wheat yield and foliage temperature: Theory and its application to infrared measurements. *Agricultural and Forest Meteorology* 36(2): 129-143.

Smith, Z.A. and S. Sokhansanj. 1989. Natural convection and temperature of stored produce – a theoretical analysis. *Canadian Agricultural Engineering* 32(1): 91-97.

Soysal, Y. 2004. Microwave drying characteristics of parsley. *Biosystems Engineering* 89(2): 167-173.

Stajnko, D., M. Lakota and M. Hocevar. 2004. Estimation of number and diameter of apple fruits in an orchard during the growing season by thermal imaging. *Computer and Electronics in Agriculture* 42(1): 31-42.

Sun, S. 2002. Effects of micronization on the physicochemical and rheological properties of wheat varieties. Unpublished M.Sc. thesis. Winnipeg, MB: Department of Human Nutritional Sciences, University of Manitoba.

Sun, X.Z., J.B. Litchfield and S.J. Schmidt. 1993. Temperature mapping in a model food gel using magnetic resonance imaging. *Journal of Food Science* 58(1): 168-172, 181.

Sun, X.Z., S.J. Schmidt and J.B. Litchfield. 1994. Temperature mapping in a potato using half fourier transform MRI of diffusion. *Journal of Food Process Engineering* 17: 423-437.

Symons, S.J. and R.G. Fulcher. 1988a. Determination of wheat kernel morphological variation by digital image analysis: I. Variations in eastern Canadian milling quality wheats. *Journal of Cereal Science* 8(3): 211-218.

Symons, S.J. and R.G. Fulcher. 1988b. Determination of wheat kernel morphological variation by digital image analysis: II. Variations in cultivars of soft white winter wheats. *Journal of Cereal Science* 8(3): 219-229.

United States Department of Agriculture. 2004. Grain Inspection Handbook. http://www.usda.gov/gipsa/reference-library/handbooks/grain-insp/grbook2/wheat.pdf . Accessed on: March 3, 2005.

Utter, O.J. 2003. Inspection on agricultural aircraft. *In Abstracts of Inframation, Infrared Camera Application Conference.* North Billerica, MA: Infrared Training Centre. Available at: http://www.inframation.org/abstracts.asp Accessed on: May 28, 2005.

Vadivambal, R., D.S. Jayas and N.D.G. White. 2005. Wheat disinfestation using microwave energy. ASAE Paper No. 056033. St. Joseph, MI: ASAE.

VanBree, K. and S. Wood. 2005. Using thermography to find a class of latent construction defect. In *Proceedings of Inframation 2005* Volume 5, 69-74, N. Billerica, MA: Infrared Training Centre.

Vanlinden, V., R. Vereycken, C. Bravo, H. Ramon and J.D. Baerdemaeker. 2003. Detection technique for tomato bruise damage by thermal imaging. In *Proceedings of Post-harvest Unlimited,* 389-394. Leuven, Belgium: International Society for Horticultural Science.

Varith, J., G.M. Hyde, A.L. Baritelle, J.K. Fellman and T. Sattabongkot. 2003. Non-contact bruise detection in apples by thermal imaging. *Innovative Food Science and Emerging Technologies* 4(2): 211-218.

Velu, V., A. Nagender, P.G.P. Rao and D.G. Rao. 2006. Dry milling characteristics of microwave dried maize grains (*Zea mays* L.). *Journal of Food Engineering* 74(1): 30-36.

Velupillai, L, L.R. Verma and J.I. Wadsworth.1989. Quality aspects of microwave-vacuum-dried parboiled rice. *Transactions of the ASAE* 32(5): 1759-1762.

Visen, N.S., D.S. Jayas, J. Paliwal and N.D.G. White. 2004. Comparison of two neural network architectures for classification of singulated cereal grains. *Canadian Biosystems Engineering* 46: 3.7-3.14.

Walde, S.G., K. Balaswamy, V. Velu and D.G. Rao. 2002. Microwave drying and grinding characteristics of wheat (*Triticum aestivum*). *Journal of Food Engineering* 55(3): 271-276.

Wallace, H.A.H. and R.N. Sinha. 1962. Fungi associated with hot spots in farm stored grain. *Canadian Journal of Plant Science* 42: 130-141.

Wallace, H.A.H., P.L. Sholberg, R.N. Sinha and W.E. Muir. 1983. Biological, physical and chemical changes in stored wheat. *Mycopathologia* 82: 65-76.

Watters, F.L. 1976. Microwave radiation for control of *Tribolium confusum* in wheat and flour. *Journal of Stored Products Research* 12(1): 19-25.

White, N.D.G. 1993. Annual costs related to stored-product pests in Canada (losses and preventive measures). Winnipeg, MB: Agriculture and Agri-Food Canada.

White, N.D.G. 1995. Insects, mites and insecticides in stored-grain ecosystems. In *Stored-Grain Ecosystems,* ed. D.S. Jayas, N.D.G.White and W.E. Muir, 123-167. New York, NY: Marcel Decker Inc.

White, N.D.G. and S.R. Loschiavo. 1986. Effects of localized regions of high moisture grain on efficiency of insect traps capturing adult *Triboliun castaneum* and *Cryptolestes ferrugineus* in stored wheat. *Tribolium Information Bulletin* 28: 97-100.

White, N.D.G., R.T. Arbogast, P.G. Fields, R.C. Hillmann, S.R. Loschiavo, B. Subramanyam, J.E. Throne and V.F. Wright. 1990. The development and use of pitfall and probe traps for capturing insects in stored grain. *Journal of the Kansas Entomological Society* 63: 505-525.

Wrigley, C.W. and I.L. Batey. 1995. Efficient strategies for variety identification. In *Identification of Food Grain Varieties,* ed. C.W. Wrigley, 19-33. St. Paul, MN: American Association of Cereal Chemists Inc.

Wurzbach, R.N. 2003. Infrared applications in farming: vision of things to come. In *Proceedings of Thermosense XXV*, No. 5073, 154-159. Bellingham, WA: The International Society for Optical Engineering.

Xu, H. and Y. Ying. 2003. Detection citrus in a tree canopy using infrared thermal imaging. In *Proceedings of SPIE No.* 5271B, 321-327. Bellingham, WA: The International Society for Optical Engineering.

Zayas, I, F.S. Lai and Y. Pomeranz. 1986. Discrimination between wheat classes and varieties by image analysis. *Cereal Chemistry* 63(1): 52-56.

Zayas, I.Y. and P.W. Flinn. 1998. Detection of insects in bulk wheat samples with machine Vision. *Transcations of the ASAE* 41(3): 883-888.

Zeleny, L. and D.A. Coleman. 1939. The chemical determination of soundness in corn. Technical Bulletin 644: United States Department of Agriculture.

Appendix A

Calibration of a thermal camera

(Source: Calibration Program Cal500 Version 2.07, User manual, 1998, Published by FLIR Systems, Publication number 557 362)

A thermal camera must be calibrated periodically in order to ensure that the temperature measurement is accurate in various environments. Since many materials used in the camera have temperature dependent properties, different techniques are needed to compensate for the temperature variations inside the camera. Some of the important operations carried out during the calibration of a thermal camera are given below:

- Determining various temperature drift properties
- Determining detector and amplifier properties
- Feeding the corresponding constants to the camera
- Determining the temperature calculation constants
- Loading the whole calculation into the camera
- Checking the quality of the calibration

Calibration of FLIR SC500 thermal camera

The camera used in this study was calibrated twice at the service station of FLIR Systems Ltd., Burlington, ON, Canada. The first calibration was done at the beginning of the research and the second was done in the middle of the research. In addition, the camera was occasionally checked for uniformity of temperature reading by imaging a hot metal plate at pre-set temperature of 90°C.